

**Redefining the *Caenorhabditis elegans* DEG/ENaC Mechanosensory Channel Complex**

Yushu Chen

Submitted in partial fulfillment of the  
Requirements for the degree of  
Doctor of Philosophy  
In the Graduate School of Arts and Sciences

COLUMBIA UNIVERSITY

2014

© 2014  
Yushu Chen  
All rights reserve

## Abstract

### **Redefining the *Caenorhabditis elegans* DEG/ENaC Mechanosensory Channel Complex**

Yushu Chen

Mechanosensation underlies multiple senses, such as touch, pain, hearing, and proprioception. The molecules that mediate most of the mechanical senses have not been identified. Genetic and molecular methods have identified several putative mechanosensitive proteins. However, how the mechanotransduction machineries organize and function remains largely unknown.

To understand the organization of the mechanotransduction complex, I studied the DEG/ENaC mechanosensory channel that detects gentle touch in the six touch receptor neurons (TRNs) of *C. elegans*. Previous studies from our lab have suggested that this channel complex contains two pore-forming subunits MEC-4 and MEC-10 (DEG/ENaC proteins) and two auxiliary subunits MEC-6 (paraoxonase-like protein) and MEC-2 (stomatin-like protein). However, questions remain about what molecules really constitute this mechanosensory channel complex. Studying this particular DEG/ENaC channel in *C. elegans* will not only elucidate the organization of one major mechanosensory complex, but also improve our knowledge of other DEG/ENaC proteins, which are found in both vertebrates and invertebrates, and involved in various functions, e.g. mechanosensation, sodium taste, acid sensation, synaptic plasticity, and sodium homeostasis.

My thesis research investigated the molecular organization and formation of the DEG/ENaC mechanosensory channel in *C. elegans*. In collaboration with Ehud Isacoff's lab, I analyzed the stoichiometry and co-localization of the potential channel subunits using single

molecule optical imaging. In *Xenopus* oocytes, MEC-4 and MEC-10 form trimers, either of MEC-4 alone or of MEC-4 and MEC-10 in a ratio of 2:1. MEC-2 and MEC-6 do not seem to colocalize with the MEC-4<sub>3</sub> or MEC-4<sub>2</sub>MEC-10 trimers at the single molecule level, and thus, may not be part of the channel complex.

To study the role of MEC-6, I characterized its homologous protein POML-1. Compared to MEC-6, POML-1 appears to play a similar but relatively minor role in the TRNs. As with *mec-6*, loss of *poml-1*, completely suppressed *mec-4(d)* induced neuronal degeneration. [*mec-4(d)* encodes a hyperactive channel and causes neuronal degeneration in vivo]. Loss of *poml-1* alone had no effect, but in sensitized background, it completely abolished touch sensitivity. Surprisingly, most of MEC-6 and POML-1 proteins were found in the endoplasmic reticulum (ER), rather than on the plasma membrane, consistent with the finding in *Xenopus* oocytes that MEC-6 is not part of the MEC-4 mechanosensory channel.

I provided several lines of compelling evidence to demonstrate that MEC-6 and POML-1 are required for MEC-4 folding and transport, and likely function as ER chaperones. First, loss of these proteins dramatically reduced MEC-4 protein level, eliminated the punctate distribution of MEC-4 in the neuronal process, and altered the MEC-4 folding status in the TRNs. These phenotypes are also shared by calreticulin (CRT-1), a chaperone in the ER. Second, MEC-6 also substantially increased MEC-4 surface expression in *Xenopus* oocytes, though POML-1 and CRT-1 did not have the same effect in oocytes. Third, overexpressing a transport protein, SEC-24, partially rescued the transport defects caused the *poml-1* and *crt-1* mutations.

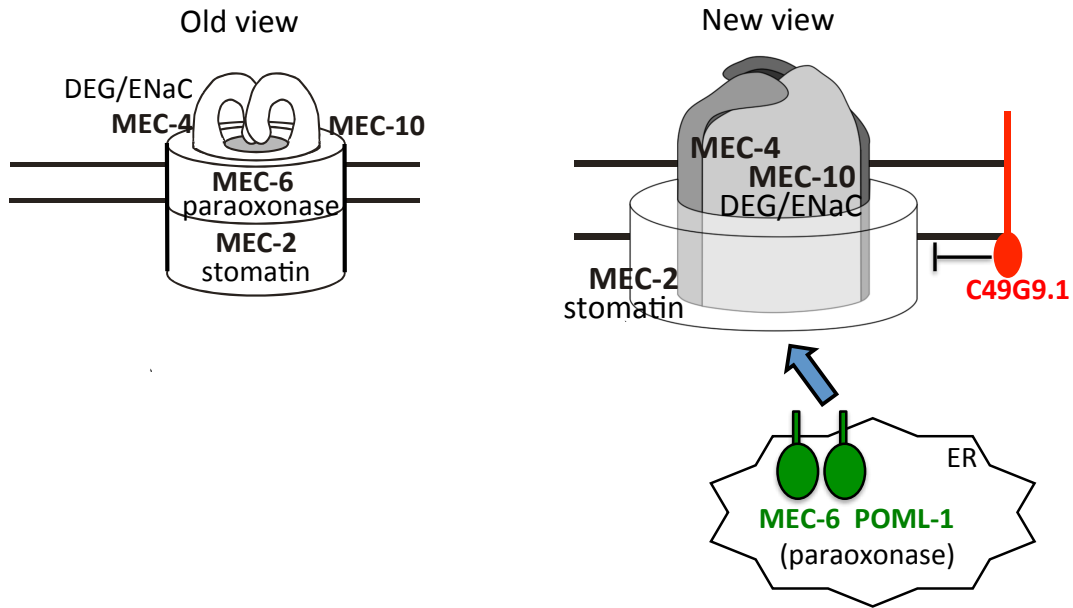
Based on the finding that loss of *poml-1* reduces MEC-4 protein levels and suppresses neurodegeneration caused by the hyperactive MEC-4(d) channel, I used the *poml-1* deletion

as a sensitized background to identify genes that normally inhibit MEC-4(d) neurotoxicity through a genetic screen. I found that the loss of two genes, *mec-10* and C49G9.1, makes *mec-4(d)* more toxic. The proteins encoded by these genes affect *mec-4(d)* neurotoxicity through different mechanisms. MEC-10 inhibits MEC-4(d) without affecting MEC-4 surface expression. In contrast, both in vivo and in vitro data suggested that C49G9.1, a membrane protein specific to nematodes, can reduce MEC-4 surface expression, which contributes to, at least in part, its inhibitory effect on MEC-4(d). C49G9.1 does not incorporate into the MEC-4/MEC-10 channel, though they may transiently interact, because C49G9.1 did not appear to co-localize with MEC-4 either in vivo or in vitro, but co-immunoprecipitated with MEC-4.

In summary, my doctoral research has refined the model of the MEC-4/MEC-10 complex. In particular, my studies resolved the subunits composition of DEG/ENaC channel at the single molecule level, by showing that they form MEC-4<sub>2</sub>MEC-10 trimers in *Xenopus* oocytes. Notably, MEC-2 and MEC-6 may not be part of the complex. Indeed, I provided compelling evidence to demonstrate that MEC-6 and POML-1 are needed for MEC-4 folding and transport, and likely function as chaperones and/or assembly factors. In addition, I identified a novel membrane protein, C49G9.1, which negatively regulates MEC-4 surface expression and/or activities. This work has revised our understanding of a major mechanosensory complex and described a new class of chaperone proteins as well as a new inhibitor protein for DEG/ENaC proteins.

Graphical Abstract

# The Mechanotransduction Complex Model



## Table of Contents

List of Figures and Tables .....	iv
Chapter I <b>Introduction</b> .....	1
Section I-A: Mechanosensitive proteins .....	4
Several putative mechanosensitive proteins .....	4
Auxiliary proteins for mechanosensitive channels .....	12
Gating mechanism .....	13
Section I-B: Touch sensation in <i>C. elegans</i> .....	15
Mechanosensation in <i>C. elegans</i> .....	15
The six touch receptor neurons .....	15
DEG/ENaC mechanosensory channel .....	18
The model of the DEG/ENaC mechanosensory channel .....	20
Other proteins that regulate the DEG/ENaC mechanosensory channel function .....	21
Section I-C: Structure and function of DEG/ENaC proteins .....	23
DEG/ENaC channels are found in many species .....	23
Sensory functions of DEG/ENaC proteins.....	23
ASICs in the central nervous system.....	27

ENaC and Na <sup>+</sup> homeostasis.....	28
Gain of function mutations of <i>C. elegans</i> degenerin .....	30
Structure and stoichiometry of DEG/ENaC proteins .....	31
 Section I-D: Paraoxonase (PONs).....	 39
PONs are multifunctional enzymes with protective activities .....	39
The PONs in <i>C. elegans</i> .....	41
 Section I-E: Membrane protein production and transport .....	 43
Classical protein synthesis and secretory pathways.....	43
Auxiliary proteins and ion channel expression and trafficking .....	49
 Chapter II <b>Reconsidering the <i>C. elegans</i> DEG/ENaC mechanosensory channel</b>	
<b>complex</b> .....	<b>52</b>
Summary .....	53
Introduction .....	54
Experimental procedures .....	55
Results .....	65
Discussion .....	93
 Chapter III <b>MEC-10 and C49G9.1 reduce the neurotoxicity of the MEC-4(d)</b>	
<b>DEG/ENaC channel</b> .....	<b>99</b>



Summary .....	100
Introduction .....	101
Experimental procedures .....	102
Results .....	106
Discussion .....	120
<b>Chapter IV Summary and Future Directions .....</b>	<b>122</b>
Summary .....	123
The MEC-4 <sub>2</sub> MEC-10 mechanosensory channel complex.....	124
MEC-6 and POML-1 in MEC-4 folding and transport .....	125
The Function of other PONs-like proteins .....	128
Inhibition of the MEC-4(d) neurotoxicity .....	129
References.....	132
<b>Appendix I The DEG/ENaC protein MEC-10 regulates the transduction channel complex in <i>Caenorhabditis elegans</i> touch receptor Neurons .....</b>	<b>155</b>
<b>Appendix II Characterization of other POML proteins .....</b>	<b>166</b>

## List of Figures and Tables

Figure I-1. Touch sensation in <i>C. elegans</i> .....	17
Figure I-2. Diagram of conserved domains in DEG/ENaC proteins .....	33
Figure I-3. The crystal structure of chick ASIC1 protein .....	36
Figure I-4. Gating mechanism of ASIC channels.....	37
Figure I-5. Sequence alignment of <i>C. elegans</i> and human PONs.....	42
Figure I-6. Synthesis of glycoproteins in and out of the ER.....	47
Figure II-1. TRN expression of MEC-6 and POML-1 .....	68
Table II-1. <i>poml-1</i> mutations .....	70
Figure II-2. <i>poml-1</i> mutations reduce the touch sensitivity .....	71
Table II-2. <i>poml-1</i> and <i>mec-6</i> mutations suppress <i>mec-4(d)</i> degenerations .....	73
Figure II-3. POML-1 increases MEC-4(d) activity in <i>Xenopus</i> oocytes.....	75
Figure II-4. Effect of <i>mec-6</i> , <i>poml-1</i> , and <i>crt-1</i> mutations on MEC-2 and MEC-4 expression in the TRNs.....	80
Figure II-5. MEC-6, POML-1 and CRT-1 may function as chaperones .....	83
Figure II-6. The FRET signal of CFP::MEC-4::YFP .....	85
Figure II-7. The effect of MEC-6, POML-1 and CRT-1 on MEC-4 surface expression .....	88
Figure II-8. The stoichiometry and co-localization of the MEC-4/MEC-10 channel .....	90
Figure II-9. MEC-2, MEC-6, POML-1, and MEC-4 do not colocalize on the plasma membrane of <i>Xenopus</i> oocytes .....	92
Table III-1. Strains used in these studies .....	104

Table III-2. <i>poml-1</i> suppression of <i>mec-4d</i> requires <i>mec-10</i> and C49G9.1 .....	108
Figure III-1. <i>mec-10</i> and C49G9 on <i>mec-4(d)</i> degeneration and touch sensitivity .....	110
Figure III-2. C49G9.1 sequence, expression and effect on MEC-4 expression .....	112
Table III-3. C49G9.1 homology identified by BLASTP .....	113
Table III-4 C49G9.1 homology recognized by Phyre2 .....	114
Figure III-3. The effect of C49G9.1 mutation on touch sensitivity and the MRC .....	116
Figure III-4. The effect of the overexpression of C49G9.1(+) .....	117
Figure III-5. C49G9.1 and MEC-4 in <i>Xenopus</i> oocytes .....	119
Figure IV. A new model of the DEG/ENaC mechanotransduction complex .....	124
Figure V. Expression pattern of POML-2, POML-3, and POML-4 .....	166
Table V. Summary of <i>C. elegans</i> PONs .....	166

## Acknowledgements

I would like to thank my advisor, Dr. Martin Chalfie. Thank you for teaching me how to think through scientific problems, and how to make presentations and write papers. I have learned a lot from you in the past seven and half years!

I am very grateful to have people in the Chalfie lab as friends and colleagues. Irini Topalidou gave me a lot of advice and support in my both professional and personal life. She was like the sunshine in my gloomy days! Anna Maria has been an essential part of nearly everything I do in the lab. Brian Cobliz helped me initiate the K11E4.3 project. I would also like to thank Robert for helping me with the microscope and talking crazy ideas to me; I thank Chaogu Zheng, Ameer Thompson, eMalick Njie, and Andrea Calixo for their friendship.

I would also like to thank several people for reagents and experiments. I thank Dr. Jian Yang and his lab members for providing frog oocytes. Without their generosity, my work is impossible. I also thank Oliver Hobert, Alexander Boyanov, and Gregory Minevich for the whole genome sequencing.

My family in China has been very supportive. I thank my parents, grandma, and brother for their love, patience, and support. My parents and grandma have sacrificed a lot, especially in the past seven and half years when I am away from them. Without them, I cannot get where I am now.

## **Chapter I**

### **Introduction**

Organisms detect various stimuli (radiant, chemical, and mechanical) from both the internal and external environments. Despite their diverse nature, these stimuli act on organisms in a similar way: activating their receptors (usually membrane proteins), eliciting electrical (membrane depolarization) and/or chemical signals (second messengers), and generating behavior (e.g. aversion or attraction).

Mechanical stimuli include, but are not limited to, physical contact, air vibration, osmolarity change, sound waves, gravity, acceleration, blood pressure, and fluid flow. These stimuli all activate mechanosensitive proteins in neurons innervating sensory organs and visceral organs, enabling animals to hear sound, feel touch, sense body position, monitor blood pressure, etc. Mechanosensation also underlies osmoregulation in microbes and gravitropism in plants. In addition to the sensory functions, mechanosensation has broader roles in bone development (Bonewald, 2006), morphogenesis (Eisenhoffer et al., 2012), cell migration, and cancer metastasis (Tadeo et al., 2014).

This thesis mainly focuses on sensory mechanosensation. The molecules that detect most mechanical stimuli remain unknown. Past studies have identified several putative mechanosensitive proteins, which are all ion channels, but how these channel proteins organize and function is poorly understood. Arguably, the *C. elegans* DEG/ENaC mechanosensory channel is the best understood eukaryotic mechanosensitive protein.

In this chapter, I first summarize the mechanosensitive proteins that have been identified so far, then introduce touch sensation in *C. elegans* and the DEG/ENaC mechanosensory channel complex, which includes two DEG/ENaC proteins (MEC-4 and MEC-10), a paraoxonase-like protein (MEC-6), and a stomatin like protein (MEC-2). In the following two sections, I also provide more specific background information about

DEG/ENaC proteins and paraoxonase proteins. Because this thesis reports that MEC-6 facilitates MEC-4 folding and transport, I provide an overview of protein synthesis and transport in the last section of this chapter.

## **Section A: Mechanosensitive (MS) proteins**

Recent studies on mechanosensation are mainly focused on identifying and characterizing mechanosensitive cells and proteins in peripheral sensory neurons and blood vessels. Here, I summarize the progress made towards identifying and characterizing mechanosensitive proteins.

Because mechanosensory transduction occurs extremely rapidly, usually with a latency of less than one millisecond, e.g. 40  $\mu$ s in hair cells (Corey and Hudspeth, 1979) and 200  $\mu$ s in fly sensory bristle (Walker et al., 2000), it is believed to result directly in an electrical signal rather than in a second messenger that mediates chemosensation. Therefore, the molecules that detect mechanical stimuli are supposed to form ion channels.

### **Putative mechanosensitive proteins**

In the past 30 years, genetic and molecular methods have identified several putative mechanosensitive proteins. They all form ion channels on the plasma membrane of the mechanosensitive cells. For most of these proteins, the requirement for mechanosensation has been proven genetically or physiologically: their absence reduces or abolishes behavioral responses to mechanical stimuli in animals, and/or the mechanosensitive currents in cells. The rest of these proteins lack the in vivo evidence, but they can form true mechanosensitive channels when expressed in heterologous systems or reconstituted on liposomes. Some of these mechanosensitive proteins are considered to be the pore-forming components of native



mechanotransducers because their point mutations can alter the physical properties (e.g. ion selectivity and gating) of the mechanosensory channels in vivo (Arnadottir and Chalfie, 2010).

Unlike the olfactory receptors and most gustatory receptors, which are G-protein coupled receptors, putative MS proteins are very diverse in protein sequence and structure. We know very little about their common nature besides their mechanosensitivity. Different sets of mechanosensitive channels are utilized by different species, for example, MscL and MscS in bacteria, TRPY in yeast, DEG/ENaC and TRP in *C. elegans*, DEG/ENaC, TRP, and Piezo in *Drosophila*, K<sup>+</sup> channel, TRP, and Piezo in mammals. One possibility is that MS proteins emerged as soon as life started on the earth and diverged over the course of evolutionary history (Kung and Blount, 2004). Moreover, diverse mechanical stimuli may have driven organisms to develop various machineries.

### **MscL and MscS**

The first MS proteins to be identified, which are also the best characterized, are mechanosensitive channel of large conductance (MscL) and mechanosensitive channel of small conductance (MscS) in bacteria (Levina et al., 1999; Sukharev et al., 1994). MscL and MscS are expressed on the bacterial membranes, open to release solutes when bacteria encounter osmotic down-shock in the environment, such as rain. Bacteria lacking both types of these MS proteins become very sensitive to hypo-osmotic shock (Levina et al., 1999). Purified MscL proteins remain mechanosensitive when reconstituted in liposomes (Sukharev et al., 1994).

Despite their similar physiological roles, MscL and MscS are very different proteins. The MscS channel is a homoheptamer of subunits with three transmembrane helices; the third

transmembrane helix of each subunit assembles together to form the channel pore (Bass et al., 2002). In contrast, MscL has two transmembrane helices and assembles as homopentamer, with the first transmembrane helix of each subunit lining the pore (Chang et al., 1998).

Four MscS-like proteins have been found in *Arabidopsis thaliana* and are implicated in mechanosensation: MSL3 can rescue the osmoregulation in bacteria that lack several MS ion channels; MSL2 and MSL3, are expressed in plastids, co-localize with plastid division proteins, and are necessary for controlling the size and shape of plastids (Haswell and Meyerowitz, 2006); membrane localized MSL9 and MSL10 are required for mechanosensitivity of root cells (Haswell et al., 2008). Proteins similar to bacterial MscS have only been found in plants and fungi, but not in animals, suggesting animals use different types of proteins for mechanosensation.

### **Degenerin/epithelial Na<sup>+</sup> channel (DEG/ENaC)**

Several DEG/ENaC proteins are mechanosensitive. DEG/ENaC proteins form amiloride sensitive and Na<sup>+</sup> selective channels found in metazoa. DEG/ENaC is trimer, and each subunit contains two transmembrane segments (Jasti et al., 2007; Mano and Driscoll, 1999).

DEG/ENaC proteins in *C. elegans*, MEC-4/MEC-10, are the first confirmed mechanosensory channels in eukaryotic sensory neurons. MEC-4 is specifically expressed in the six touch receptor neurons (TRNs, Lai et al., 1996), while MEC-10 is expressed in TRNs and two other types of mechanosensory neurons, FLP and PVD (Huang and Chalfie, 1994). MEC-4 is essential for touch sensitivity and the mechanoreceptor current (MRC), as verified by the phenotype of its null mutants (O'Hagan et al., 2005). Moreover, animals with a *mec-4*

missense mutation *u2* (G716D), which alters channel ion selectivity, completely lost the MRC and touch response. In contrast, we have shown that MEC-10 appears to be required but not essential, because loss of *mec-10* reduced but did not eliminate the MRC and touch sensitivity; but several gain-of-function mutations of *mec-10* altered ion selectivity of the mechanotransduction channel and completely eliminated the MRC and touch responses, validating the contribution of MEC-10 to the mechanosensory channel (Arnadottir et al., 2011).

Another *C. elegans* DEG/ENaC protein, DEG-1, is an essential pore-forming component of the major mechanotransducer in the nociceptive ASH neuron. Loss of *deg-1* completely eliminated the Na<sup>+</sup> permeable and amiloride sensitive current, which constitutes approximately 80% of the total MRC; *deg-1* missense mutations affecting the predicted pore-forming domain altered the MRC ion selectivity (Geffeney et al., 2011).

Several DEG/ENaC proteins from *Drosophila* and mammals are also implicated in mechanosensation, but little evidence exists for their direct role in transduction (see more details in section B).

### **Transient receptor potential (TRP) channels**

Transient receptor potential (TRP) channels are involved in multiple senses, including vision, taste, smell, hearing, touch, and temperature. In these different sensory modalities, TRP channels can function as either the direct transducers or downstream molecules. The *trp* gene was first identified in a *Drosophila* mutant with defective vision (Montell et al., 1985; Montell and Rubin, 1989), and later was found to encode a large family of Ca<sup>2+</sup> permeable but non-selective cation channels conserved from yeast to mammals. Based on sequence and

topological similarity, TRP channels can be divided into seven subfamilies: TRPA, TRPC, TRPM, TRPN, TRPV, TRPP, and TRPML; more distantly related yeast TRPs comprise another subfamily (Venkatachalam and Montell, 2007). TRP proteins have similar topology: six transmembrane segments and intracellular N and C-termini (Montell, 2005).

Nearly every subfamily (except TRPM and TRPML) has members that are potential mechanotransducers, but only two of them have been confirmed. Yeast TRPY1 (also called Yvc1p) mediates the release of  $\text{Ca}^{2+}$  from vacuoles to cytoplasm upon hyperosmotic shock. This protein can be activated by pressure either on whole vacuole or the vacuole excised on patch (Zhou et al., 2003). *C. elegans* TRP-4 (TRPN member) is an essential pore-forming subunit of the mechanosensory channel in CEP neuron, because loss of TRP-4 completely eliminated the MRC in CEP neuron, and the mutations in the predicted pore altered ion selectivity of the mechanosensory channel (Kang et al., 2010). TRP-4 is also required for the function of DVA neuron in sensing body stretch and regulating locomotion in *C. elegans* (Li et al., 2006).

Several other TRP channels are potential mechanotransducers, though none have been experimentally confirmed. One of the most likely candidates is *nompC*, which was first recovered by genetic screening for mutants defective in mechanoreception in *Drosophila* (Kernan et al., 1994). *nompC* (TRPN) is expressed in *Drosophila* mechanosensory organs (e.g. bristles, proprioceptors, and auditory system), and its mutation eliminated 90% MRC in the mechanosensory bristles, and 40% of sound-evoked electrical response in hair cells (Kamikouchi et al., 2009; Walker et al., 2000). It has been suggested that NOMPC is the mechanotransducer in the auditory organ of *Drosophila*, because its mutation disrupted the non-linear signal amplification in hair cells which requires the functional transducers (Gopfert

et al., 2006). In zebrafish, NOMPC is also a potential transducer for hearing because the reduction of its expression eliminated the mechanical response in hair cells (Sidi et al., 2003).

Another likely candidate is TRPV. *C. elegans* TRPV channels, OSM-9 and OCR-2, are located on the cilia of the poly-modal nociceptor ASH neuron, and are required for avoidance of hyperosmolarity and nose touch in *C. elegans* (Colbert et al., 1997; Tobin et al., 2002). Mouse TRPV4 can restore the osmotic avoidance and nose touch avoidance to the *osm-9* mutant worms, and *trpv4* knockout mice displayed impaired osmotic regulation, suggesting a conserved role of TRPV in mechanosensation (Liedtke and Friedman, 2003; Liedtke et al., 2003).

TRPA1 is also implicated in mechanosensation. *C. elegans* TRPA1 is required for foraging and nose touch response. Moreover, the heterologously expressed worm and rat TRPA1 proteins can produce currents in response to negative pressure and hyperosmolarity, respectively (Kindt et al., 2007; Zhang et al., 2008).

### **Transmembrane channel-like (TMC) proteins**

TMC1 and TMC2 are implicated in mechanosensation in hair cells. They both encode  $\text{Ca}^{2+}$  permeable cation channels with six predicted transmembrane segments. TMC1 and TMC2 are expressed in mouse hair cells, and are required for hearing and vestibular function (Kawashima et al., 2011). But whether TMC proteins act as the mechanotransduction channel in hair cells remains controversial, based on studies from two groups. The Holt group reported that TMC1 and TMC2 act as essential components of the hair cell mechanotransducer in the mouse inner ear, because deletion of both genes reduced the mechanotransduction current and a *Tmc1* point mutation reduced  $\text{Ca}^{2+}$  permeability and the single channel conductance (Pan et

al., 2013). In contrast, the Fettiplace group observed that outer hair cells with deletion of both Tmc1 and Tmc2 produced currents of normal amplitude when hair bundles deflected to the negative position (wild type hair cells respond to the positive deflection), suggesting that TMC1 and TMC2 do not form the pore of the transduction channel (Kim et al., 2013). It is likely that TMC1 and TMC2 contribute to mechanotransduction through interaction with tip links, because hair cells with defective tip links produced the similar negative phase current to that in Tmc1/Tmc2 double knockout (Alagramam et al., 2011). The defects observed by the Holt group may arise from loss of one auxiliary component of the transduction complex.

### **Piezo**

Recently, Piezo proteins (Piezo1 and Piezo2) were identified as essential components of mechanosensitive channels through siRNA screens for potential ion channels needed for mechanosensitive current in Neuro A neuroblastoma cells (Coste et al., 2010). Piezo proteins encode a new class of non-selective cation channels that are found in animals, plants, and fungi, but not in yeast and bacteria. These proteins each contain over 30 putative transmembrane regions, and assemble as homo-tetramers. Both *Drosophila* and mouse Piezo can produce mechanically activated currents when expressed in many cell types and reconstituted in lipid bilayers, suggesting Piezo proteins alone can form mechanosensitive channels (Coste et al., 2012). *Drosophila* Piezo is required for mechanical nociception, and acts in parallel with DEG/ENaC pickpocket (ppk), because the loss of Piezo alone reduced the response, whereas in combination with ppk knockdown, it completely abolished the response to noxious mechanical stimuli (Kim et al., 2012). Mouse Piezo proteins are expressed in bladder, colon, kidney, lung, and dorsal root ganglion (DRG) neurons, suggesting a role for

Piezo proteins as native mechanotransducers (Coste et al., 2010). Piezo 2 has been shown to be required for mechanosensation in mouse Merkel cells, because its deficiency in the skin reduced the firing rate of the slow adapting response to mechanical stimuli in Merkel cells, and decreased the behavioral response to touch in animals (Woo et al., 2014).

### **K<sup>+</sup> channel**

Several potassium channels are also mechanosensitive. Two-pore domain potassium channels (K<sub>2P</sub>) form homo- or heterodimeric channels; each subunit contains four predicted transmembrane regions and two pore-forming domains. They are poly-modal channels and open in response to a wide range of stimuli, including mechanical stimuli, membrane depolarization, heat, lower intracellular pH, and lipids (e.g. volatile anesthetics, polyunsaturated fatty acids, and lysophospholipids) (Honore, 2007). Membrane stretch and lipids can directly activate three K<sub>2P</sub> members, TREK-1 (TWIK-related K<sup>+</sup> channel), TREK-2, and TRAAK (TWINK-related arachidonic acid-stimulated K<sup>+</sup> channel) in heterologous systems (Bang et al., 2000; Maingret et al., 1999; Patel et al., 1998). Their responses to lipids also hint at a mechanosensitive property, because lipid is thought to change membrane geometry and may activate the channel directly through mechanical forces within the lipid bilayer.

Although heterologously expressed K<sub>2P</sub> proteins exhibit mechanosensitivity, the role of K<sub>2P</sub> in mechanosensation has not been proven in vivo. TREK-1 may function as a modulator rather than a transducer, because *trek-1* knockout mice are more sensitive to mechanical stimuli than wild-type animals (Alloui et al., 2006). In contrast to the opposing effect on mechanical sensitivity, TREK-1 may mediate the cellular response to volatile

anesthetics, because TREK-1 is highly expressed in mammalian CNS, and the genetic knockout mice showed a significant decrease in sensitivity to chloroform, halothane, sevoflurane, and desflurane (Franks and Honore, 2004).

Kv 1.1 proteins are also mechanosensitive. Recently, Kv 1.1 was found to produce mechanosensitive current, which can modulate mechanical threshold of C-mechanoreceptors and adaptation of A $\beta$ -mechanoreceptors (Hao et al., 2013).

In addition to the above potential mechanically-gated ion channels, Kv Shaker channel (Laitko et al., 2006; Laitko and Morris, 2004) and HCN2 (Lin et al., 2007) can be mechanically modulated, because membrane stretch can alter their rate of activation and inactivation.

### **Auxiliary proteins for mechanosensitive channels**

As with many ion channels, MS channels also require auxiliary proteins for their function and/or expression. The first identified auxiliary proteins are a stomatin-like protein (MEC-2) and a paraoxonase-like protein (MEC-6) in *C. elegans* DEG/ENaC mechanosensory channels (Chelur et al., 2002; Goodman et al., 2002). The two proteins have different functions: MEC-6 is needed for the channel localization (Chelur et al., 2002); MEC-2 binds to cholesterol and may contribute to channel gating through regulating the lipid microenvironment surrounding the channel (Huber et al., 2006). A MEC-2 homolog, mouse STOML3 (also called SLP3), is needed for the function of multiple potential mechanosensitive proteins, because 1) loss of STOML3 resulted in several types of mechanosensory DRG neurons that exhibited deficits in producing the mechanosensitive



current (Poole et al., 2014; Wetzel et al., 2007); 2) STOML3 co-immunoprecipitated with ASIC2a, ASIC2b, and ASIC3 in HEK-293 cells, and inhibited the activities of ASICs in both HEK-293 cells and mouse DRG neurons (Wetzel et al., 2007); 3) in N2A neuroblastoma cells, STOML3 increased the mechanosensitivity of Piezo1 and Piezo2 (Poole et al., 2014). However, how these auxiliary proteins contribute to mechanosensory channel function remains unclear.

### **Gating mechanism of MS proteins**

One important open question is how transduction occurs. Based on their gating properties, MS proteins can be divided into two groups: the first group can be directly activated by membrane stretch without any additional proteins, including bacterial MscS and MscL, yeast TRPY1, mammalian  $K_{2P}$  and Piezo; the second group requires other proteins (intracellular cytoskeleton, extracellular proteins, or other auxiliary proteins) for mechanical activation, e.g. *C. elegans* DEG/ENaC channels, the unidentified hair cell transduction channel, and some TRP channels (Arnadottir et al., 2011).

Two gating models are proposed: the membrane force model for the first group and the tethered model for the second group (Kung, 2005). In the membrane force model, the MS channel is directly gated by force on the membrane, through interaction between lipids and proteins. In the tethered model, the MS channel is tethered to intracellular and extracellular components; the membrane bending caused by force stretches the tethering to open the MS channels. For example, hair cells project multiple stereocilia composed of cross-linked actin bundles on the surface, and these stereocilia are connected via tip links composed of cadherin

and protocadherin. Deflection of the tip links activates the membrane-localized hair cell transduction channel, which is thought to be tethered to the actin bundle inside and the tip link outside (Pickles and Corey, 1992). But little direct evidence exists. The function of *C. elegans* MEC-4/MEC-10 mechanotransduction complex requires extracellular matrix (ECM) proteins and intracellular 15-protofilament microtubules (15-p MTs). But a couple of experiments raised the doubt about the tethered model for MEC-4: 1) membrane-localized MEC-4 proteins do not appear to associate with either ECM proteins or the 15-p MTs, as imaged by electron microscopy (Cueva et al., 2007); 2) disrupting the 15-p MTs reduces but does not completely eliminate the mechanoreceptor current (O'Hagan et al., 2005).

Understanding the molecular organizations and architecture of mechanosensory channels will pave ways to the understanding of the function and regulation of mechanosensory channels. The function and organization of the mechanotransduction complex is not understood except for the bacterial MscL and MscS channels. *C. elegans* MEC-4/MEC-10 is perhaps the best characterized eukaryotic MS channel. The major part of my PhD research is studying the organization of MEC-4/MEC-10 mechanosensory channel complex (more details in Chapter II).

## **Section B: Touch Sensation in *C. elegans***

### **Mechanosensation in *C. elegans***

*C. elegans* is a great model organism to study mechanosensation for several reasons. First, it is a simple organism with a small and transparent body composed of only 959 cells (1031 cells in male), including 302 neurons (383 neurons in male) in adult hermaphrodites. Second, it is a great genetic tool because of its short life cycle, easy maintenance, and sexual forms containing predominant self-fertilizing hermaphrodites as well as males (Riddle, 1997). Third, its wild-type cell lineage (Deppe et al., 1978) and neuroanatomy (White et al., 1986) have been determined; its entire genome has been sequenced (Consortium, 1998).

*C. elegans* has 30 mechanosensory neurons in hermaphrodites, e.g. the six touch receptor neurons sensing gentle touch and plate tap, the multi-dendritic PVD and FLP detecting harsh touch, the ciliated neurons CEP, ADE, and PDE sensing texture during crawling, the polymodal sensory neuron ASH responding to mechanical and osmotic stimuli. Males have an additional 52 putative mechanosensory neurons for mating (Goodman, 2006).

### **The six touch receptor neurons**

Among all these mechanosensory neurons, the six touch receptor neurons (TRNs) are the best characterized. TRNs consist of three pairs of neurons laying against the hypodermis (Figure I-1A): two pairs of neurons are located on the lateral anterior (ALML and ALMR) and posterior (PLML and PLMR) sides of the worm; a third pair of neurons lie on the ventral

side of the mid anterior (AVM) and mid posterior (PVM) of the worm (Chalfie and Sulston, 1981). The TRN has a simple morphology: a cell body and a process that extends from the cell body anteriorly for nearly half of the worm's length. In addition, PLM neurons each have a shorter posterior process, and some ALM neurons also have a posterior process, which is shorter than that of a PLM. The processes of TRNs sense physical touch through the mechanotransduction complex localized on the membrane and make synaptic connection with other neurons through their anterior branches. All TRNs have physical features unique to them, including the prominent extracellular proteins that ensheathe the TRNs and the intracellular 15-protofilament microtubules (most other cells have 13-protofilament microtubules) (Bounoutas and Chalfie, 2007).

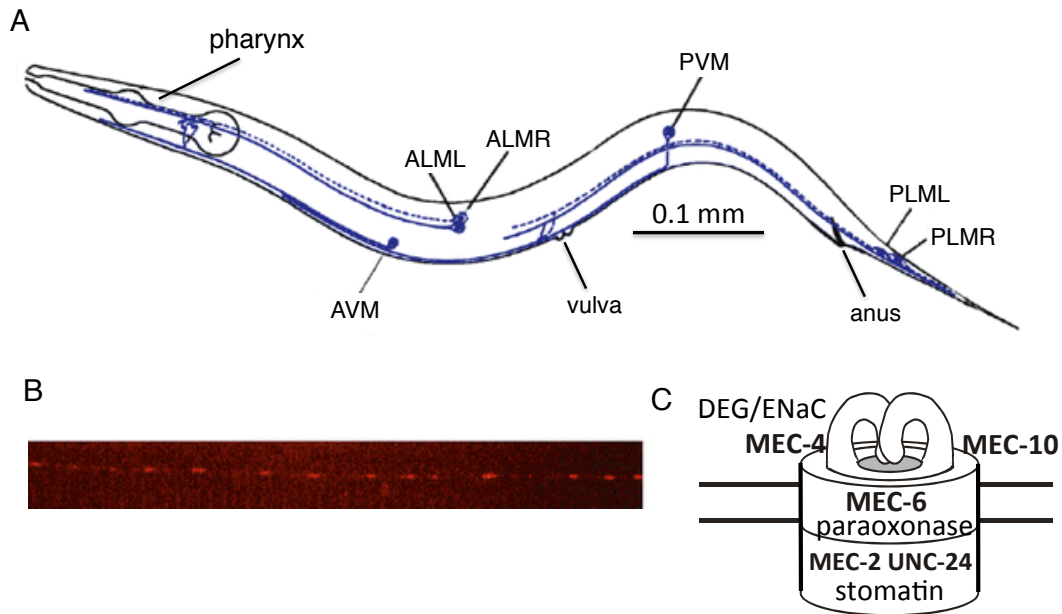


Figure I-1. Touch sensation in *C. elegans*. (A) Diagram of the six TRNs (blue) in *C. elegans* (adapted from Chalfie and Sulston, 1981). (B) MEC-4::GFP (false colored) puncta along the TRN process (from Emtage et al., 2004). (C) Membrane proteins required for the mechanotransduction complex (adapted from O'Hagan and Chalfie, 2006)

The development and function of TRNs requires 15 *mec* (MECHANOSENSORY abnormal) genes, which were identified by genetic screens for mutants defective in body-touch sensitivity (Chalfie and Au, 1989; Chalfie and Sulston, 1981). These *mec* genes encode a transcription factor with a LIM-type homeodomain (MEC-3), an RNA processing factor (MEC-8), extracellular matrix proteins (MEC-1, MEC-5, and MEC-9), microtubule proteins (MEC-7 / $\beta$ -tubulin and MEC-12/ $\alpha$ -tubulin), DEG/ENaC proteins (MEC-4 and MEC-10), a stomatin-like protein (MEC-2), a paraoxonase-like protein (MEC-6), a F-box protein implicated in protein degradation pathway (MEC-15; Bounoutas et al., 2009b), a tubulin acetyltransferase (MEC-17; Topalidou et al., 2012), a luciferase and coA ligase-like protein

(MEC-18), and a protein similar to the shaker-type K<sup>+</sup> channel  $\beta$ -subunit (MEC-14; Chalfie et al., unpublished work).

### **DEG/ENaC mechanosensory channel**

Among those 15 MEC proteins, four membrane proteins are necessary for the function of the mechanotransduction channel complex, which can produce amiloride sensitive Na<sup>+</sup> current in response to mechanical stimuli (O'Hagan et al., 2005). These proteins include two pore-forming subunits MEC-4 and MEC-10 (DEG/ENaC proteins), MEC-2 (a stomatin-like protein), and MEC-6 (a paraoxonase-like protein) (Chelur et al., 2002; Goodman et al., 2002).

Although both MEC-4 and MEC-10 form the pore of the mechanosensory channel (more details in Section A), MEC-4 plays a major role in the channel function while MEC-10 plays a relatively minor role. First, the null mutations of *mec-4* and *mec-10* produce different effects on touch sensitivity. *mec-4* null mutation completely eliminated touch sensitivity and the mechanoreceptor current (MRC) in worms (O'Hagan et al., 2005). In contrast, a *mec-10* deletion that is considered to be a null mutation reduced the touch response by 40% and the MRC peak amplitude by 25% in vivo (Arnadottir et al., 2011). Second, their gain-of-function (d) mutations that encode amino acid substitutions produce different effects. In *Xenopus* oocytes, MEC-4(d) alone forms the hyperactive channel that produces Na<sup>+</sup> selective and amiloride inhibited currents (similar to the in vivo MRC), whereas MEC-10(d) alone is inactive, and modestly reduces the MEC-4(d) current amplitude when co-expressed with MEC-4(d) (Brown et al., 2007; Chelur et al., 2002; Goodman et al., 2002). In vivo, *mec-4(d)* induces over 90% TRN degeneration and its toxicity does not require *mec-10* (Driscoll and

Chalfie, 1991), whereas *mec-10(d)* causes only 30% TRNs death and its toxicity requires *mec-4* (Huang and Chalfie, 1994).

MEC-10 has only modest effects on the physical properties of the channel. MEC-10 does not affect the single channel conductance both in vivo and in vitro (Arnadottir et al., 2011; Brown et al., 2008). Loss of MEC-10 did not affect the MRC responses to varying stimulus pressure, suggesting MEC-10 is not involved in gating (Arnadottir et al., 2011). Loss of MEC-10 modestly altered channel kinetics, resulting in an MRC with slower activation and adaptation (Arnadottir et al., 2011). Moreover, MEC-10 has no effect on MEC-4 distribution and expression on the plasma membrane either in vivo or in vitro (Arnadottir et al., 2011; Goodman et al., 2002). Probably, MEC-10 plays a modulatory role in the MEC-4/MEC-10 mechanosensory channel.

Several experiments suggest that MEC-6 and MEC-2 play different roles in the mechanosensory channel. First, MEC-2 and MEC-6 act synergistically to increase MEC-4(d) activities in *Xenopus* oocytes, suggesting that they function in parallel (Goodman et al., 2002). Second, MEC-2 reduces amiloride K<sub>i</sub> and increases the single channel conductance of MEC-4(d) by 30% in *Xenopus* oocytes; whereas MEC-6 has no effect on channel properties (Brown et al., 2008; Goodman et al., 2002). Third, MEC-6 is required for MEC-4 channel localization, whereas MEC-2 punctate distribution requires MEC-4 and MEC-6 (Chelur et al., 2002; Zhang et al., 2004), suggesting MEC-2 and MEC-6 may act downstream and upstream of the MEC-4/MEC-10 channel respectively. Because MEC-2 associates with the inner leaflet of lipid bilayer, and can bind to cholesterol, it may regulate the lipid environment surrounding the transduction channel and contribute to the channel gating. This hypothesis is supported by experiments that disrupting MEC-2 binding to cholesterol reduced the touch sensitivity in

animals (Huber et al., 2006). In contrast, MEC-6 functions, at least in part, through regulating MEC-4 channel localization.

### **The model of DEG/ENaC mechanosensory channel**

Several experiments suggested that MEC-2, its similar protein UNC-24, and MEC-6 were the auxiliary subunits of the mechanosensory channel. First, MEC-2 and MEC-6 are essential for the production of MRC in vivo (the role of UNC-24 is not tested) (O'Hagan et al., 2005). Second, MEC-2 and MEC-6 dramatically increased the whole cell current of MEC-4(d) when expressed in *Xenopus* oocytes, without apparently increasing the amount of surface localized MEC-4(d) in a biotinylation assay (Brown et al., 2008; Chelur et al., 2002; Goodman et al., 2002); UNC-24 reduced the MEC-4(d) current amplitude by 30% (Zhang et al., 2004). Third, MEC-2 and MEC-6 co-immunoprecipitated with MEC-4(d), MEC-10, and each other in *Xenopus* oocytes or CHO cells (Chelur et al., 2002; Goodman et al., 2002; Zhang et al., 2004); while UNC-24 co-immunoprecipitated with MEC-2 and MEC-4(d) in *Xenopus* oocytes (Zhang et al., 2004). Fourth, MEC-2 (detected by the MEC-2 antibody) and MEC-6::FLAG (detected by the FLAG antibody) formed discrete puncta in the TRN process, which appeared to colocalize with MEC-4::YFP (Chelur et al., 2002; Zhang et al., 2004); UNC-24::GFP co-localized with MEC-2 puncta (Zhang et al., 2004).

This mechanotransduction complex model (MEC-4/10, MEC-2, MEC-6, and UNC-24) is possible but not proven. No sufficient evidence supports that these MEC proteins complex together. The co-immunoprecipitation only suggests these proteins have physical interaction in the whole cells, which can be transient; the co-localization of these proteins within puncta



along the TRN process is acquired by the conventional light microscopy rather than the single molecule imaging, and thus, does not necessarily indicate that these proteins complex together.

Several experiments also raise doubts about this model. First, MEC-10 puncta have not been detected in the TRN process (Chatzigeorgiou et al., 2010). Second, the function of the puncta was questioned by the *in vivo* electrophysiological studies (O'Hagan et al., 2005), which estimated that the amount of functional channel was similar to the number of puncta in the TRN process. The single channel should not be visible in previous experiments, so most proteins localized to the puncta are probably inactive. Third, loss of MEC-6 eliminated MEC-4::YFP puncta in the TRN process, but had no effect on MEC-4 surface expression in *Xenopus* oocytes (Chelur et al., 2002).

### **Other proteins that regulate the DEG/ENaC mechanosensory channel function**

The proper function and localization of the DEG/ENaC mechanosensory channel also requires extracellular matrix (ECM) proteins (MEC-1, MEC-5, and MEC-9) and 15-protofilament microtubules (MEC-7/ $\beta$ -tubulin and MEC-12/ $\alpha$ -tubulin). ECM proteins are essential for the MEC-4 channel localization in the neuronal process, because loss of any of these proteins eliminated the MEC-4 puncta (Emtage et al., 2004). The TRN specific 15-protofilament microtubules have general roles in gene expression and intracellular transport of TRNs. Microtubule disruption caused by mutations or colchicine treatment eliminated MEC-2 punctate distribution in the TRN process (Bounoutas et al., 2011; Bounoutas et al., 2009a). In addition, the 15-protofilament microtubules also play specific roles in mechanosensation, perhaps by providing the rigidity for TRNs (Bounoutas et al., 2009a).

The previous microarray experiment identified two additional membrane proteins that may regulate the function of the MEC-4/MEC-10 transduction channel (Topalidou and Chalfie, 2011). POML-1::GFP fusion (originally called K11E4.3) formed discrete puncta along the TRN process; *poml-1* mutation resulted in very mild defects in touch sensitivity. C49G9.1::GFP fusion was detected in TRNs, FLP, and PVD, and appeared to co-localize with MEC-2 in the TRN process (Topalidou and Chalfie, 2011).

## **Section C: Structure and Function of DEG/ENaC proteins**

### **DEG/ENaC channels are found in many species**

Degenerin and epithelial Na<sup>+</sup> channels (DEG/ENaC) form amiloride sensitive and Na<sup>+</sup> selective channels. DEG/ENaC can be divided into four groups: *C. elegans* degenerins (Driscoll and Chalfie, 1991), mammalian ENaCs (Canessa et al., 1993; Lingueglia et al., 1993), the acid-sensing ion channels (ASICs; Waldmann et al., 1997), and FMRFamide-gated channels (FNaC) found in snail and *Aplysia* (Furukawa et al., 2006; Lingueglia et al., 1995).

DEG/ENaC proteins are found in invertebrates and vertebrates, but not in yeast and bacteria (Mano and Driscoll, 1999). Invertebrates have a larger number of DEG/ENaC proteins: the *C. elegans* genome encodes 30 DEG/ENaC proteins; the *Drosophila* genome encodes 31 DEG/ENaC-like proteins (Ben-Shahar, 2011). Mammalian genomes encode three ENaC proteins (ENaC  $\alpha$ ,  $\beta$ ,  $\gamma$ ) and at least six ASIC (also called ACCN) proteins (ASIC-1a, 1b, 2a, 2b, 3, 4) from four genes loci (Ben-Shahar, 2011; Wemmie et al., 2013).

DEG/ENaC channels can be activated by mechanical force (O'Hagan et al., 2005), low extracellular pH (Waldmann et al., 1997), and peptides (Lingueglia et al., 1995). ENaC is constitutively open (Canessa et al., 1993; Lingueglia et al., 1993). DEG/ENaC proteins have a wide range of functions, e.g. mechanosensation, sour and sodium taste detection, peripheral pain, synaptic plasticity, learning and memory, and Na<sup>+</sup> homeostasis.

### **Sensory functions of DEG/ENaC proteins**

## **Mechanosensation**

After studies in *C. elegans* first identified degenerin proteins, MEC-4 and MEC-10, as pore-forming subunits of the mechanotransducers in the TRNs (Arnadottir et al., 2011; Chalfie and Sulston, 1981; O'Hagan et al., 2005), more DEG/ENaC proteins were found to be involved in mechanosensation. DEG-1 has been shown to be the major mechanosensory channel in the *C. elegans* nociceptor, ASH neuron (Geffeney et al., 2011). UNC-8 and UNC-10 are potential mechanosensitive channels, but have not been confirmed by experiments yet. UNC-8 was proposed to act as a mechanosensitive channel that regulate locomotion in *C. elegans*, because UNC-8 was expressed in sets of motor neurons that were thought to sense body stretch, and *unc-8* null mutation produced severe locomotion defects (Tavernarakis et al., 1997). UNC-105 may be a mechanosensitive protein in muscles, and its hyperactivation caused hypercontraction of muscle (Liu et al., 1996).

A couple of *Drosophila melanogaster* DEG/ENaC proteins have been shown to be required for mechanosensation. *Drosophila* pickpocket (*ppk*) is essential for the mechanical nociception in larvae, because mutation or RNAi knock down of this gene reduced the larvae's response to harsh mechanical stimuli without affecting the general physiology of the nociceptive neurons (Zhong et al., 2010). *Drosophila* *ppk28* mediates water detection, likely through sensing mechanical tension in membrane caused by changes in external osmolarity (Cameron et al., 2010; Chen et al., 2010).

Mammalian ASICs also contribute to mechanosensation but may not function as the transducers. ASICs are abundant in the peripheral sensory neurons, including cutaneous mechanoreceptors (Meissner corpuscles, Lanceolate endings, Merkel cell complex, and Ruffini endings), proprioceptors of the muscle, nociceptors, arterial baroreceptors, gastric

DRG neurons, suburothelium nerve complex of bladder, and vestibular ganglia (Chen and Wong, 2013). ASICs may modulate rather than mediate mechanosensation in the skin, because knocking out ASIC2 and 3 caused only subtle and controversial effects on mechanosensation in behavioral and electrophysiological assays (Chen and Wong, 2013; Drew et al., 2004; Price et al., 2001; Roza et al., 2004), and transgenic expression of a dominant-negative ASIC3 subunit, which eliminates all ASIC channel activities, led to increased mechanosensitivity (Mogil et al., 2005). In contrast to the weak modulatory effects on skin mechanosensation, ASIC2 is required for the mechanosensory function of arterial baroreceptors. The ASIC2 knockout mice developed hypertension, baroreceptor neurons isolated from ASIC2 null mice showed reduced membrane depolarization upon mechanical stimuli than WT neurons, and baroreceptor neurons overexpressing ASIC2a had increased mechanically-induced membrane depolarization (Lu et al., 2009). Further investigation needs to verify the role of ASIC2 as a component of the mechanotransducer in baroreceptors.

### **Chemosensation - sodium and acid**

Studies in *Drosophila* and mice have suggested that DEG/ENaC proteins mediate the taste of sodium salt in taste-receptor neurons. Disrupting two DEG/ENaC genes *ppk11* and *ppk19* reduced flies' response to low concentrations of KCl and NaCl, but had no effect on other taste modalities (Liu et al., 2003). ENaC $\alpha$  knockout mice completely lost sodium taste responses, suggesting an essential role of ENaC in mammalian sodium taste (Chandrashekar et al., 2010).

ASICs can be activated by lower extracellular pH (Waldmann et al., 1997; Wemmie et al., 2006), but their role in mammalian sour taste detection is unclear. Rat taste bud cells

express ASIC2 (ASIC2a and ASIC2b), and produce a current that is predominantly carried by  $\text{Na}^+$  and can be partially suppressed by amiloride (very similar to the ASIC2 current in vitro), suggesting a role of ASIC2 in sour perception (Lin et al., 2002; Ugawa, 2003; Ugawa et al., 1998). However, studies in mice challenged the potential role of ASICs as the universal sour taste receptors in mammals: gene expression of ASIC1 and ASIC3, but not ASIC2, was detected in mice; ASIC2 knockout mice had normal acid-evoked  $\text{Ca}^{2+}$  response (Richter et al., 2004). These conflicting results suggest that multiple receptors exist in mammals, and different species utilize different receptors to perceive sour taste. Indeed, polycystic kidney disease (PKD) related protein, PKD2L1 (TRP channel), has been identified as the sour taste receptor in mice (Chandrashekar et al., 2009; Huang et al., 2006; Kataoka et al., 2008; Nelson et al., 2010). Both ASICs and PKD proteins may contribute to human sour taste perception, because two sour ageusia (inability to detect low pH in ingested food) patients were found to have reduced gene expression of ASICs (ASIC1a, 1b, 2a, 2b, and 3) and PKD channels (PKD2L1 and 1L3) (Huque et al., 2009).

Two *C. elegans* DEG/ENaC proteins are required for acid sensation. ACD-1 (acid-sensitive channel), in parallel with DEG-1, mediates acid avoidance and chemotaxis to amino acid lysine (Wang et al., 2008; Wang and Bianchi, 2009).

### **Peripheral pain**

All ASICs except ASIC4 are expressed in DRG nociceptive neurons, but their roles in mediating acid-induced pain appear to be controversial based on studies from different species. Genetically disrupting ASIC3, whose homomeric channel is most sensitive to pH among all ASIC channels and can be potentiated by several inflammatory molecules, resulted

in mice that had increased response to acidic stimuli (Mogil et al., 2005; Price et al., 2001). In contrast, pharmacological inhibition and genetic knock down of ASIC3 reduced acid-induced pain in humans and rats (Deval et al., 2010; Ugawa et al., 2002).

### **ASICs in the central nervous system (CNS)**

ASICs also detect protons produced by acidic neurotransmitter release, metabolism, and diseases in the CNS, and are implicated in synaptic plasticity, learning and memory, neuronal injury and neurological diseases (Wemmie et al., 2013). ASIC1a, ASIC2a and ASIC2b are all expressed in CNS, but only ASIC1a is required.

Several studies suggested that ASIC1a is an essential component of the H<sup>+</sup>-gated channel that regulates synaptic plasticity. First, ASIC1a is abundant in brain regions with high synaptic density, and is localized to dendritic synapses (Wemmie et al., 2003). Second, ASIC1a is essential for the acid-evoked currents that are predominantly carried by Na<sup>+</sup> and are also permeable to Ca<sup>2+</sup> (similar to ASIC1a currents in a heterologous system) in hippocampal, amygdala, and cortical neurons (Wemmie et al., 2003; Wemmie et al., 2002; Xiong et al., 2004). Third, ASIC1a increases the density of dendritic spines in hippocampal slices, through the H<sup>+</sup>-evoked intracellular Ca<sup>2+</sup> increase and downstream CaMKII phosphorylation (Zha et al., 2006). Fourth, consistent with the physiological studies, ASIC1 knockout mice showed impaired long-term potentiation in hippocampus, and exhibited deficits in several learning behaviors that depend on hippocampus, cerebellum, and amygdala (Wemmie et al., 2003; Wemmie et al., 2002).

ASICs are also implicated in neuronal injury and neurological diseases, e.g. ischemic stroke, multiple sclerosis, Huntington's disease, Parkinson's disease, spinal cord injury, and epilepsy (Wemmie et al., 2013; Xiong et al., 2004). These diseases and their related metabolic stress induce local acidosis, which results in hyperactivation of ASIC1a and causes brain injury. Pharmacological blockade of ASIC1a can protect against the acidification-induced neuronal injury (Xiong et al., 2004).

### **ENaC and Na<sup>+</sup> homeostasis**

ENaC is responsible for Na<sup>+</sup> reabsorption on several epithelial tissues, including distal kidney nephron, distal colon, urinary bladder, and lung, and thus, plays a crucial role in regulating Na<sup>+</sup> balance, blood volume and pressure (Schild, 2010). ENaC comprises three homologous subunits  $\alpha$ ,  $\beta$ , and  $\gamma$ , which share 30-40% identical amino acid sequence. Among the three homologues, only the  $\alpha$  subunit is able to form functional homomeric channels and is essential for the ENaC activities, whereas the  $\beta$  and  $\gamma$  subunits allow the maximal channel expression and activities on the plasma membrane (Canessa et al., 1994). A fourth subunit  $\delta$  has been found to assemble with  $\alpha$ ,  $\beta$ , and  $\gamma$  subunits in lung epithelial cells, and alter several channel properties, such as cation selectivity, amiloride inhibition, proton activation, and self inhibition time (Ji et al., 2006). Activation of ENaC needs the proteolytic cleavage of the extracellular loops of  $\alpha$  and  $\gamma$  subunits by furin and other proteases, which can occur both along secretory pathways and on the plasma membrane (Carattino et al., 2008; Hughey et al., 2007; Kleyman et al., 2009). Similar activation by proteases was also observed in MEC-4(d) channels expressed in *Xenopus* oocytes (Brown et al., 2008).



Because ENaCs play crucial roles in regulating Na<sup>+</sup> balance and blood pressure, their expression and activities need to be tightly regulated. Apical expression of ENaC is largely regulated through ubiquitination and subsequent retrieval from the apical surface. Specifically, the E3 ubiquitin ligase, Nedd4-2, binds to PPxY motifs in the C-terminus of ENaC  $\alpha$ ,  $\beta$ , and  $\gamma$  subunits and mediates the ubiquitination of lysine residues in the N-terminus of ENaC proteins. Mutations affecting Nedd4-2 and ENaC interaction lead to increased ENaC surface expression and hypertension in Liddle syndrome (Goulet et al., 1998; Hansson et al., 1995a; Hansson et al., 1995b; Shimkets et al., 1994; Snyder, 2002; Staub et al., 1996). The ubiquitinated ENaC is internalized through clathrin-mediated endocytosis. Most internalized ENaCs are destined for either endosomes or lysosomes for degradation, but a small number of proteins can be deubiquitinated and routed to a cycling compartment (early endosome and/or recycling endosome) to return to the apical surface.

Multiple hormones and kinases can regulate the activities and expression of ENaC proteins, at least in part, through Nedd4-2 mediated ubiquitination. Several hormones (e.g. aldosterone and vasopressin) regulate ENaC expression at the apical membrane through ENaC trafficking and recycling (Loffing and Korbmacher, 2009). ENaC expression is mainly up-regulated by aldosterone in kidney, which increases both protein insertion (rapid process) to the apical membrane and gene transcription (slow process) and also inhibits ENaC degradation (Loffing et al., 2001). Part of the above hormonal regulation is mediated by their downstream kinases (e.g. aldosterone and insulin induced kinase SgK1, PI3K, and Akt). These kinases phosphorylate ENaC  $\alpha$  subunit (Diakov and Korbmacher, 2004; Staruschenko et al., 2007) to increase the ENaC open probability. Moreover, these kinases phosphorylate Nedd4-2 to inhibit Nedd4-2 binding to ENaC and thus increase ENaC surface expression (Lee

et al., 2007; Snyder et al., 2004). Several other kinases, including G protein-coupled receptor kinase, Grk2 (Dinudom et al., 2004), protein kinases A and C (Shimkets et al., 1998), extracellular regulated kinase (Shi et al., 2002a; Shi et al., 2002b), and Casein kinases 2 (Shi et al., 2002b), have also been reported to mediate phosphorylation of the C-termini of ENaC  $\beta$  and  $\gamma$  subunits, and regulate ENaC/Nedd4-2 interaction.

Moreover, self-inhibition of ENaC by  $\text{Na}^+$  provides a negative feedback loop to control  $\text{Na}^+$  absorption (Turnheim, 1991). Extracellular  $\text{Na}^+$  rapidly reduces channel open probability (Bize and Horisberger, 2007; Volk et al., 2004). In contrast, intracellular  $\text{Na}^+$  decreases channel surface expression and open probability in a slower manner (Anantharam et al., 2006).

### **Gain of function mutations of *C. elegans* degenerin**

Gain of function (d) mutations of *C. elegans* degenerin genes encode hyperactive channels that can lead to necrosis-like cell death [*mec-4* (Driscoll and Chalfie, 1991; Goodman et al., 2002), *mec-10* (Huang and Chalfie, 1994), *deg-1* (Chalfie and Wolinsky, 1990; Garcia-Anoveros et al., 1995), *unc-8* (Shreffler et al., 1995; Tavernarakis et al., 1997; Wang et al., 2013)], or muscle hypercontraction [*unc-105* (Garcia-Anoveros et al., 1998; Park and Horvitz, 1986)]. Cells expressing degenerin with the d mutations accumulate membranous whorls and cytoplasmic vacuoles, swell to several times of their original size, and often die (Hall et al., 1997).

The d mutations usually result in the substitution of large-side chain amino acids (e.g. Thr, Val, and Leu) for Ala or Gly at either the pore forming domain preceding the second

transmembrane segment (A713T in MEC-4, A707T in DEG-1, A692V in UNC-105, A673V in MEC-10) or the extracellular regions (A404V in MEC-4, A393V in DEG-1, P134S in UNC-105, G387E and A586T in UNC-8) (Brown et al., 2007; Garcia-Anoveros et al., 1998; Driscoll and Chalfie, 1991; Tavernarakis et al., 1997; Garcia-Anoveros et al., 1995; Huang and Chalfie, 1994). The residual substitution interferes with gating, locking the DEG/ENaC channel in a constitutively open state (Brown et al., 2007; Garcia-Anoveros et al., 1998; Wang et al., 2013). Unlike the sequence containing the d position on the extracellular loop (Garcia-Anoveros et al., 1995), which is specific to *C. elegans*, the region containing the d position near the second transmembrane domain is highly conserved (Brown et al., 2007). Indeed, a similar mutation also activates mammalian ASIC1 (also called BNaC2) and ASIC2 (also called MDEG and BNaC1) and *Drosophila* PPK, leading to cell death (Adams et al., 1998; Bassilana et al., 1997; Waldmann et al., 1996).

The neuronal degeneration induced by the d mutations affecting DEG/ENaC proteins (MEC-4, DEG-1, and UNC-8) requires calreticulin (a Ca<sup>2+</sup> binding chaperone in the ER) and intracellular Ca<sup>2+</sup> increase due to the release of Ca<sup>2+</sup> from the ER (Xu et al., 2001). The hyperactive DEG/ENaC channels are permeable to Ca<sup>2+</sup>, and may also contribute to the intracellular Ca<sup>2+</sup> increase (Bianchi et al., 2004; Brown et al., 2008; Xu et al., 2001). Moreover, the d mutation induced neurodegeneration also requires MEC-6 (Chalfie and Wolinsky, 1990; Garcia-Anoveros et al., 1995; Harbinder et al., 1997; Shreffler et al., 1995), which is needed for MEC-4 channel localization (Chelur et al., 2002).

### **Structure and stoichiometry of DEG/ENaC proteins**

DEG/ENaC proteins have a simple topology (Figure I-2): two short intracellular N and C-termini, two transmembrane helices (TM1 and TM2), and a large extracellular region, which contains two cysteine rich domains (CRD); while *C. elegans* degenerin proteins have one additional CRD and extracellular regulatory domain (ERD) (Lai et al., 1996; Sherwood et al., 2012). The two transmembrane helices, the sequence preceding them, and CRDIII are particularly important for gating and ion conductance of the MEC-4/MEC-10 mechanosensory channel, because most *mec-4* missense mutations and all of the *mec-10* missense mutations that alter ion selectivity are located on these regions (Arnadottir et al., 2011; Hong et al., 2000).

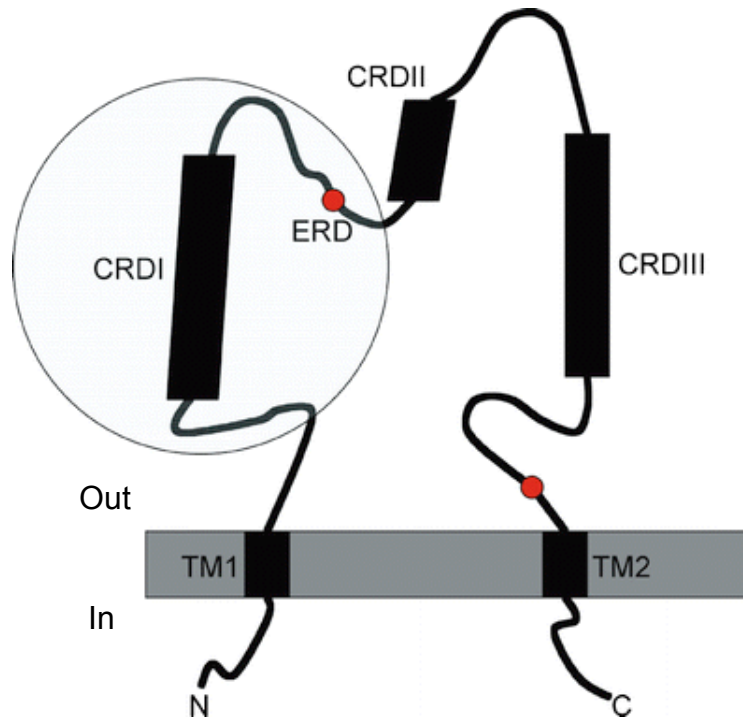


Figure I-2. Diagram of the conserved domains in DEG/ENaC channels (from Bounoutas and Chalfie, 2007). The CRDI and ERD (in shaded circle), is only found in *C. elegans* degenerated mutations in the ERD and preceding TM2 (in red), can produce hyperactivate channel and cause neurodegeneration. In indicates inside the cell; out indicates outside the cell. Domains are not drawn in proportion to the real size.

The first crystal structure of a DEG/ENaC protein, chick ASIC, provides a structural basis for the stoichiometry and subunit-subunit interaction (Jasti, et al., 2007). First, ASIC is trimeric (Figure I-3A). Second, in each subunit, the extracellular region resembles a clenched hand and contains multiple domains that represent palm,  $\beta$ -ball, knuckle, finger, and thumb (Figure I-3B). The two conserved CRDs are located at palm,  $\beta$ -ball, and thumb domains. The intracellular termini were not seen in crystal structure, probably because they do not form an ordered structure. Third, in the trimeric channel, each subunit interacts extensively with the other two between the two transmembrane helices, the palm domains, and the palm domain of

one subunit and the thumb domain belonging to the other. Weak interaction between subunits also exists between knuckle and finger domains, and palm domain and  $\beta$ -ball domain.

The ASIC1 structure also suggests mechanisms about how the *mec-4* and *mec-10* mutations affect ion selectivity or gating. Both TM1 and TM2 define the interior pore, but TM2 makes the predominant contribution, consistent with the fact TM2 harbors most point mutations that alter ion selectivity and gating. Gly 435, equivalent to the d position whose mutation into bulky residues results in hyperactive degenerin channels and neurodegeneration in *C. elegans*, resides on TM2, facing the TM1 of the adjacent subunit. It suggests that d mutations produce hyperactive channels through disrupting gating.

The snake toxin bound open state of the ASIC channel reveals more details about its pore architecture and ion selectivity (Baconguis, et al, 2014). The second transmembrane is discontinuous, and makes a turn at Gly-Ala-Ser, allowing the one third cytoplasmic TM2 of one subunit to swap with that of the other subunit within the trimer (Figure I-3C). The Gly-Ala-Ser peptide each adopts a belt-like conformation aligning nearly parallel to the membrane plane. The GAS belts from three subunits form triangular rings and define the selectivity filter with a radius of 3.6 Å (Figure I-3C), matching the size of hydrated  $\text{Na}^+$  (3.8 Å) and hydrated  $\text{Li}^+$  (3.5 Å). It provides structural basis for the DEG/ENaC proteins high permeability for  $\text{Na}^+$  and  $\text{Li}^+$ , and also suggests that DEG/ENaC adopts a barrier mechanism for ion selectivity. The open ion channel pore is lined with carbonyl oxygen atoms of Gly 436, 439, 443, Thr 448, and Glu 451. All of these residues are highly conserved among DEG/ENaC proteins, and their mutations in MEC-4 and MEC-10 disrupt touch sensitivity in *C. elegans* (Eastwood and Goodman, 2012), suggesting other DEG/ENaC proteins may also have the similar ion pore structures and ion selectivity mechanism.

Comparing the desensitized state and the open state of the ASIC channels suggests the structural domains that are crucial for ASICs gating (Baconguis and Gouaux, 2012; Baconguis, et al., 2014). Superimposition of the desensitized and the toxin bound open state channel indicates that the upper palm and knuckle domains have the same conformation, which may comprise the rigid structural scaffold. Relative to the desensitized state, the lower palm flexes and undergoes conformational changes. The toxin forms extensive interactions with the thumb, palm, and wrist domains, suggesting that these regions may play major roles in channel gating. On the basis of ASIC structures, the channel gating may involve conformational changes to varying extent of the flexible domains of thumb, finger, lower palm, and wrist, which lead to the rotation and tilt of the transmembrane helices and the opening of the channel pore (Baconguis, et al., 2012; Figure I-4).

The mechanical gating mechanism of MEC-4 and MEC-10 still remains elusive. If they adopt a gating mechanism similar to that of ASICs, it would suggest that the gating initiates from the extracellular domains, and transduces into the transmembrane helices, favoring the previous tethered model over the membrane force model.

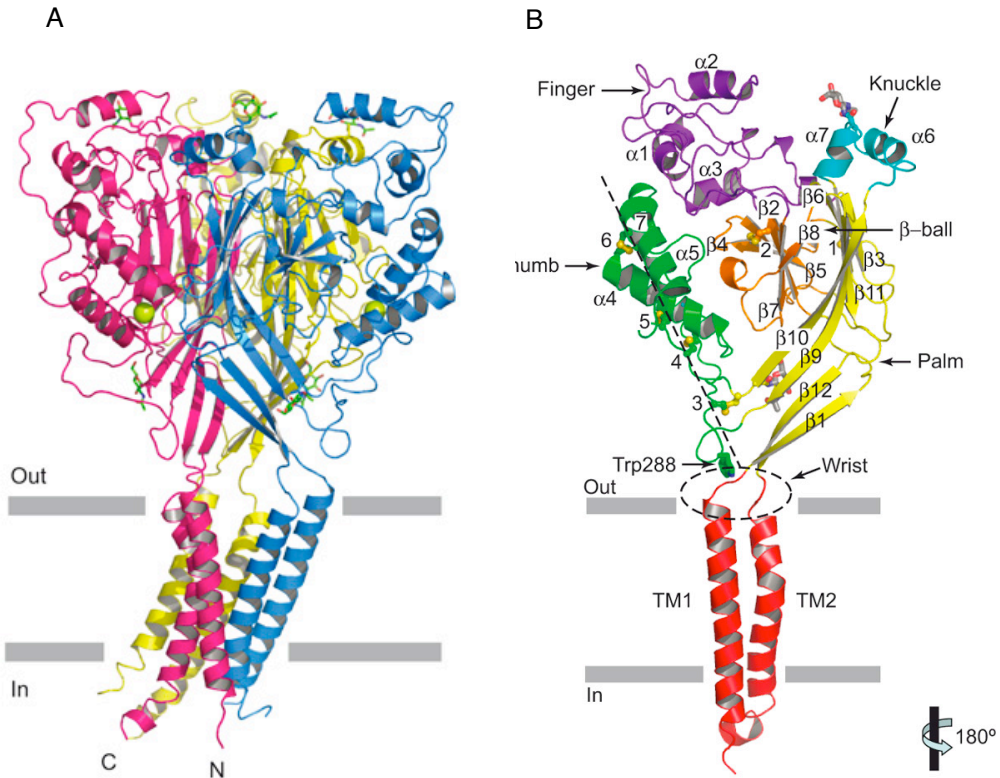
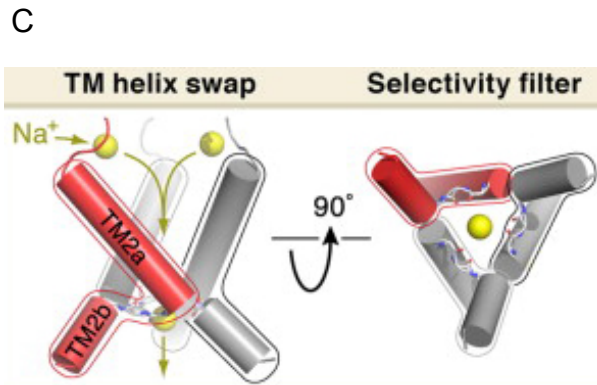


Figure I-3. Crystal structure of chick ASIC1 protein (A and B are adapted from Jasti et al., 2007). (A) Homotrimeric ASIC1. Three subunits are indicated in red, yellow and blue. (B) Domain organization of one subunit. (C) Swapping of transmembrane helix and the selectivity filter (from Bacongus et al., 2014).





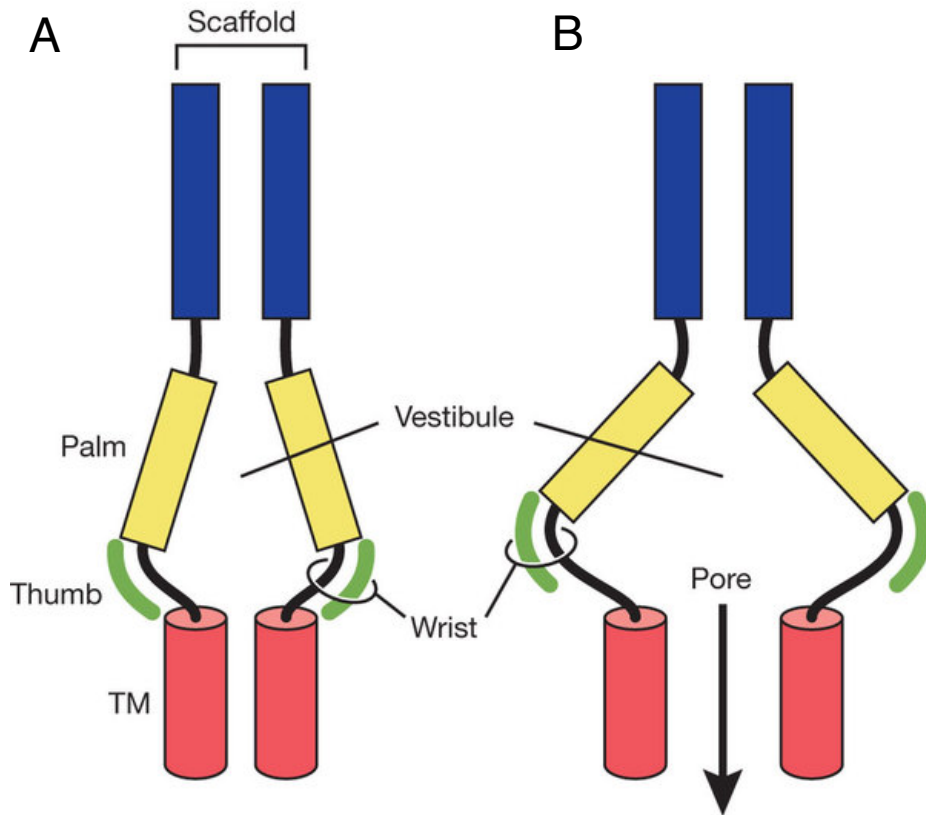


Figure I-4. The gating model of the ASIC channel (adapted from Bacongus and Gouaux, 2012). A, The closed and desensitized state conformation. B, The open state conformation.

Although several experiments suggested that functional DEG/ENaC channels consisted of four, eight, or nine subunits (Coscoy et al., 1998; Eskandari et al., 1999; Firsov et al., 1998; Snyder et al., 1998), the crystal structure of the chick ASIC channel provides the most convincing evidence that DEG/ENaC is trimeric. Additionally, fluorescence intensity ratio analysis also suggested that ENaC  $\alpha\beta\gamma$  prefer to form heteromeric channels containing an equal number of each subunit when co-expressed in COS-7 cells (Staruschenko et al., 2005). Consistent with the chick ASIC structure, this thesis reports that MEC-4 and MEC-10

also form trimeric channels (MEC-4<sub>3</sub> or MEC-4<sub>2</sub>MEC-10) in *Xenopus* oocytes, with preference for MEC-4<sub>2</sub>MEC-10 when co-expressed.

DEG/ENaC proteins can form both homomeric and heteromeric channels. Only some DEG/ENaC proteins can form functional homomeric channels, while other subunits contribute to heteromeric channels and modulate channel activities. For example, among ENaC  $\alpha$ ,  $\beta$ , and  $\gamma$ , only  $\alpha$  subunit can form functional channels, while the  $\beta$  and  $\gamma$  subunits regulate channel expression and activities on the plasma membrane (Canessa et al., 1994). Among the six ASICs (1a, 1b, 2a, 2b, 3 and 4), four of them can form functional homomeric channels with different desensitization rate and pH sensitivity in heterologous systems (ASIC1a,  $\text{pH}_{0.5} = 6.2$ ; ASIC1b,  $\text{pH}_{0.5} = 5.9$ ; ASIC2a,  $\text{pH}_{0.5} = 4.4$ ; ASIC3,  $\text{pH}_{0.5} = 6.5$ ;  $\text{pH}_{0.5}$  indicates pH of half-maximal activation); ASIC2b and ASIC4 are pH insensitive by themselves (Wemmie et al., 2006; Wemmie et al., 2013). But ASIC2b has been reported to associate with other ASICs and modulate the channel activities, e.g. inactivation kinetics and peak current amplitude (Lingueglia et al., 1997). Different ASICs are expressed in different neurons: ASIC1a, 2a, 2b, and 4 in central nervous system and ASIC1a, 1b, 2a, 2b, and 3 in peripheral nervous system (Wemmie et al., 2013).

Similar to other DEG/ENaC proteins, this thesis reports that MEC-4 alone can form homotrimers in *Xenopus* oocytes; MEC-10 incorporates into the heterotrimer MEC-4<sub>2</sub>MEC-10 channel in *Xenopus* oocytes. MEC-10 is also expressed in other two types of mechanosensory neurons, FLP and PVD, and may contribute to other DEG/ENaC channels complex. These studies suggest that combination of different subunits could produce diverse receptors in different neuronal populations.

## Section D: Paraoxonase (PON)

### **PONs are multifunctional enzymes with protective activities**

Paraoxonases (PONs) are a family of enzymes with a wide range of activities, including deoxidization of lipids and detoxification of organophosphates. Human and mice have three PON proteins, PON1, PON2, and PON3 (Primo-Parmo et al., 1996). These three proteins share approximately 60% sequence identity. PONs exhibit enzymatic activities of arylesterases, paraoxonases, and lactonases (Draganov et al., 2005; Khersonsky and Tawfik, 2005; Rodrigo et al., 2003; Rosenblat et al., 2003; Smolen et al., 1991). Although this protein family is named as paraoxonase, only PON1 has paraoxonase activity. PON1 is capable of hydrolyzing toxic organophosphates, including pesticide products, such as paraoxon, diazoxon, chlorpyrifos oxon, and even neurotoxins such as sarin and soman (Davies et al., 1996; Smolen et al., 1991). All three PONs, however, have lactonase activity (Draganov et al., 2005). In vitro evidence suggests that the lactonase activity may enable human and mouse PONs to hydrolyze and therefore inactivate acyl-homoserine lactones, which are quorum-sensing signals of some pathogenic bacteria (e.g., *Pseudomonas aeruginosa*) (Chun et al., 2004; Estin et al., 2010).

Studies in the past twenty years have demonstrated a relationship of the PONs to the risk of atherosclerosis. PON1 associates with high density lipoprotein (HDL), and is needed for two key HDL activities: inhibition of lipid oxidation in low density lipoprotein (LDL) and mediation of cholesterol efflux (Lund-Katz et al., 2003), such as from macrophage foam cells in atherosclerotic lesions. In vitro data suggests that the anti-atherogenic property of PON1 is

related to its lipolactonase activities, by hydrolyzing oxidized lipids (Rosenblat et al., 2006). PON2 and PON3 also protect against atherosclerosis. Like PON1, human PON3 is primarily expressed in the liver and secreted into the plasma, where it associates with HDL particles and prevents atherosclerosis (Aviram and Rosenblat, 2004; Mackness et al., 1993; Reddy et al., 2001). Similarly, PON2 also exhibits anti-atherogenic ability by reducing oxidized lipids in LDL and macrophage (Ng et al., 2001).

PON2 and PON3 also exhibit anti-oxidative effects in various tissues and can protect against cell death. In contrast to PON1, PON2 (human and mouse) and mouse PON3, are not detected in HDL, but are widely expressed in many tissues, such as liver, adipose, and macrophage (Shih et al., 2010). PON2 and PON3 are expressed on the mitochondrial membrane; they interact with coenzyme Q10 and protect against cell death by reducing mitochondrial superoxide formation in several human cell lines (Altenhofer et al., 2010; Schweikert et al., 2012). The anti-oxidative effects appear to be independent of their enzymatic activities, because the point mutations that abolish the lactonase activity of PON2 have no effect on its anti-oxidative or anti-apoptotic function (Altenhofer et al., 2010). Moreover, PON2 and PON3 are present in the endoplasmic reticulum (ER), increase their expression upon ER stress caused by unfolded proteins, and reduce the ER stress induced apoptosis (Horke et al., 2007; Schweikert et al., 2012). However, their function and mechanism in the ER is not understood.

Despite the extensive research on mammalian PONs, the physiological roles and native substrates of PONs still remain elusive. Even for their well-studied anti-atherogenic function, the mechanism still remains debated.

## The PONs in *C. elegans*

PON-like proteins have been identified from many species, including nematode (Chelur et al., 2002). In addition to MEC-6, the *C. elegans* genome also encodes four more PON-like proteins, which we have renamed POML (paraoxonase and mec-6-like): POML-1 (K11E4.3), POML-2 (E01A2.7), POML-3 (E01A2.10), and POML-4 (K05F6.11). All of the five PON-like proteins have a 13-amino acid sequence that is only found in *C. elegans*, right after the predicted transmembrane domain. POML-2, POML-3, and POML-4 are more closely related because their sequences are over 60% identical to each other; POML-3 and POML-4 are 98% identical, and may arise from gene duplication. In contrast, MEC-6 and POML-1 share only 20-30% identical sequence to that of the other three POMLs and each other.

*C. elegans* PON-like proteins share 20-30% identical sequence with human PONs over the conserved C-terminal domain (Figure I-4), but they resemble human PONs more in the overall structure. For example, all the *C. elegans* PON-like proteins have the disulfide bonds (Cys42 and C353) required for stability in human PONs (Josse et al., 1999; Rosenblat 2006). All the five PON-like proteins have predicted hydrophobic N-termini, a similar feature to mammalian PONs. Both human PON1 and *C. elegans* MEC-6 bind to lipid with their N-termini [PON1 to HDL phospholipids (Harel et al., 2004) and MEC-6 to the TRNs plasma membrane (Chelur et al., 2002)]. However, among the five *C. elegans* PONs, only POML-2, POML-3, and POML-4 retain some of the amino acids required for lactonase and esterase activities in human PONs (Figure I-5), including H115, H134 (catalytic histidine dyad), H155, E53, D269 (catalytic Ca<sup>2+</sup> binding sites), and W281 (Harel et al., 2004; Josse et al., 1999).



## **Section E: Membrane protein production and transport**

Nearly all eukaryotic membrane proteins are synthesized in the endoplasmic reticulum (ER), modified in the Golgi, and transported to the plasma membrane and other target sites. The mechanism and machineries used for production and transport of membrane proteins are highly conserved across species and have been extensively studied in both yeast and mammals. Similar features also exist in *C. elegans*. Here I summarize the classical protein synthesis and secretory pathways.

### **Classical protein synthesis and secretory pathways**

#### **Protein translocation into the endoplasmic reticulum (ER)**

After ribosomes translate the signal peptide or the first transmembrane segment in the cytosol, the elongating polypeptide translocates across the ER membrane, in either a co-translational or a post-translational manner. The entire process includes the targeting (signal-recognition particle dependent) and translocation (the Sec61 channel mediated) phases (Rapoport, 2007). During translocation, many auxiliary components contribute to the folding of transmembrane segments and efficiency of translocation, including ER membrane proteins [e.g. translocon-associated membrane protein (TRAM), the translocon-associated protein (TRAP), Sec62/63], and the ER luminal chaperones [e.g. heat shock protein BiP and protein disulfide isomerase (PDI) (Zimmermann et al., 2011)].

Most membrane proteins insert in the ER membrane during their synthesis. The orientation of the first transmembrane region usually follows “positive inside rule”(more

positively charged segments in cytosol; Andersson and von Heijne, 1994), and determines that of the subsequent transmembrane segments. The hydrophilic segments between transmembrane regions alternate between the ER lumen and the cytosol (Rapoport et al., 2004).

### **Protein folding in the ER**

After entering ER, nascent polypeptides undergo a series of folding and modifications to acquire their native conformation, assisted by molecular chaperones and folding enzymes. The entire folding process involves N-linked glycosylation, protein folding, disulfide bond formation, proline-isomerization, and oligomerization (Braakman and Hebert, 2013). Most membrane proteins receive polysaccharide (Glc3Man9GlcNAc2) attached to the Asn residue of Asn-X-Ser/Thr sequence from the oligosaccharyltransferase (OST). Glucosidase I and II sequentially remove the two residual glucoses from the N-glycan attached to the nascent protein. After this, the mono-glucosylated protein associates with ER lectin chaperones, calnexin and calreticulin, which are paralogous proteins residing on the ER membrane and lumen, respectively. Oxidoreductase ERp57 also binds to the nascent chains and catalyzes disulfide bond formation. Calnexin and calreticulin bind to GlcMan9GlcNAc2 ( $\text{Ca}^{2+}$  dependent, Vassilakos et al., 1998) and ERp57 through a globular N-domain and an extended arm-like P-domain, respectively (Leach et al., 2002; Michalak et al., 2009). The calnexin/calreticulin/ERp57 complex releases most nascent proteins in their native conformation. These folded proteins undergo deglycosylation and partial demannosylation before entering transport vesicles to leave the ER (Hebert and Molinari, 2007).



Oligomerization of subunits and assembly of protein complexes can occur before (Copeland et al., 1988) or after (Prabakaran et al., 1996) an individual protein completely matures.

In addition to the lectin chaperones (calnexin and calreticulin), heat shock proteins, such as Hsp70 and Hsp90 families, constitute the other major chaperone group. They directly bind to the maturing or misfolded polypeptides to promote folding efficiency and/or prevent aggregation (Braakman and Hebert, 2013). ER chaperones have diverse substrates. It remains largely unknown how newly synthesized polypeptides choose their folding chaperones and enzymes. Some proteins may have their own specific chaperones. In this thesis, I report that MEC-6, POML-1, and calreticulin function as chaperones and/or assembly factors for MEC-4 folding and transport.

Chaperone activities can be assayed both in vitro and in vivo. In vitro, chaperones can suppress thermal aggregation of glycosylated proteins (e.g. IgY and  $\alpha$ -mannosidase) and/or non-glycosylated proteins (e.g. citrate synthase and malate dehydrogenase), as monitored by light scattering; they promote refolding of denatured proteins, as monitored by recovery of activities; they interact with substrates (usually unfolded proteins rather than native proteins), as analyzed by size exclusion chromatography, co-immunoprecipitation, and electron microscopy (Ihara et al., 1999; Saito et al., 1999; Stronge et al., 2001). In vivo assays have analyzed the effect of chaperones on the assembly and transport of the major histocompatibility complex (MHC) class I molecules in mammalian cells or *Drosophila* S2 cells. MHC molecules each comprise transmembrane heavy chain, light chain  $\beta_2$ -microglobulin, and peptides, which assemble in the ER before leaving for the membrane. Their folding and assembly stages can be probed by several antibodies that recognize different intermediates (Paquet et al., 2005).

### **ER associated degradation (ERAD)**

The ER has a protein quality control mechanism to ensure only the properly folded proteins can either stay and function in the ER or travel to the Golgi and beyond; misfolded proteins are rapidly removed through ERAD pathways. Although it remains largely unknown how the cells select the terminally misfolded proteins from the well folded proteins and the folding intermediates, a growing number of ER-resident factors have been proposed to recognize and target substrates, such as BiP, PDI, calnexin, UBL domain containing membrane protein (Usa1 in yeast, and HERP in mammal), ER degradation-enhancing  $\alpha$ -mannosidase-like lectin (EDEMs), and Mannose-6-phosphate receptor-like lectin (Yos9 in yeast, OS9 and XTP3-B in mammals; Vembar and Brodsky, 2008). Targeted substrates retro-translocate across the ER membrane to the cytosol, and get degraded by the ubiquitin-proteasome pathway. A few candidates are proposed as the putative dislocation channel on the ER membrane, including Sec61, derlin, and membrane spanning E3 ubiquitin ligases Hrd. AAA+ ATPase (Cdc48 in yeast and p97 in mammal) associates with the dislocation channel and pulls substrates out of the ER (Olzmann et al., 2013; Vembar and Brodsky, 2008).

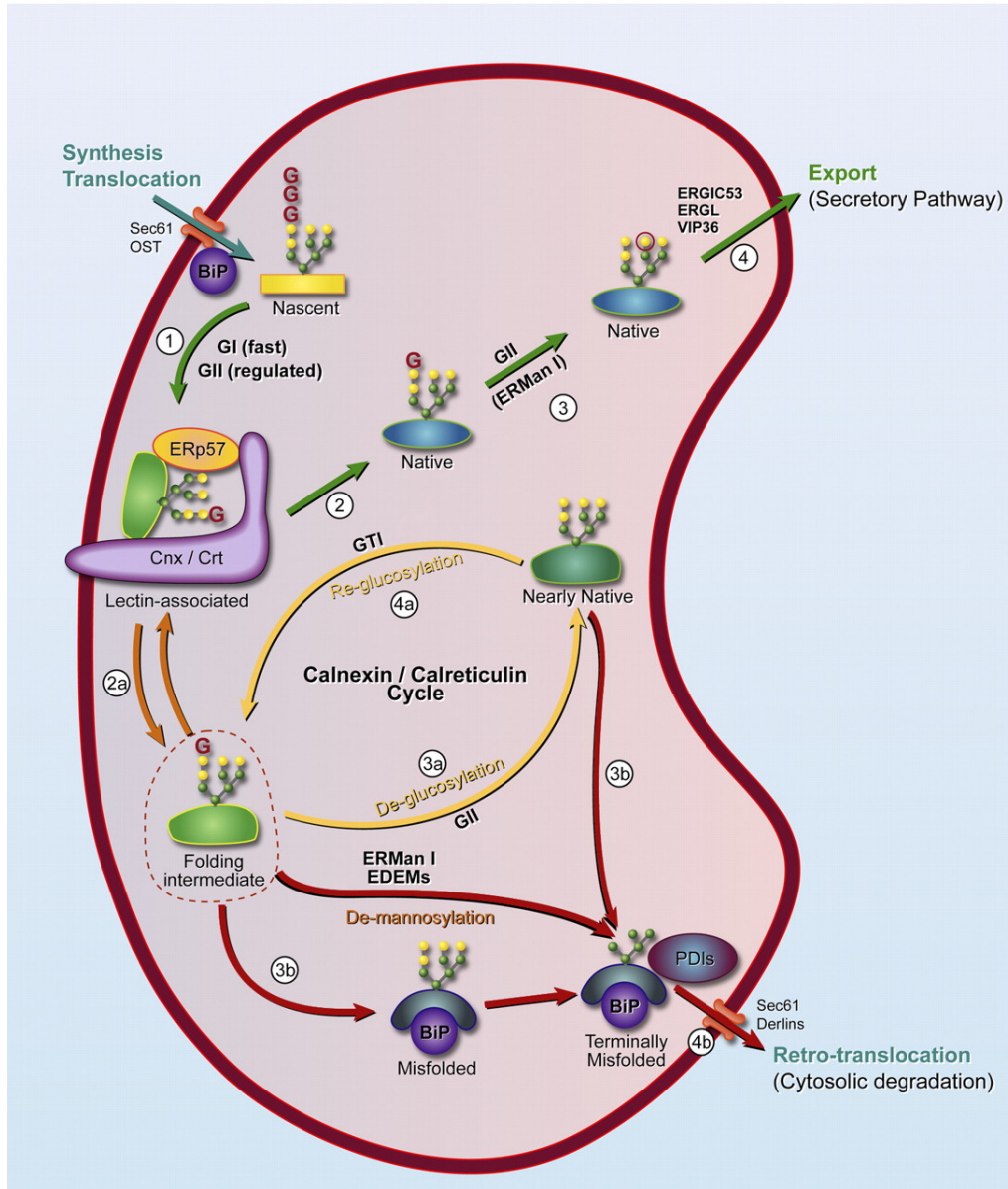


Figure I-6. Synthesis of glycoproteins in and out of the ER (from Hebert and Molinari, 2007).

## **ER-to-Golgi-to-plasma membrane transport**

After passing the “quality control” checkpoint, newly synthesized proteins are exported from the ER to the Golgi via COPII-coated vesicles. The COPII machinery comprises cytosolic proteins: the small GTPase Sar1, Sec23/24, and Sec13/31 (Schekman, 2002). ER membrane protein Sec12, which is the guanine nucleotide exchange factor, activates Sar1 and recruits Sar1 to the ER membrane (Barlowe and Schekman, 1993). Sar1 initiates vesicle formation and subsequent recruitment of Sec23/Sec24 and Sec13/31 (Bi et al., 2002; Lee et al., 2005). Sec24 binds to cargo molecules and recruits them into vesicles (Miller et al., 2002; Miller et al., 2003; Peng et al., 1999; Shimoni et al., 2000; Springer and Schekman, 1998). Sec23 functions as a Sar1 GTPase activating protein. Sec13 and Sec31 form the outer layer of vesicles and promote membrane bending and vesicle fission (Barlowe et al., 1994; Copic et al., 2012). COPII vesicles depart from the ER exit sites and travel along microtubules towards the Golgi in a dynein/dynactin dependent manner (Presley et al., 1997). Once reaching their destination, GTP hydrolysis by Sar1 induces disassembly of the COPII complex; vesicles fuse with the cis-Golgi or ER-Golgi intermediate compartment (ERGIC) to release the cargo proteins.

After the forward transport, the transport proteins and escaped ER proteins return from the Golgi to the ER through the COPI mediated retrograde transport. The cargo proteins of COPI vesicles include proteins bearing an ER retrieval signal at the C-terminus (KDEL or HDEL for ER luminal proteins, KKXX or KXKXX motif for membrane proteins), KDEL receptors, SNARE, etc. Moreover, the COPI-coated vesicle is also implicated in intra-Golgi traffic. The COPI machinery comprises the small ras-like GTPase ARF1, ARFGAPs, and oligomeric coatomer (Duden, 2003).

Proteins undergo further modification and processing in the Golgi before heading to their final destination. One major modification affects protein glycosylation. Most proteins enter the cis-Golgi with N-glycans of high mannose type (Endo H sensitive), which mature into complex N-glycans (Endo H resistant), after glycosylation enzymes remove mannoses and add other sugars (Stanley, 2011).

Mature membrane proteins leave the trans-Golgi for the plasma membrane via multiple routes, including Rab GTPase positive endosomes (Weisz and Rodriguez-Boulan, 2009) and non-endosome compartments in some cases (Hou and Pessin, 2007). Lipid rafts have also been shown to be involved in protein sorting and trafficking (Helms and Zurzolo, 2004). Vesicle budding and trans-Golgi network (TGN) exit utilizes machineries different from COPI and COPII vesicles, and requires dynamin, cofilin, microtubules, actin, and motor proteins kinesin and non-muscle myosin. After exiting the TGN, vesicles travel along microtubules to the plasma membrane (Weisz and Rodriguez-Boulan, 2009).

### **Auxiliary proteins and ion channel expression and trafficking**

The proper function of ion channels largely depends on the right number of ion channels localized at the right sub-cellular positions. Aberration in channel protein expression and localization results in cellular dysfunction and is linked to many diseases, such as epilepsy, ataxia, and Liddle syndrome. Cells utilize multiple molecular pathways to control the protein synthesis, secretory, and endocytic pathways. The regulation can be very specific for particular proteins.

Many ion channels need their own auxiliary proteins for expression and transport. For example, cytoplasmic Kv $\beta$ 2 subunit facilitates Kv1 axonal transportation, but not surface expression, through interaction with (MT) plus-end tracking protein (+TIP) EB1 and KIF3/kinesin II (Gu et al., 2006). Cav $\beta$  subunit stabilizes Cav channels and increases total Cav protein expression by preventing ubiquitination and ERAD of the Cav channels (Altier et al., 2011; Waithe et al., 2011). AMPA receptor regulatory proteins (TARPs) increase synaptic AMPA receptor expression via direct interaction with the post-synaptic density (PSD), and also modulate channel properties and agonist-binding affinity (Straub and Tomita, 2012). Cornichon (CNIH) proteins negatively regulate the AMPA receptor export from the ER to control the neuronal excitability (Brockie et al., 2013). My thesis reports that paraoxonase-like proteins MEC-6 and POML-1 act as chaperones or assembly factors for the folding and transport of the DEG/ENaC mechanosensory channel in *C. elegans*. These auxiliary proteins differ in mechanism, sequence, and structure. Little common nature has been found among them.

In summary, mechanosensitive proteins mediate multiple senses. But except in bacteria, how these molecules organize and function remains largely unknown. In eukaryotes, the well-known mechanosensory complex is the DEG/ENaC channel that mediates gentle touch sensation in the six touch receptor neurons of *C. elegans*. The function of this channel complex requires four membrane proteins: DEG/ENaC proteins MEC-4 and MEC-10, stomatin-like protein MEC-2, and paraoxonase-like protein MEC-6. Past work suggested that all these four proteins form the mechanotransduction complex. But this model has some problems.

This thesis has refined the mechanosensory channel model. In chapter II, I used single molecule imaging to analyze the composition of the channel complex, and found that it is simply MEC-4<sub>3</sub> or MEC-4<sub>2</sub>MEC-10. Neither MEC-2 nor MEC-6 incorporates into the channel. I provided several lines of evidence to demonstrate that MEC-6 and its similar protein POML-1 appear to act as chaperones that facilitate MEC-4 folding and transport. In chapter III, I screened for mutations that can enhance the neurotoxicity of *mec-4(d)* in *poml-1* background, and found two genes *mec-10* and C49G9.1. C49G9.1 encodes a novel membrane protein, which can negatively regulate MEC-4 channel surface expression. In Appendix II, I summarize the gene expression pattern and the loss of function phenotypes of all the *C. elegans* PONs-like proteins.

## Chapter II

### **Reconsidering the *C. elegans* DEG/ENaC Mechanosensory Channel Complex**

(The following manuscript has been submitted to *J. Neurosci.* with other authors: Shashank Bharill, Zeynep Altun, Robert O'Hagan, Brian Coblitz, Ehud Y. Isacoff, and Martin Chalfie. Shashank Bharill performed the single molecule imaging experiment in *Xenopus* oocytes and collected the data of MEC-4 surface expression using TIRF. Zeynep Altun identified the cells where POML-1 is expressed. Robert O'Hagan collected the in vivo electrophysiology data. Brian Coblitz helped with cloning POML-1 cDNA. I performed the remaining experiments.)



## Summary

*Caenorhabditis elegans* senses gentle touch in the six touch receptor neurons (TRNs) using a mechanotransduction complex that contains the pore-forming DEG/ENaC proteins MEC-4 and MEC-10. Past work has suggested these proteins interact with the paraoxonase-like MEC-6 and the cholesterol-binding stomatin-like MEC-2 proteins. Using genetics, molecular biology, electrophysiology and single molecule optical imaging, we have refined the model for the MEC-4/MEC-10 complex. In *Xenopus* oocytes MEC-4 and MEC-10 form MEC-4<sub>3</sub> and MEC-4<sub>2</sub>MEC-10 trimers. The other proteins do not associate with these trimers and, thus, may not be part of the transduction complex. MEC-2, however, colocalizes with MEC-4 in vivo and, thus, may affect the lipid environment of the trimeric channels. In contrast, MEC-6 and a similar protein, POML-1, do not appear to colocalize with MEC-4 either in vivo or in vitro. Several lines of evidence suggest that they act as chaperones and/or assembly factors for MEC-4 folding and transport.

## Introduction

Few of the sensory transduction molecules needed to detect touch, sound, and other mechanical stimuli are known (Chalfie, 2009; Geffeney and Goodman, 2012), and the molecular organization of most of those that are known have not been studied. In *C. elegans*, for example, gentle touch is transduced in the six touch receptor neurons (TRNs) by the DEG/ENaC proteins MEC-4 and MEC-10 (O'Hagan, 2005), but the exact nature of the transduction complex is not known. Several of our previous experiments, however, suggested that several other membrane proteins, including the stomatin-like protein MEC-2 (Huang et al., 1995), and the paraoxonase-like protein MEC-6 (Chelur et al., 2002), also contributed to the transduction complex. First, MEC-2, MEC-6, and MEC-4 are essential for the production of the transduction current, whereas MEC-10 has relatively minor effects on it (O'Hagan et al., 2005; Arnadóttir et al., 2011). Second, MEC-2 and MEC-6 increased the activity of MEC-4(d) channels five days after injection of their cRNAs into frog oocytes without apparently changing the amount of surface-localized MEC-4(d) protein (Chelur et al., 2002; Goodman et al., 2002; Zhang et al., 2004). [The *mec-4(d)* mutation, which results in an A713T substitution, produces a hyperactive channel that is constitutively active (Driscoll and Chalfie, 1991; Goodman et al., 2002; Brown et al., 2007) and leads to TRN degeneration.] Third, in frog oocytes MEC-2 and MEC-6 co-immunoprecipitated with MEC-4(d), MEC-10, and each other (Chelur et al., 2002; Goodman et al., 2002). Fourth, antibodies to MEC-2 and FLAG-tagged MEC-6 labeled puncta in vivo, which appeared to colocalize with MEC-4::YFP (Chelur et al., 2002; Zhang et al., 2004).

Recently, other observations made us reinvestigate this model. First, although MEC-6 did not affect MEC-4 abundance in frog oocytes, loss of *mec-6* in vivo led to a drastic reduction in MEC-4::YFP expression in the TRNs (Chelur et al., 2002). Second, studies in *Drosophila melanogaster* found that although DEG/ENaC proteins needed for mechanosensation were present (Liu et al., 2003; Zhong et al., 2010), obvious MEC-6-like proteins were not (Hicks et al., 2011). Third, we wondered about the importance of the puncta and the apparent colocalization of the proteins in them, since in vivo electrophysiological studies of the TRNs (O'Hagan et al., 2005) showed that the estimated number of active channels equaled the number of puncta, but single channels were unlikely to be visible by fluorescence microscopy. Moreover, MEC-10::GFP did not form puncta in vivo (Chatzigeorgiou et al., 2010).

Here we study the interactions and stoichiometry of the proteins of the TRN transduction channel complex and the particular role of MEC-6 and a second MEC-6-like protein, K11E4.3 ([renamed POML-1 (paraoxonase and MEC-6-like)] in the production of the complex. These studies suggest that the ENaC proteins form a MEC-4<sub>2</sub>MEC-10 trimer that does not form a high-affinity complex with MEC-2 or MEC-6. Moreover, our data suggest that MEC-6, POML-1, and the endoplasmic reticulum (ER) chaperone CRT-1/calreticulin regulate MEC-4 production, maturation, and transport from the ER.

## **Experimental Procedures**

### ***C. elegans* strains**

Unless otherwise indicated, strains were maintained and studied at 20°C on the OP50 strain of *E. coli* according to Brenner (1974). Strains with the *poml-1(ok2266)*, *poml-1(tm4234)*, *mec-10(ok1104)*, *crt-1(ok948)*, and *uba-1(it129)* mutations were obtained from the *C. elegans* Genetic Center and National Bioresource Project-Japan. Strains with the *poml-1(u881)* and *poml-1(u882)* mutations were obtained by Mos1-mediated deletion as described below. *poml-1(u851, u852, u853, u854)* were obtained by ethyl methanesulfonate mutagenesis as described below. The two *mec-6* hypomorphic alleles [*mec-6(u511)* with a G235E change and *mec-6(u518)* with a G213E change] were identified in a genetic screen for suppressors of the cold lethality of *deg-1(506)* (García-Añoveros, 1995). *mec-6(u450)*, *mec-6(u247)*, *mec-4d(e1611)*, *mec-4(u45)*, *mec-4(u253)*, and *mec-5(u444)* have been previously described (Chalfie and Sulston, 1981; Chalfie and Au, 1989; Driscoll and Chalfie, 1991; Huang and Chalfie, 1994). IA404 [*fog-2(q71) pha-4(q490)/sec-23(ij13) rol-9(sc148)*; *uEx(sec-23::gfp)*] (Roberts et al., 2003) was a kind gift from Dr. Meera Sundaram. Double or triple mutants were created using standard genetics (Brenner, 1974) and verified either phenotypically or by PCR.

The following strains were generated during this study: TU3380 [*uls31; mec-4d(e1611) poml-1(ok2266)*], TU3393 [*mec-6(u450); uls31; mec-4d(e1611)*], TU3553 [*uls77(poml-1::yfp)*], TU3555 [*uls78(poml-1::yfp; mec-6::3xflag)*], TU3583 [*dpy-5(e61); uls83(Pmec-4::mec-4(d), Pmec-17::gfp, Pmyo2::mcherry)*], TU3930 [*uEx834(Pmec-4::yfp::tram-1)*], TU3969 [*uls144(Pmec-4::yfp::pisy-1)*], TU3970 [*uls145(Pmec-4::aman-2::yfp)*], TU3971 [*uls146(mec-4::tagrfp)*], TU3973 [*uls149(mec-6::tagrfp)*], TU4109 [*uEX849(Ppoml-1::poml-1::tagrfp)*], TU4339 [*uls31; poml-1(ok2266) mec-4d(e1611); uEx863(Pmec-18::sec-24.1::unc-54 3'UTR, Pmec-18::sec-24.2::unc-54 3'UTR,*

*Pmyo2::mCherry*), TU4340 [*uIs31; poml-1(ok2266) mec-4d(e1611); uEx864(Pmec-18::sec-24.1::unc-54 3'UTR, Pmec-18::sec-24.2::unc-54 3'UTR, Pmyo2::mCherry)*], TU4352 [*uIs146 (mec-4::tagrfp); uEx871(Pmec-10::mec-10::gfp, Pmyo2::mCherry)*], TU4353 [*uIs146 (mec-4::tagrfp); uEx872(Pmec-10::mec-10::gfp, Pmyo2::mCherry)*], TU4356 [*mec-6(u450); uIs31; mec-4d(e1611); uEx865(Pmec-18::sec-24.1::unc-54 3'UTR, Pmec-18::sec-24.2::unc-54 3'UTR, Pmyo2::mCherry)*], TU4357 [*mec-6(u450); uIs31; mec-4d(e1611); uEx866(Pmec-18::sec-24.1::unc-54 3'UTR, Pmec-18::sec-24.2::unc-54 3'UTR, Pmyo2::mCherry)*], TU4358 [*crt(ok948); uIs31; mec-4d(e1611); uEx867(Pmec-18::sec-24.1::unc-54 3'UTR, Pmec-18::sec-24.2::unc-54 3'UTR, Pmyo2::mCherry)*], TU4359 [*crt(ok948); uIs31; mec-4d(e1611); uEx868(Pmec-18::sec-24.1::unc-54 3'UTR, Pmec-18::sec-24.2::unc-54 3'UTR, Pmyo2::mCherry)*], TU4563 [*mec-6(u450); uIs94(Pmec-4::channelrhodopsin-2::yfp, Pmec-17::gfp, Pmyo2::mCherry); poml-1(ok2266)*], TU4564 [*uIs94; crt-1 (ok948)*], TU4565 [*uIs94; crt-1(ok948); poml-1(ok2266)*], TU4569 [*uEx903(Pmec-4::cfp::mec-4::yfp, Pmyo2::mCherry)*], TU4570 [*uEx904(Pmec-4::cfp::mec-4::yfp, Pmyo2::mCherry)*], TU4600 [*uEx905(Pmec-4::cfp::mec-4::yfp, Pmyo2::mCherry)*], TU4615 [*uIs188(Pmec-4::mec-4::yfp, Pmyo2::mCherry); uEx919(Pmec-4::cfp::mec-4, Pinx20::cfp)*], TU4616 [*uIs188; uEx920(Pmec-4::cfp::mec-4, Pinx20::cfp)*], TU4618 [*uIs188*], TU4619 [*uIs189(Pmec-4::cfp::mec-4, Pmyo2::mCherry)*], TU4628 [*uEx912 (Pmec-4::mec-4::yfp, Pmec-18::mec-6::3xflag; Pmyo2::mCherry)*], TU4629 [*uEx913 (Pmec-4::mec-4::yfp, Pmec-18::mec-6::3xflag; Pmyo2::mCherry)*], TU4630 [*uIs193(Pmec-10::mec-10::gfp, Pmyo2::mCherry); uEx914 (Pmec-4::mec-4, Pinx20::gfp)*], TU4631 [*uIs193; uEx915(Pmec-4::mec-4, Pinx20::gfp)*]

## cDNA and plasmids

A 1050 bp *poml-1* fragment encoding the cDNA coding sequence was generated by RACE PCR using FirstChoice RLM-RACE kit (Ambion, Grand Island, NY) with mRNA from wild-type animals.

Fluorescence fusion plasmids were generated from pPD95.75 ([www.addgene.org/static/cms/files/Vec95.pdf](http://www.addgene.org/static/cms/files/Vec95.pdf)). TU#1171 was made by replacing GFP in pPD95.75 with YFP. A *poml-1::yfp* (TU#1172) translational fusion was created by cloning *poml-1* promoter (3008 bp of genomic sequence before start codon) and coding sequence (from the start codon to the end of genomic sequence right before the stop codon) into TU#1171 between HindIII and BamHI. *poml-1::tagrfp* (TU#1173), *mec-6::tagrfp* (TU#1174) and *mec-4::tagrfp* (TU#1175) were generated by removing *yfp::unc-54* 3'UTR from *poml-1::yfp*, *mec-6::yfp*, and *mec-4::yfp* (Chelur et al., 2002) using *KpnI* and *ApaI* and replacing it with *tagrfp::unc-54* 3'UTR from TU#930 (J. Kratz and M.C., unpub.). TU#1190 was made by replacing GFP in pPD95.75 with 3xFLAG from p3XFLAG-CMV-14 (Sigma-Aldrich, St. Louis, MO). *mec-6::3Xflag* (TU1191) was made by cloning 3787bp sequence upstream of the start codon and 2872bp of coding sequence (without the stop codon) of the *mec-6* genomic DNA into TU#1190. *mec-10::gfp* (TU#1176) was made by cloning the 1925 bp sequence upstream of the start codon and the 4232 bp of coding sequence (without the stop codon) of the *mec-10* genomic DNA into pPD95.75. The *Pmec-18::mec-6::3Xflag* construct has been previously described (Chelur et al., 2002).

A plasmid (TU#1177) containing *Pmec-4::mec-4(d)* was generated by taking wild-type genomic DNA from 1019 bp upstream of the *mec-4* start codon to 541 bp downstream of the stop codon and inserting it into pPD95.75 digested with *BamHI* and *ApaI* and producing

the *mec-4(d)* mutation (A713T) using QuickChange Site-Directed Mutagenesis Kit (Agilent Technologies, Santa Clara, CA)

Subcellular markers were from plasmid generated by Rolls et al. (2002). The *Pmec4::yfp::tram-1*(TU#1178) plasmid was constructed by replacing the *rpl-28* promoter with the MEC-4 promoter in 28y-TRAM via *SalI-NotI* digestion. Similarly, The *Pmec-4::yfp::pisy-1*(TU#1179) plasmid and the *Pmec-4::aman-2::yfp* (TU#1180) plasmid were constructed by replacing the *glr-1* promoter with *mec-4* promoter in gy-PIS via *PstI-NotI* digestion and in gy-Manns via *PstI-NotI* digestion.

*Pmec-18::sec-24.1::unc-54* 3'UTR (TU#1182) and *Pmec-18::sec-24.2::unc-54* 3'UTR (TU#1183) were made using the Three-Fragment Vector Construction Kit (Invitrogen). The *mec-18* promoter (400 bp genomic sequence upstream of start codon) was cloned into pDONRP4P1R. The *sec-24.1(+)* and *sec-24.2(+)* coding sequences (genomic sequence from the start codon to the stop codon) were cloned into pDONR221. *unc-54* 3'UTR (865 bp from pPD95.75) was cloned into pDONRP2RP3. *Pmec-18::sec-24.1(m)::unc-54* 3'UTR (TU#1184) and *Pmec-18::sec-24.2(m)::unc-54* 3'UTR (TU#1185) were produced by site direct mutagenesis. *Pmec-4::cfp::mec-4::yfp* (TU#1186) was made using the Three-Fragment Vector Construction Kit. *mec-4* promoter and *cfp* coding sequence was cloned into pDONRP4P1R. *mec-4* coding sequence w/o ATG and stop codon was cloned into pDONR221. *yfp* and *unc-54* 3'UTR (from TU#1171) was cloned into pDONRP2RP3. *Pmec-4::cfp::mec-4* (TU#1187) was also made using the three-fragment vector. *Pmec-4::mec-4::yfp* was described by Chelur et al. (2002).

### **Transgenic animals**

Transgenic animals were generated by microinjection and integrated transgenes were generated by UV irradiation (Chelur and Chalfie, 2007). For all expression experiments, we microinjected *lin-15* (*n756ts*) with 5-20 ng/μl of the relevant GFP or TagRFP (Merzlyak et al., 2007) fusion plasmid (unless otherwise indicated) and 40 ng/μl of the *lin-15*(+) plasmid and pBluescript SK plasmid to bring the total DNA to 100 ng/μl. Integration of transgenes was induced by γ-irradiation (Chelur and Chalfie, 2007). Integrated lines have been out crossed at least three times. The function of the Integrated arrays with *poml-1::yfp*, *mec-4::tagrfp* and *mec-6::tagrfp* was tested by rescuing *poml-1*, *mec-4*, and *mec-6* mutations.

For the rescuing experiments, we microinjected 1-10 ng/μl of the relevant plasmid, 2 ng/μl *Pmyo2::mCherry* (PCFJ90, Addgene, Cambridge, MA), 40 ng/μl of the *lin-15*(+) plasmid, and pBluescript SK to bring the total DNA to 100 ng/μl.

### **Mutageneses**

Additional *poml-1* mutations were obtained by mutagenizing TU3699 [*dpy-5(e61)*; *uls83* (*Pmec-4::mec-4(d)*, *Pmec-17::gfp*, *Pmyo2::mcherry*)] with ethyl methanesulfonate (Brenner, 1974), crossing them with *poml-1(ok2266)* males, and screening for non-Dpy hermaphrodite progeny with GFP in the TRNs. These animals should carry a new *poml-1* mutation failing to complement *poml-1(ok2266)*. Four mutants were recovered from approximately 15,000 hermaphrodites.

We generated a targeted deletion of *poml-1* by excision (Frokjaer-Jensen et al., 2012) of the Mos1 insertion ttTi23097 (obtained from Dr. Kathrin Gieseler), which is 10 kb downstream of *poml-1*. The plasmid that enabled the deletion (TU#1192) was made using the Three-Fragment Vector Construction kit. 2105 bp of genomic DNA downstream of the



ttTi23097 Mos1 insertion site was cloned into pDONRP4P1R. Genomic DNA of *C. briggsae* *unc-119* (including the promoter, coding sequence, and 3'UTR) from pCFJ151 (Addgene, Cambridge, MA) was cloned into pDONR221. 2506 bp of genomic DNA upstream of the *poml-1* start codon was cloned into pDONRP2RP3. Two independent deletion lines were recovered, verified by PCR, and outcrossed seven times. These deletions (*u881* and *u882*) each removed a 14.6 kb sequence from the *poml-1* start point ATG to the ttTi23097 Mos1 insertion as expected, and replaces it with *cb-unc-119(+)*. The deletion starts with ATGCTACAGCTAAGCCCGTTTGCTAGTAACTGT and ends at CGCAACGGCGTCGGCTGCGCGAACGTCTCTCACGCCACAT.

### **TRN activity**

We studied gentle touch sensitivity in blind tests as described (Chalfie and Sulston, 1981). We quantified the response by counting the number of response to ten touches delivered alternately near the head and tail in 30 animals.

We performed in vivo electrophysiology as previously described (O'Hagan et al., 2004). We also used blue light and channelrhodopsin-2 expressed in the TRNs to stimulate these cells as described by Chen and Chalfie (2014).

### **Immunofluorescence and *C. elegans* microscopy**

Immunostaining of larvae and adults was performed according to Miller and Shakes (1995). Isolated, embryonic TRNs that had been cultured for 15-24 hrs (Zhang et al., 2002) were fixed in 4% paraformaldehyde, blocked in PBS with 1% BSA (in some experiments 0.2% Triton-X-100 was added to permeabilize the plasma membrane), incubated with primary

antibody at 4°C for 2 hours, washed 3X in PBS, incubated with secondary antibodies at room temperature for 30 min, and washed 3X in PBS. The following antibodies were used: anti-MEC-18 (Zhang, 2004), anti-MEC-2 N-terminus (Zhang, 2004), anti-MEC-4 (mouse, Abcam ab22184), and anti-GFP (rabbit and mouse; Invitrogen, Carlsbad, CA) diluted 1:200, tetramethylrhodamine isothiocyanate-conjugated goat anti-mouse/rabbit IgG (Jackson ImmunoResearch Laboratories, West Grove, PA), and Alexa Fluor 488/555-conjugated goat anti-rabbit/mouse (Invitrogen, Carlsbad, CA) diluted 1:1000.

Fluorescence and immunofluorescence were observed using a Zeiss Axio Observer Z1 inverted microscope equipped with a Photometrics CoolSnap HQ<sup>2</sup> camera (Photometrics, Tucson, AZ) and a Zeiss Axioskop II equipped with SPOT 2 slider camera (SPOT Imaging Solutions, Sterling Heights, MI). Confocal images were acquired using a Confocal ZEISS LSM700. Live animals were anesthetized using 100 mM 2-3 butanedione monoxime in 10 mM HEPES, pH 7.4.

We measured MEC-4::TagRFP intensity in the cell body by selecting the cell body area (20-30  $\mu\text{m}^2$ ), and measuring the mean intensity subtracted from the background of the same size area by Image J ([rsbweb.nih.gov/ij/](http://rsbweb.nih.gov/ij/)).

The intensity of the MEC-4::TagRFP puncta intensity was measured in the best focused image of six images taken at different z planes using the Puncta Analysis Toolkit beta developed by Dr. Mei Zhen, Samuel Lunenfeld Research Institute, Toronto, Canada. Puncta were examined over a region approximately equivalent to ten cell body lengths starting near the cell body.

MEC-2 and POML-1 immunofluorescence puncta were also analyzed using Image J and the Puncta Analysis Toolkit beta. The width of puncta was the length at half-maximum of

each peak and the average distance between puncta were calculated as  $1/(\text{number of puncta per } \mu\text{m})$ .

FRET was performed on L4 to young adult animals glued with Dermabond (Ethicon Inc., Somerville, NJ) onto 2% agarose pads according to the method of Youvan et al. (1997) using a Confocal ZEISS LSM700. Mean fluorescence intensity minus background was determined in the cell body (and in the puncta for wild type) for three channels: CFP (CFP<sub>excitation=405nm</sub> - CFP<sub>emission=420-475nm</sub>); YFP (YFP<sub>excitation=488nm</sub> - YFP<sub>emission $\geq$ 520nm</sub>), and FRET (CFP<sub>excitation=405nm</sub> - YFP<sub>emission $\geq$ 520nm</sub>). The cross talk of CFP into the FRET channel ( $Df = \text{FRET}/\text{CFP} = 84\%$ ) was determined in animals expressing  $P_{mec-4}::cfp::mec-4$ . Similarly, the cross talk co-efficiency of YFP to the FRET channel is determined by expressing  $P_{mec-4}::mec-4::yfp$  only, and calculated as  $Af = \text{FRET}/\text{YFP} = 1.4\%$ . Net FRET was calculated as  $\text{FRET} - 0.84 \times \text{CFP} - 0.014 \times \text{YFP}$  (Youvan, 1997). Normalized FRET was calculated as  $\text{Net Fret}/(\text{CFP} \times \text{YFP})^{1/2}$  (Xia and Liu, 2001).

We performed single molecule fluorescence *in situ* hybridization to count *mec-4* mRNA as previously described (Topalidou et al., 2011).

### **Electrophysiology in *Xenopus* oocytes**

cRNA expression and electrophysiology in *Xenopus laevis* oocytes followed the procedures and used the plasmids described in Goodman et al. (2002). 10 ng cRNA of MEC-4, MEC-2, and 1 ng MEC-6 cRNA were injected unless noted. In addition *poml-1* cDNA was cloned in pGEM-HE (Liman et al., 1992) and 5 ng of cRNA was injected in *Xenopus laevis* oocytes unless noted (Xenopus I, Dexter, MI or Nasco, Fort Atkinson, WI). Oocytes were maintained as previously describe (Arnadóttir et al., 2011). Membrane current was measured

4-6 days after RNA injection unless noted using a two-electrode voltage clamp as previously described (Goodman et al., 2002).

cDNA for C-terminally FLAG-tagged POML-1 was cloned into pGEM-HE. N-terminally Myc-tagged MEC-4(d) and C-terminally HA-tagged MEC-6 were expressed in oocytes as described previously (Goodman et al., 2002). Immunoprecipitation were performed 5-6 days after cRNA injection and detected by using antibodies against the FLAG, Myc and HA tags (Sigma) and horse radish peroxidase-conjugated secondary antibodies (Jackson ImmunoResearch Laboratories, West Grove, PA).

### **Single molecule imaging**

For stoichiometry and co-localization experiments, DNA constructs for C and/or N-terminally EGFP and mCherry tagged proteins were generated in vector pGEMHE-X-EGFP/mCherry and/or pGEMHE-EGFP-X (Ulbrich and Isacoff, 2007). Plasmids propagation and cRNA synthesis were done as before (Goodman et al. 2002).

Imaging of individual protein complex in *Xenopus* oocyte membrane by TIRF microscopy was performed as previously described (Abuin et al., 2011; Ulbrich and Isacoff, 2007, 2008). Briefly, oocytes were manually devitellinized after 1-2 days of expression at 18°C and placed on high refractive index coverglass ( $n = 1.78$ , Olympus America Inc.) and imaged using Olympus 100X, NA 1.65 oil immersion objective at room temperature.

EGFP and mCherry tagged MEC proteins were excited using a phoxX 488 (60 mW) laser and a 593 nm DPSS laser, respectively. For subunit counting with EGFP tags, a 495 nm long-pass dichroic mirror was used at excitation in combination with a 525/50 nm band-pass filter at emission. For co-localization experiments where both EGFP and mCherry were

excited sequentially, a z488/594 rpc polychroic (Chroma) was used at excitation and 525/50 and 629/53 nm band-pass filters for EGFP and mCherry, respectively, were used at emission. Five to eight hundred frames at the rate of 20 Hz were acquired for subunit counting, whereas 1000 frames (~200 for mCherry and ~800 for EGFP, sequentially) were acquired at the same rate for co-localization using an EMCCD (Andor iXon DV-897 BV) camera. Only single, immobile and diffraction-limited spots were analyzed. The number of bleaching steps was determined manually for each single spot included in the analysis. 200-800 spots from 5-10 oocytes from 3-5 different batches were analyzed for most of the constructs. Observed frequency distribution of photobleaching steps for each construct was plotted and compared with the expected binomial distributions for a dimer, trimer, tetramer and pentamer that were calculated using a fixed probability of 80% of mEGFP being fluorescent, and 66% of mCherry being fluorescent.

Single-molecule co-localization of red (mCherry) and green (EGFP) spots were analyzed as previously described (Abuin et al., 2011).

### **Statistics**

Data are presented with their mean  $\pm$  S.E.M. Statistical significance was determined using the Student t-test unless otherwise noted.

### **Results**

#### **MEC-6 and POML-1 are found in the TRN ER**

The POML-1 sequence is 30% identical and 42% similar to that of MEC-6. As with MEC-6, POML-1 contains a transmembrane domain and a nematode-specific region of 15 amino acids in the N-terminus (Figure 1A; Chelur et al., 2002). In contrast to MEC-6, which is expressed in many cells (Chelur et al., 2002), POML-1 was expressed in only a few neurons. In addition to the TRNs (Topalidou and Chalfie, 2011), POML-1 was found in the IL1, AIM, ALN, and BDU neurons.

In the TRNs, rescuing and tagged translational fusions of MEC-6 and POML-1 formed a mesh-like structure in the cell body and puncta in the proximal process. (In general, the POML-1 fusion was brighter than that of MEC-6 and could be seen further along the process.) In the cell body, translational fusions for both proteins co-localized with markers for the ER (YFP::TRAM-1 and YFP::PISY-1, Figures 1B-D), but not with a marker for the Golgi apparatus (AMAN-2::YFP, Figure 1E).

MEC-6 and POML-1 puncta appeared to co-localize in the TRN process (Figure 1F). These puncta differed and did not co-localize with the MEC-4::TagRFP or MEC-2 puncta (Figures 1G, 1H, 1I, and 1J) although some overlap was observed. In general, the MEC-6 and POML-1 puncta were smaller and closer together than the MEC-4 and MEC-2 puncta: POML-1 puncta were  $0.90 \pm 0.02 \mu\text{m}$  wide and were separated by  $1.17 \pm 0.08 \mu\text{m}$  ( $n=25$  PLM processes), and MEC-2 puncta were  $1.95 \pm 0.05 \mu\text{m}$  wide and were separated by  $3.86 \pm 0.13 \mu\text{m}$  (mean  $\pm$  SEM,  $n=30$  PLM processes).

We cannot explain why these results differed from our previous work (Chelur et al., 2002), which did show colocalization of MEC-6 and MEC-4. Unfortunately the strain used in those previous studies has been lost, but our new experiments used the same plasmids to generate a new strain. Perhaps the relative overexpression in the previous work (higher

concentrations of DNA were injected in Chelur et al., 2002) or the different microscopes used in the experiments resulted in the very different results.

Previous work suggested that MEC-6 was a membrane protein that extended its C-terminus extracellularly (Chelur, et al., 2002). Specifically, LacZ fused to the C-terminus of MEC-6 produced no  $\beta$ -galactosidase activity unless a synthetic transmembrane domain was inserted between MEC-6 and LacZ (LacZ only produces  $\beta$ -galactosidase activity intracellularly). MEC-6 was glycosylated when expressed in CHO cells, and C-terminally HA tagged MEC-6 was detected by surface immunostaining against HA in CHO cells (Chelur, et al., 2002). We found, however, that antibodies directed against C-terminal epitopes of MEC-6 and POML-1 only detected the proteins in cultured TRNs from wild-type embryos when the cells were permeabilized (Figures 1K and 1L). In contrast, surface MEC-4 could be detected in intact cells (data not shown). The failure to detect MEC-6 or POML-1 on the TRN surface suggests that most, if not all, of both proteins is located within the cell. Because some of these molecules were found on the surface of *Xenopus* oocytes and CHO cells in previous experiments (Chelur, et al., 2002), either control over the subcellular localization is tighter in the TRNs or a small, undetected amount of MEC-6 and POML-1 goes to the TRN surface. Most of MEC-6 and POML-1, however, appears to reside in the ER.

The above fusion constructs, including *poml-1::yfp*, *poml-1::tagrfp*, *mec-4::tagrfp*, *Pmec-18::mec-6::3Xflag*, *mec-6::3Xflag*, and *mec-6::tagrfp* were proven to be functional by rescuing *poml-1*, *mec-4*, and *mec-6* null mutations. *mec-4::yfp* rescued *mec-4* mutations poorly, but formed the puncta that co-localized with MEC-4::TagRFP along the TRN process (data not shown).

**A** MLQLSPFASNCLFFTSFAIVTTLFGKLLLHIDINKRTYNHVPGECEGVIPNLPGILGLTT  
 STTGRLYMTTNSKDINTDQTHLFTFYSDNRTAREIEIRGGPPKWRLTPGALSINSETS  
 ↓(u851) ↓(u852)  
 NPNVVFVHNKRTNNIDVFETNEQNDAWQYRKTfKDEQFEGLTDISAAGLNSFFVVK  
 SSIFGTNFALNIER VVPIPTGYIYFVSGNNIQISRVSFPTGIVYDSVKKSIFVTSSTRN  
 ↓(u853)  
 SIYRMKVQVKNIEIVSSKEYDLGCSPIWKFDFGSLTCHPVKFRYLLSLFVITSSP  
 ↓(u854)D  
 SLILRVAVPTDKDKPLTITQLYSNDGATISNANVTVRAGRSLLISDGTKILNCHL

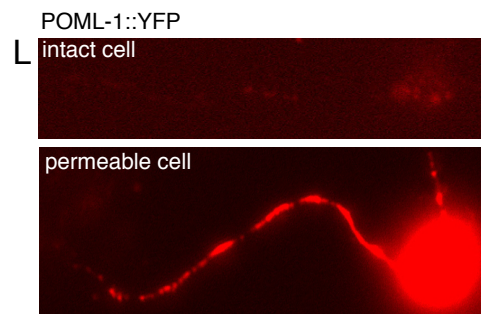
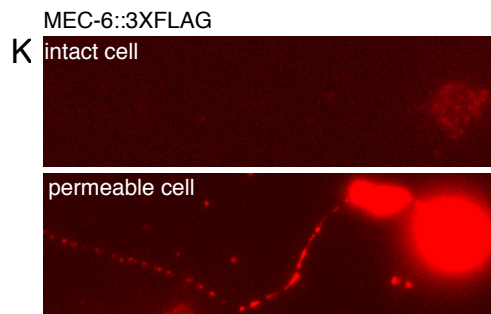
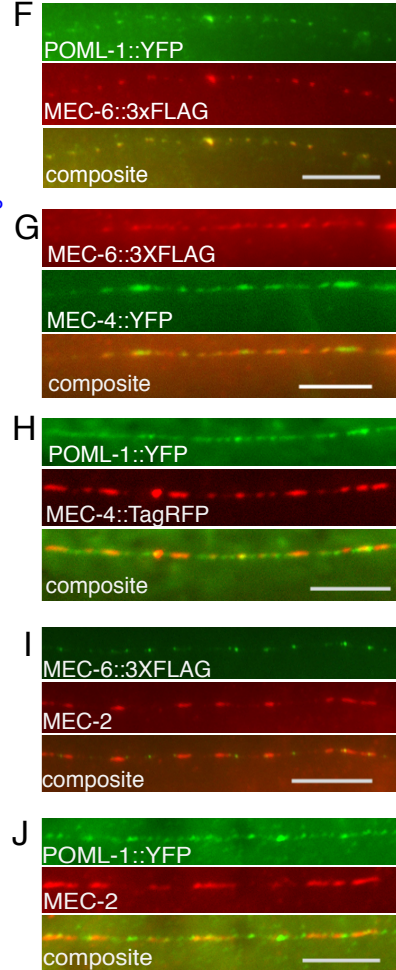
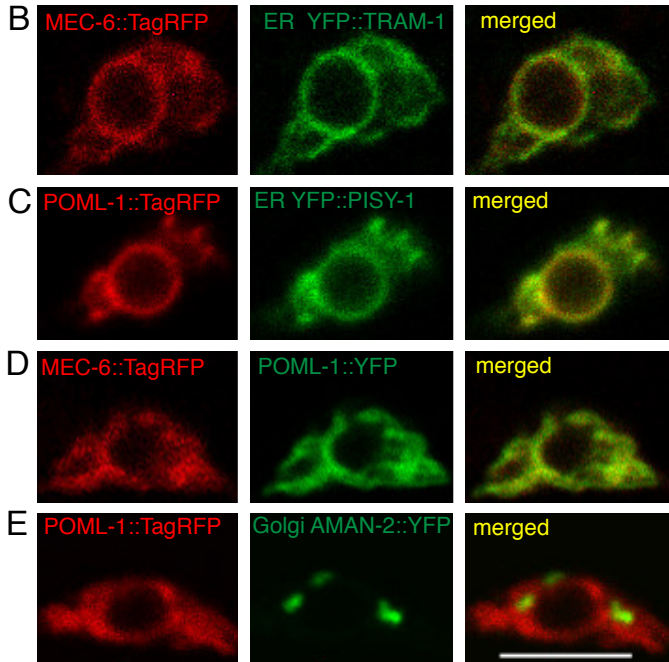




Figure 1 (II-1). TRN expression of MEC-6 and POML-1. (A) The deduced POML-1 protein sequence. The *C. elegans* specific domain (underline) and the predicted transmembrane domain (red) are indicated. Splice-site (arrow) and missense (inverted triangle) mutations are indicated above the affected amino acid for each mutant allele (in parentheses). The sequences deleted in *ok2266* and *tm4234* alleles are indicated in gray and blue, respectively. Confocal sections of TRN cell bodies of (B) MEC-6::TagRFP and the ER marker YFP::TRAM-1, (C) POML-1::TagRFP and the ER marker YFP::PISY-1 (D) MEC-6::TagRFP and POML-1::YFP, and (E) POML-1::TagRFP and the Golgi marker AMAN-2::YFP. Process expression of (F) POML-1::YFP and *Pmec-18*::MEC-6::3XFLAG, (G) *Pmec-18*::MEC-6::3XFALG and MEC-4::YFP, (H) POML-1::YFP and MEC-4::TagRFP, (I) *Pmec-18*::MEC-6::3xFLAG and MEC-2, and (J) POML-1::YFP and MEC-2. Anti-FLAG, anti-GFP, and anti MEC-2 antibodies were used to label the proteins in (F), (G), (H), (I), and (J). (K) MEC-6::3XFLAG expression as detected by an anti-FLAG antibody in intact (top panel) and permeabilized (lower panel) cultured TRNs. (L) POML-1::YFP expression as detected by an antiGFP antibody in intact (top panel) and permeabilized (lower panel) TRNs in culture. The faint immunofluorescence in intact cells (K and L) was not specific because it was often observed in cells that did not express MEC-6::3XFLAG or POML-1::YFP. Scale bars = 5  $\mu$ m.

### **POML-1 affects MEC-4 function**

The failure of MEC-6 and POML-1 to colocalize with MEC-4 suggests that MEC-6 and POML-1 may not function directly in transduction. To study the role of *poml-1*, we first generated a *poml-1* null allele. Using Mos1-mediated gene deletion (Frokjaer-Jensen et al., 2010), we obtained two null mutations, *u881* and *u882*, which lacked the entire *poml-1* coding sequence. We obtained four additional mutations using ethyl methanesulfonate mutagenesis: three splicing junction mutations (*u851*, *u852*, and *u853*) and one missense mutation (*u854*; Figures 1A and Table 1). Two *poml-1* alleles (*ok2266* and *tm4234*) with the gene partially deleted previously known. For many of the experiments we used the *ok2266* allele, which acted as a null since it produced the same phenotype as *poml-1(u881)*; see below).

Table 1 (II-1). *poml-1* mutations

Allele	Mutation
<i>ok2266</i>	exons 2-4 deleted
<i>tm4234</i>	exons 6-8 deleted
<i>u851</i>	g-a at splice junction of exon 3 – intron 3
<i>u852</i>	g-a at splice junction of intron 4 – exon 5
<i>u853</i>	g-a at splice junction of exon 7 – intron 7
<i>u854</i>	ggt>gat, missense mutation G320D
<i>u881</i>	Deletion from <i>poml-1</i> start to ttTi23097 Mos1 insertion site
<i>u882</i>	Deletion from <i>poml-1</i> start to ttTi23097 Mos1 insertion site

None of the eight mutations produced touch insensitivity or any other obvious phenotype. The mutations, however, did render animals containing sensitizing mutations touch insensitive (Figure 2). These sensitizing mutations were temperature-sensitive alleles of *mec-4* and *mec-6* (Gu et al., 1996), two hypomorphic alleles of *mec-6* [*u511*(G235E) and *u518*(G213E)] (García-Añoveros, 1995), and two *crt-1* null alleles (Xu et al., 2001). Except for the *crt-1* mutations, which lower MEC-4 protein level and cause slight touch defects (Xu et al., 2001), none of the sensitizing mutations produced touch insensitivity on their own. All the mutations produced severe touch insensitivity in *poml-1* homozygotes. These synthetic results suggest a role for *poml-1* in TRN touch sensitivity. [The loss of MEC-6, POML-1, or CRT-1 did not affect the general physiology of the TRNs, since light-activation of TRN-

expressed channelrhodopsin-2 (Nagel et al., 2003) produced the same response in *crt-1*, *mec-6*; *poml-1*, and *crt-1*; *poml-1* animals as wild type (data not shown).]

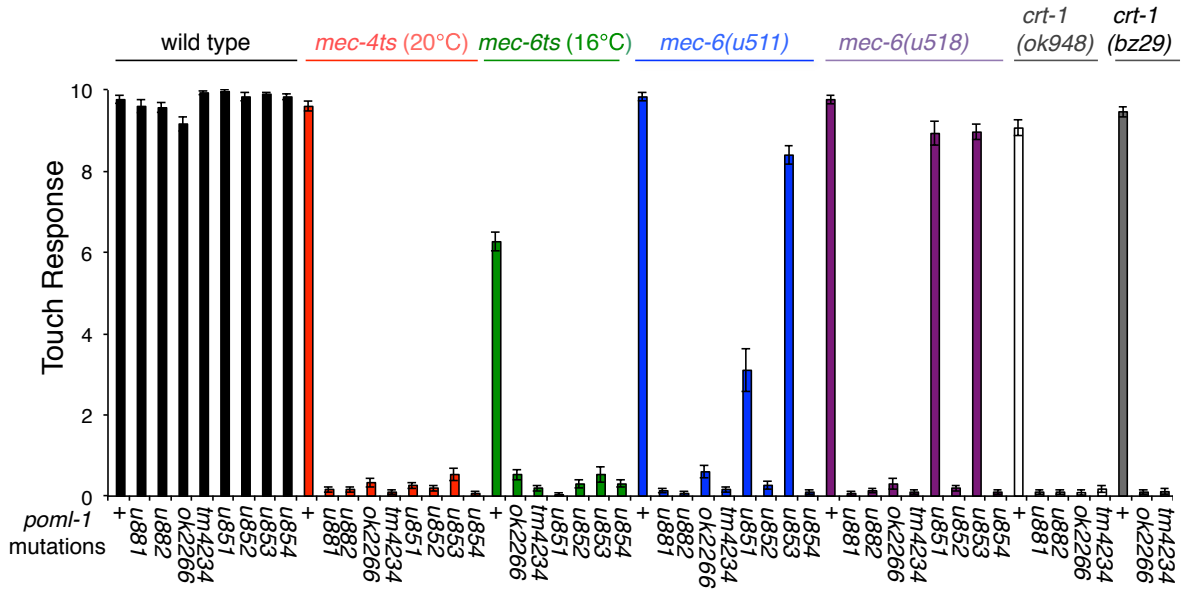


Figure 2 (II-2). *poml-1* mutations dramatically reduce the touch sensitivity in sensitized backgrounds (mean  $\pm$  SEM, n=30).

Other evidence for a role in MEC-4 function comes from the suppression by *poml-1* mutations of the TRN degeneration caused by the *mec-4(d)* gain-of-function mutation *e1611*. *mec-6* mutations but not those of other touch sensitivity genes, suppressed these deaths (Chalfie and Wolinsky, 1990; Huang and Chalfie, 1994). In contrast to their weak effects on touch sensitivity, seven of the eight *poml-1* alleles (all but the missense mutation *u854*) strongly suppressed *mec-4(d)* neuronal degeneration to different extents (Table 2) and did so on their own. The suppressed animals were all touch insensitive, suggesting that either insufficient MEC-4(d) is available for touch sensitivity or that the mutant channels cannot transduce touch. Overexpressing wild-type *poml-1*, but not *mec-6*, resulted in TRN degeneration in *poml-1 mec-4(d)* animals (Table 2). Similarly, *poml-1(+)* did not rescue *mec-6; mec-4(d)* mutants (data not shown). Overexpressing *mec-4(d)* by the multiple copy insertion *uIs83* partially caused degeneration in *poml-1* animals, but not in *mec-6(u450)*, which deletes most of *mec-6* coding sequence and is considered to be a null allele (Chelur et al., 2002; Table 2). Unlike *mec-6* mutations (Chalfie and Wolinsky, 1990; Shreffler et al., 1995), *poml-1* mutations did not suppress other DEG/ENaC gain-of-function mutations, including *deg-1*, *unc-8*, and *unc-105*, even though *poml-1* and *deg-1* are both expressed in IL1 neurons. These results suggests that POML-1 is critical for the MEC-4(d)-induced degeneration, and has a separate role from MEC-6, which functions more broadly.

Table 2 (II-2). *poml-1* and *mec-6* mutations suppress *mec-4(d)* degenerations

Genotype			% Surviving TRNs	
<i>poml-1</i>	<i>mec-6</i>	<i>mec-4(d)</i>	ALM	PLM
+	+	<i>e1611</i>	1±1	1±1
<i>ok2266</i>	+	<i>e1611</i>	97±1	90±2
<i>u881</i>	+	<i>e1611</i>	92±2	89±2
<i>ok2266/u881</i>	+	<i>e1611</i>	93±2	86±4
<i>u881; uEx[poml-1(+)]</i>	+	<i>e1611</i>	1±1	1±1
+	<i>u450</i>	<i>e1611</i>	99±1	99±1
+	+	<i>uls83</i>	0±0	0±0
<i>u851</i>	+	<i>uls83</i>	50±3	29±3
<i>u852</i>	+	<i>uls83</i>	70±3	32±3
<i>u853</i>	+	<i>uls83</i>	23±3	11±2
<i>u854</i>	+	<i>uls83</i>	1±1	0±0
<i>ok2266</i>	+	<i>uls83</i>	73±3	38±4
<i>tm4234</i>	+	<i>uls83</i>	60±3	23±3
<i>u881</i>	+	<i>uls83</i>	62±3	26±3
<i>u882</i>	+	<i>uls83</i>	68±3	35±3
+	<i>u450</i>	<i>uls83</i>	98±1	100±0

TRNs with GFP in L4 and young adult animals were scored as having survived. *uls83* is an integrated array that overexpresses *mec-4(d)*. The percentage of surviving TRNs is given as the mean ± SEM. n > 100 except for the *ok2266/u881* heterozygotes (n = 30) and the rescue

experiments using extrachromosomal arrays of *poml-1(+)* (*uEx[poml-1(+)]*); n = 61 from four stable lines).

### **POML-1 increases MEC-4(d) channel activity in *Xenopus* oocytes**

As with MEC-6 (Chelur et al., 2002), POML-1 increased the activity of the MEC-4(d) channel in *Xenopus* oocytes (Figure 3A). POML-1 increased the amiloride-sensitive Na<sup>+</sup> current by three-fold, a smaller effect compared to the 10-fold increase by MEC-6. Like MEC-6, POML-1 worked synergistically with MEC-2, but not with MEC-6, to increase channel activity ~12-fold (Figure 3A). The effects of POML-1 on channel activity suggest that POML-1 up-regulates MEC-4(d) channel activity through a similar mechanism to that of MEC-6, but different from that of MEC-2. We did, however, find that coexpression of POML-1 with MEC-4d, MEC-2, and MEC-6 doubled MEC-4(d) channel activity over that in oocytes without POML-1. Either, POML-1 also regulates MEC-2 expression or activity or the larger current with MEC-2 and MEC-6 revealed a small effect of POML-1 [At higher concentrations POML-1 on its own, like MEC-6 (Chelur et al., 2002), produced an amiloride-resistant current in *Xenopus* oocytes (Figure 3B).]

To study protein-protein interactions, we tagged these proteins and expressed them in *Xenopus* oocytes. Antibodies against the tags on MEC-4(d) and MEC-6 bound a small amount of POML-1::3XFLAG, suggesting a weak physical interaction between POML-1 and these proteins (Figure 3C).

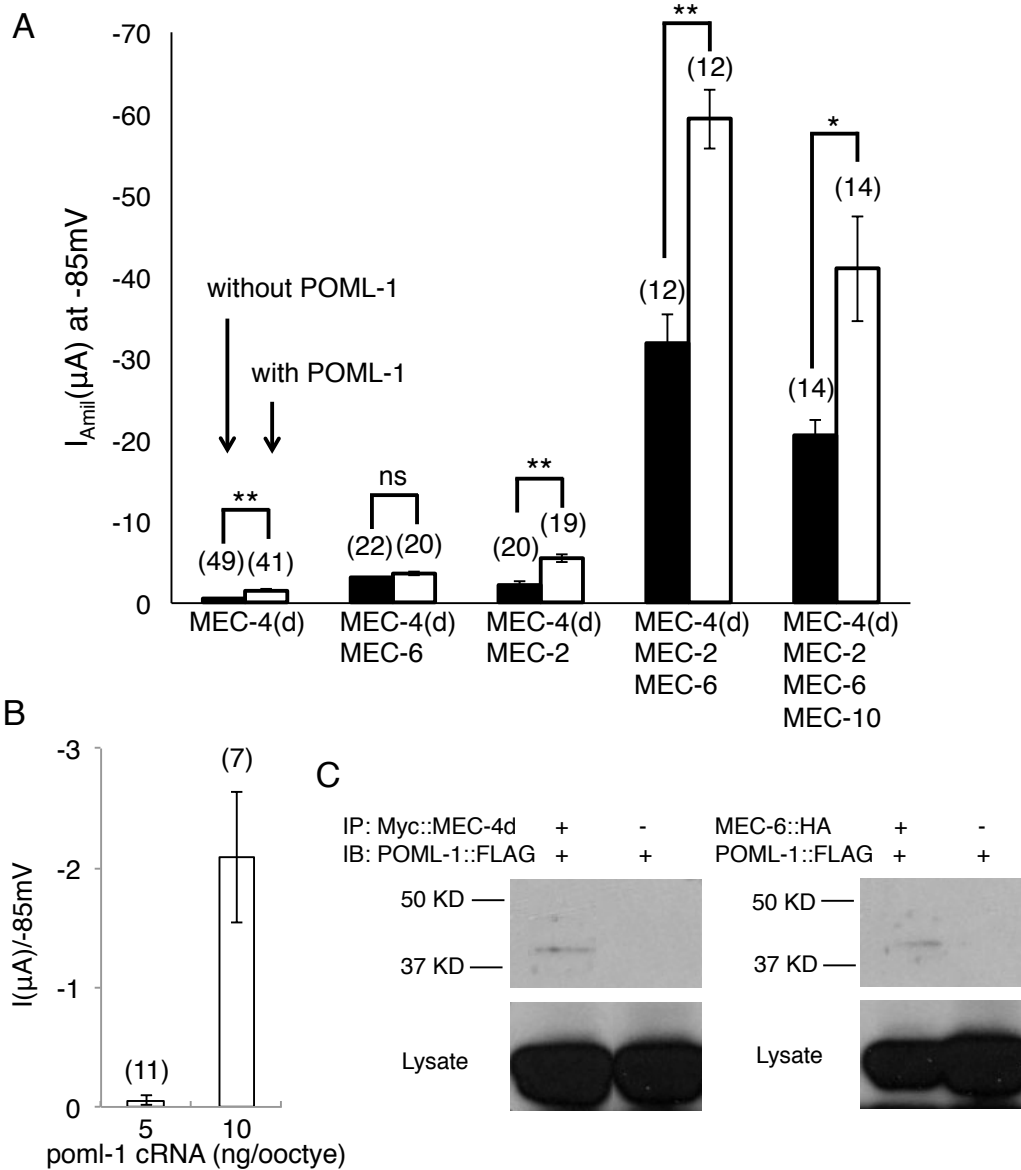


Figure 3 (II-3). POML-1 increases MEC-4(d) activity in *Xenopus* oocytes. (A) The effect of POML-1 (white bars) on the MEC-4(d) amiloride-sensitive current at -85 mV (mean  $\pm$  SEM) in the presence and absence of other MEC proteins. The number of oocytes tested is given in parentheses (here and in B). The oocytes were from at least two frogs. \* $p=0.005$ ; \*\* $p<0.0001$ ; ns, not significant. (B) Amiloride-resistant membrane current produced by expressing POML-1 alone in *Xenopus* oocytes at -85 mV (mean  $\pm$  SEM). (C) Co-immunoprecipitation of POML-1 by MEC-4(d) and MEC-6 in *Xenopus* oocytes.

## POML-1 and MEC-6 affect the amount and distribution of MEC-4

MEC-2 and MEC-4 are predominantly distributed in TRN processes as puncta (Chelur et al., 2002; Zhang et al., 2004). This distribution requires MEC-6 (Chelur et al., 2002), and the production of MEC-2 puncta requires MEC-4 (Emtage et al., 2004; Zhang et al., 2004). We tested the role of POML-1 on MEC-2 distribution using an anti-MEC-2 antibody in *poml-1* mutants, the two *mec-6* hypomorphic mutants [*u511*(G235E) and *u518*(G213E)], *crt-1* mutants, and *mec-6*(*u511* or *u518*); *poml-1* and *crt-1*; *poml-1* double mutants. No single mutation caused obvious defects in MEC-2 puncta. In contrast, the double mutants had disrupted MEC-2 puncta (Figure 4A), a result that is consistent with the need for the doubles to cause touch insensitivity.

We also tested the effect of *mec-6* and *poml-1* mutations on the production and distribution of MEC-4. We examined wild-type MEC-4 expression using several fluorescent protein tags and with an anti-MEC-4 antibody. Tagged MEC-4 appeared as large spots in the TRN cell body and smaller puncta in the process (in some cases the spots were less prominent in the cell body and a meshwork was seen). In the cell body, MEC-4::TagRFP spots partially co-localized with ER (YFP::TRAM-1), but some were always adjacent to the Golgi (AMAN-2::YFP, n= 20 TRNs) and the ER exit site (SEC-23::GFP; n = 10 TRNs, Figure 4B). Thus, cell body MEC-4 may reside in ER-Golgi intermediate compartment (Appenzeller-Herzog and Hauri, 2006) or trans-Golgi network (Traub and Kornfeld, 1997).

*mec-6* and *poml-1* mutations reduced MEC-4 protein levels as seen with anti-MEC-4 antibody (Figure 4C) and fusion proteins (Figure 4D). The reduction, was stronger with *mec-6* (Figures 4C, 4D, and 4E), and, thus, correlates with the stronger phenotype of *mec-6* with



regard to touch sensitivity and *mec-4(d)* degeneration. Protein was mainly found in the TRN cell body with faint expression in the proximal process. In general, MEC-4 was more evenly distributed in the cell body and puncta were not seen in the process (Figure 4C and 4D). Since *poml-1* animals had nearly normal touch sensitivity and MEC-2 puncta, the animals must have functional, surface-localized MEC-4 channels that are below our level of detection. In addition, the mechanoreceptor current (MRC) of *poml-1* TRNs responded slightly differently from that in wild-type TRNs to pressure (*poml-1*  $P_{1/2} = 7.7 \pm 0.8$  nN/ $\mu\text{m}^2$  versus wild type  $P_{1/2} = 4.5 \pm 0.7$  nN/ $\mu\text{m}^2$ ), but peak MRC amplitude was not changed (data not shown).

The effects of *mec-6* and *poml-1* mutations on MEC-4 protein levels and distribution suggest that MEC-6 and POML-1 act early in MEC-4 production and/or transport. Consistent with this hypothesis defects that presumably affect touch sensitivity after MEC-4 is made [mutation of *mec-5* and *mec-9*, genes that encode ECM proteins needed for touch sensitivity (Emtage et al., 2004)], disrupted the process localization of MEC-4 without affecting the level of MEC-4 protein or its distribution in the cell body (Figure 4D).

### **MEC-6 and POML-1 may be chaperones**

Calreticulin (CRT-1), a calcium-binding chaperone in the ER lumen (Park et al., 2001), is also required for the degeneration caused by hyperactive degenerin channels containing MEC-4, UNC-8, DEG-1, or UNC-105 (Xu et al., 2001). Like the *mec-6* and *poml-1* mutations, *crt-1* mutations reduced the amount of MEC-4 and its appearance as puncta in TRN cell bodies and processes (Figure 4D). *crt-1* mutation resulted in a slight defect in touch

sensitivity and a slight reduction in MEC-2 puncta, but *crt-1* and *poml-1* together completely abolished touch sensitivity and disrupted MEC-2 puncta (Figures 2 and 4A), suggesting CRT-1 and POML-1 act redundantly.

MEC-6, POML-1, and CRT-1 affected the expression and distribution of MEC-4 protein, rather than the amount of *mec-4* mRNA as seen with single molecule fluorescence *in situ* hybridization (data not shown). The similarity of the phenotypes of *crt-1*, *mec-6*, and *poml-1* mutants, the expression of all three proteins primarily in the ER, and the additivity of their phenotypes suggest that MEC-6 and POML-1, like CRT-1, may, at least in part, act as chaperones.

If these proteins facilitate the folding of MEC-4 in the ER, the reduction in MEC-4 could be a consequence of protein degradation. Indeed, the loss of CRT-1, MEC-6, or POML-1 caused an ubiquitin-dependent reduction in MEC-4 levels. Mutation of the ubiquitin-activating (E1) enzyme gene *uba-1* (Jones et al., 2002) or treatment of L3-4 larvae for 8 hours (animals got very sick if treated with bortezomib for longer periods) with 50  $\mu$ M proteasome inhibitor bortezomib increased MEC-4 levels 2-3 fold in *mec-6*, *poml-1*, and *crt-1* mutants (*uba-1* only increased MEC-4 level by 20% in wild type; Figure 4E).

This increase, however, did not restore MEC-4 levels to those seen in wild type, in part, perhaps, because less MEC-4 protein was produced in *mec-6*, *poml-1*, and *crt-1* mutants even when the degradation pathway was blocked or the *uba-1* mutation and bortezomib treatment only partially suppressed the degradation pathway. Although these treatments increased the amount of MEC-4, they did not change its distribution. MEC-4 was still largely restricted to the same mesh-like structure in the cell body seen in the mutants without the *uba-1* mutation or bortezomib (Figure 4D). Moreover, the MEC-4 present in the proximal process

was diffuse (Figure 4D). Additionally, because these treatments did not restore touch sensitivity to *mec-6* null mutants or *crt-1; poml-1* double mutants (data not shown) and only resulted in a modest increase (16% for *uba-1* in ALM) of touch cell deaths in *poml-1 mec-4(d)* animals but not in *mec-6; mec-4(d)* animals (Figure 4F), the increased MEC-4 does not function, perhaps because it is misfolded or not properly localized.

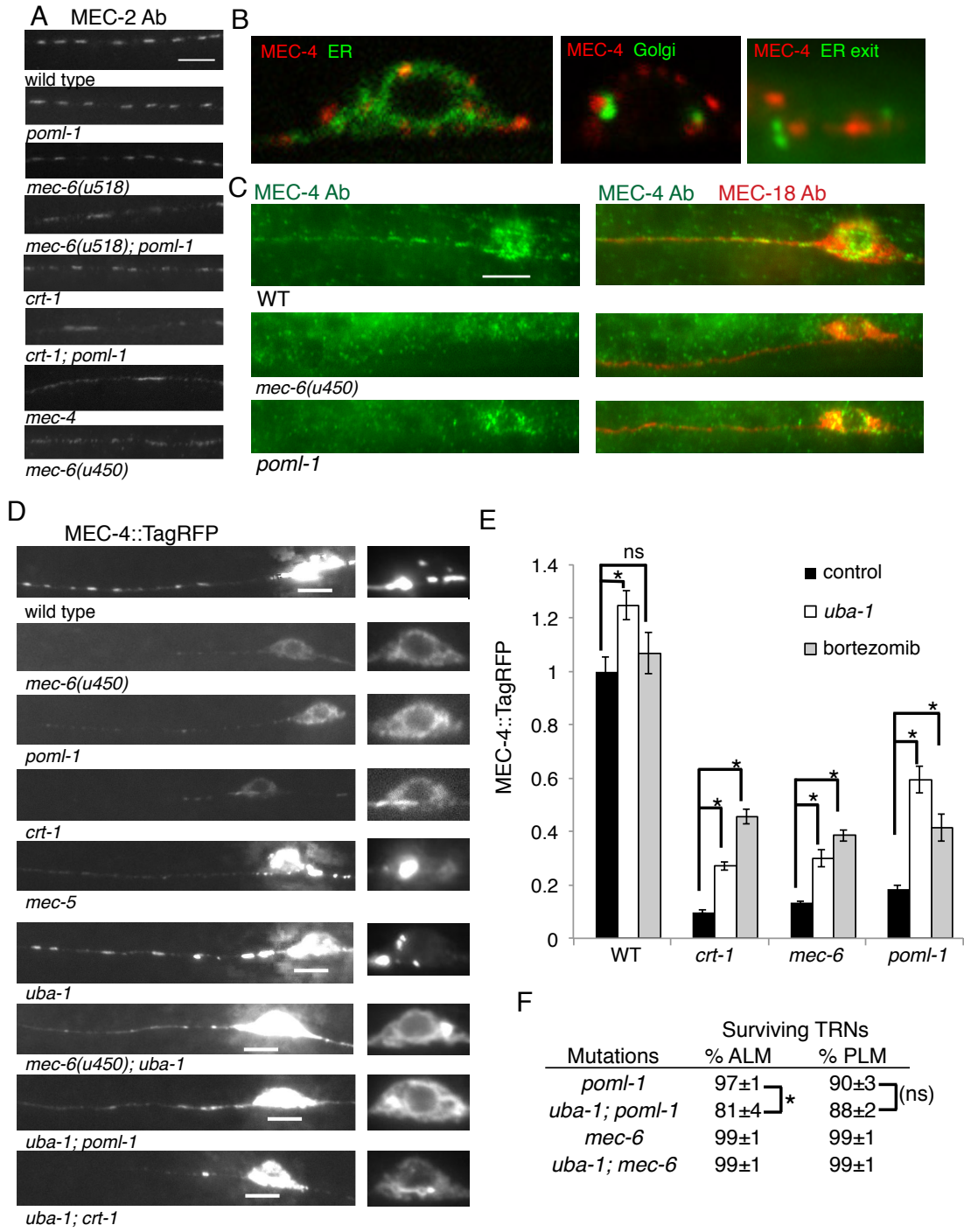


Figure 4 (II-4). Effect of *mec-6*, *poml-1*, and *crt-1* mutations on MEC-2 and MEC-4 expression in the TRNs. (A) MEC-2 puncta in the TRN process. (B) Coexpression of MEC-4::TagRFP with YFP::TRAM-1 (an ER marker), AMAN-2::YFP (a Golgi marker), and SEC-23::GFP (an ER exit site marker). (C) *mec-6* and *poml-1* mutations reduce the amount of endogenous MEC-4 as detected by an anti-MEC-4 antibody (green). TRNs were labeled with an anti-MEC-18 antibody (red). The left panels show MEC-4 immunofluorescence; the right panels show the merged MEC-4 and MEC-18 immunofluorescence. (D) MEC-4::TagRFP expression. Left panels show the merged images of expression at ten focal planes; right panels are images of the single plane showing the best focused images of the same cell body. (E) Normalized MEC-4::TagRFP fluorescence intensity in the TRN cell bodies of L4 larvae and young adults of wild type, *crt-1*, *mec-6(u450)*, and *poml-1* animals that were either untreated, had a *uba-1* mutation, or were treated with 50  $\mu$ M bortezomib for 8 hrs (mean  $\pm$  SEM, n = 30-50, \*p<0.0001; ns, not significant). (F) Lack of a strong effect of *uba-1* mutation on TRN degeneration in *poml-1 mec-4(d)* or *mec-6; mec-4(d)* animals (mean  $\pm$  SEM, n = 40-70, \*p<0.001). Unless noted the following mutations were used: *crt-1(ok948)*, *mec-4(u253)*, *mec-5(u444)*, *uba-1(it129)*, and *poml-1(ok2266)*. Scale bar = 5  $\mu$ m.

Since overexpression of the ER transport protein SEC-24 rescued trafficking defects caused by the loss of a putative ER chaperone/escort receptor in yeast (Elizabeth Miller, pers. comm.), we tested whether overexpression of the genes for *C. elegans* SEC-24 (*sec-24.1* and *sec-24.2*) in the TRNs could similarly suppress *crt-1*, *mec-6*, and *poml-1* mutations. The effects were partial: about 50% of the TRNs died in *poml-1 mec-4(d)* animals and 30% in *crt-1; mec-4(d)* animals, but no TRNs died in *mec-6; mec-4(d)* animals overexpressing the *sec-24* genes (Figure 5A). Most of the remaining TRNs had morphological defects: wavy processes, extra neurites and misplaced cell bodies (Figure 5B). These defects were also found, though less severe, in wild-type animals that overexpressed *sec-24(+)*, but they were rarely observed in mutants that did not overexpress them. Overexpressing SEC-24 in *poml-1* mutants doubled the amount of MEC-4::TagRFP in TRN processes, but not in the cell bodies (Figure 5C). In addition, overexpression of SEC-24 did not restore touch sensitivity to *mec-6(u511); poml-1* animals. Overexpressing the *C. elegans sec-24* genes with mutated potential cargo-binding sites [corresponding to Yeast SEC-24 R230A, R235A, L616W (Miller et al., 2003)] reduced but did not eliminate the effect; 20% of the TRNs died *poml-1 mec-4(d)* animals (Figure 5A).

The partial recovery of *mec-4(d)*-induced death by SEC-24(+) in *poml-1* and *crt-1* animals might result from an increase in MEC-4 transport to the plasma membrane. POML-1 and CRT-1 may act, at least in part, as chaperones to facilitate MEC-4 transport. We do not know why SEC-24 overexpression did not affect the *mec-6* phenotype; either the amount of SEC-24 could not overcome the loss of MEC-6 or MEC-6 may have an additional, essential role.

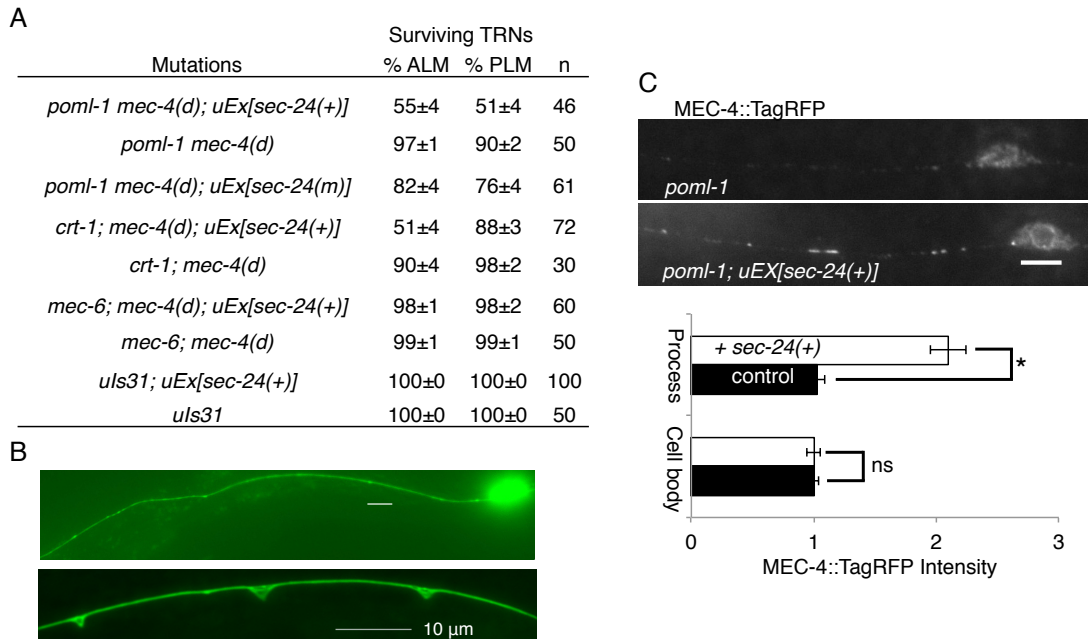


Figure 5 (II-5). MEC-6, POML-1 and CRT-1 may function as chaperones. (A) The effect of SEC-24(+) overexpression on the suppression of *mec-4(d)* deaths by *poml-1*, *crt-1*, and *mec-6* (mean ± SEM). *sec-24(m)* is *sec-24.1* and *sec-24.2* with mutated cargo-binding sites. n = the number of animals examined. The results with *uEx[sec-24(+)]* and *uEx[sec-24(m)]* were collected from 2-5 stable lines. (B) Overexpression of *sec-24(+)* caused morphological defects in the majority of surviving TRNs in *poml-1 mec-4(d)* animals. (C) Effect of overexpressing SEC-24(+) on MEC-4::TagRFP fluorescence intensity in the TRN cell bodies and proximal processes of *poml-1* L4 larvae and young adults (mean ± SEM, n = 34-40, \*p<0.001). Fluorescence intensity was normalized to that of *poml-1* mutants. Scale bar = 5 μm.

Because Förster resonance energy transfer (FRET) can be used to monitor protein folding (Miyawaki et al., 1997; Philipps et al., 2003), we used a CFP::MEC-4::YFP fusion to examine whether MEC-6, POML-1, and CRT-1 affect the MEC-4 protein folding. This fusion was expressed in the TRNs: the protein formed puncta in the process and a mesh-like structure and spots in the cell body, though the spots in the cell body appeared to be smaller and dimmer than with MEC-4::TagRFP (Figure 6A). In *mec-6*, *poml-1*, or *crt-1* animals CFP::MEC-4::YFP was restricted to the cell body, where the fluorescence was reduced by 50%, but formed a similar mesh-like structure and spots to those seen in the wild type (Figure 6A and data not shown). CFP::MEC-4::YFP produced an efficient FRET signal in wild type animals, suggesting that CFP and YFP were close to each other. The FRET signal of CFP::MEC-4::YFP was mainly produced intramolecularly, rather than intermolecularly because co-expression of CFP::MEC-4 (CFP fused to the N-terminus of MEC-4) and MEC-4::YFP (YFP fused to the C-terminus of MEC-4) did not produce the FRET signal (Figures 6A and 6B). Thus, the FRET signal is likely to reflect the folding status of individual MEC-4 polypeptides, rather than their aggregation or trimerization. In contrast to the FRET signal in wild type, FRET from CFP::MEC-4::YFP was reduced by 50%-70% in *mec-6*, *poml-1*, or *crt-1* animals (Figure 6B). The reduction of FRET in these mutants was less likely to be due to their reduced CFP::MEC-4::YFP expression, because the FRET signal was normalized to CFP and YFP intensity (see Experimental Procedure), and wild-type animals expressing similar level of CFP::MEC-4::YFP as that in these mutants still produced robust FRET signals (data not shown). These data suggested that MEC-4 had not folded or assembled correctly in these mutants.



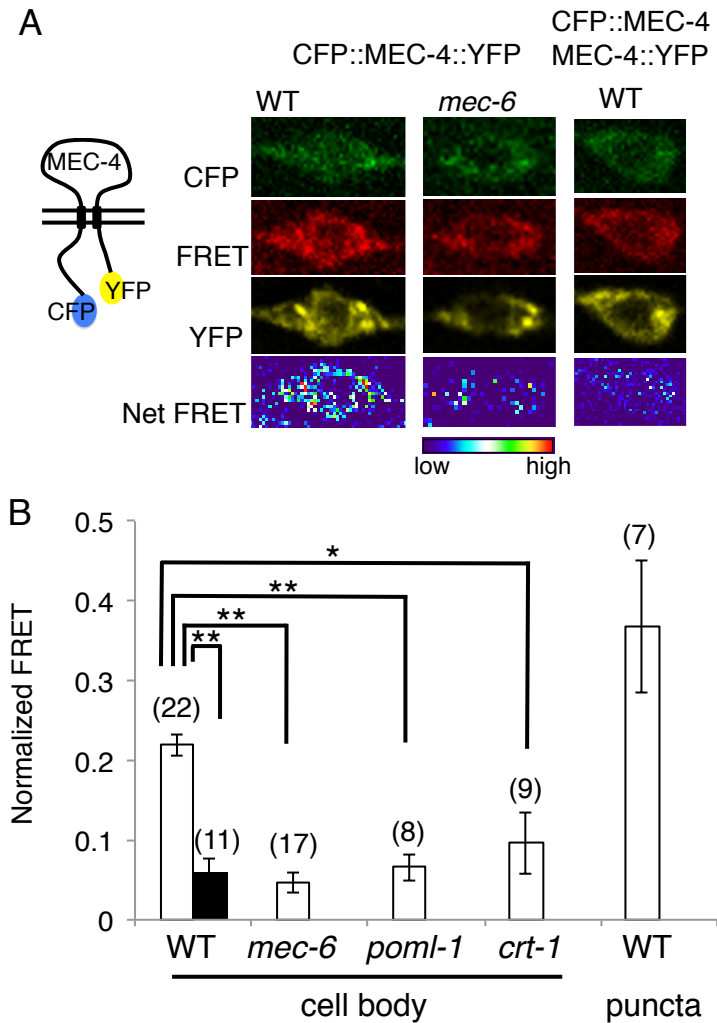


Figure 6 (II-6). The FRET signal of CFP::MEC-4::YFP. (A) Schematic of CFP::MEC-4::YFP protein (left panel) and images of CFP::MEC4::YFP or CFP::MEC-4 with MEC-4::YFP taken with the CFP (green), FRET (red), and YFP (yellow) channels, respectively (right panel). The Net FRET signal is given by a pseudocolored image to show the relative intensity. (B) The normalized FRET signal (see Experimental Procedures, mean  $\pm$  SEM) of CFP::MEC-4::YFP (white bar) in the cell body of WT and mutants and in the puncta of WT. The black bar represents the normalized FRET signal (mean  $\pm$  SEM) in the TRN cell bodies containing CFP::MEC-4 and MEC-4::YFP. The number of cell bodies or strongly fluorescent puncta tested (from 2-3 stable lines with extrachromosomal arrays) is given in parentheses. \*  $p < 0.001$ ; \*\* $p < 0.0001$ . Unless noted the following mutations were used: *crt-1(ok948)*, *mec-6(u450)*, and *poml-1(ok2266)*.

## **MEC-6 increases the surface expression of MEC-4**

In keeping with a role for MEC-6 as a chaperone, we found that it greatly increased the amount of surface expression of MEC-4 in *Xenopus* oocytes using total internal reflection (TIRF) microscopy. The number of MEC-4::EGFP spots increased 50-fold in the presence of MEC-6 (from  $3.5 \pm 1.3$  spots to  $180 \pm 60$  spots; mean  $\pm$  SEM, Figures 7A and 7B). These results appear specific to MEC-6 since no significant increase of MEC-4 surface expression was observed with MEC-2, POML-1, or CRT-1 (Figures 7A and 7B). This result supports the hypothesis that MEC-6 assists the folding of MEC-4 and/or its transport to the plasma membrane.

In our previous study (Chelur et al., 2002), we did not detect an effect of MEC-6 on the surface expression of MEC-4 in *Xenopus* oocytes 5-6 days post injection using a biotinylation assay. These different results could have been due to the larger amount of MEC-4 cRNA used in the original experiments and to the relative lack of sensitivity of the biotinylation assay. Indeed, when we used the larger amount of MEC-4::EGFP cRNA (equivalent to what was used in our previous experiments), we observed a smaller difference (2.5-fold increase) in surface MEC-4-EGFP with MEC-6 (from  $86 \pm 16$  spots to  $305 \pm 40$  spots). The longer period of expression used in the previous study (5 days vs 2 days) may have also contributed to our not finding any difference in MEC-4 surface expression. One possibility is that the amount of MEC-4 at the latter times is approximately the same with or without MEC-6, but at earlier times the MEC-6-dependent MEC-4 expression on the surface is more obvious.

Because the change in surface MEC-4 was seen so early following oocyte injection, we tested whether an early change could also be seen in MEC-4(d) currents in the frog oocytes. Indeed, MEC-6 increased the MEC-4(d) current over 30 fold to about 50% of the maximum current two days post injection (Figure 7C) (the fold difference is greater here than above because these oocytes had been injected with the lesser amount of *mec-4* cRNA, so the MEC-4(d) current was lower). In contrast, MEC-2 and POML-1 barely increased the MEC-4(d) current two days post injection (Figure 7C). [CRT-1 did not increase MEC-4(d) current at any time tested (data not shown).] Thus, MEC-6 shortened the amount of time required for MEC-4 to reach the surface and produce observable currents in *Xenopus* oocytes.

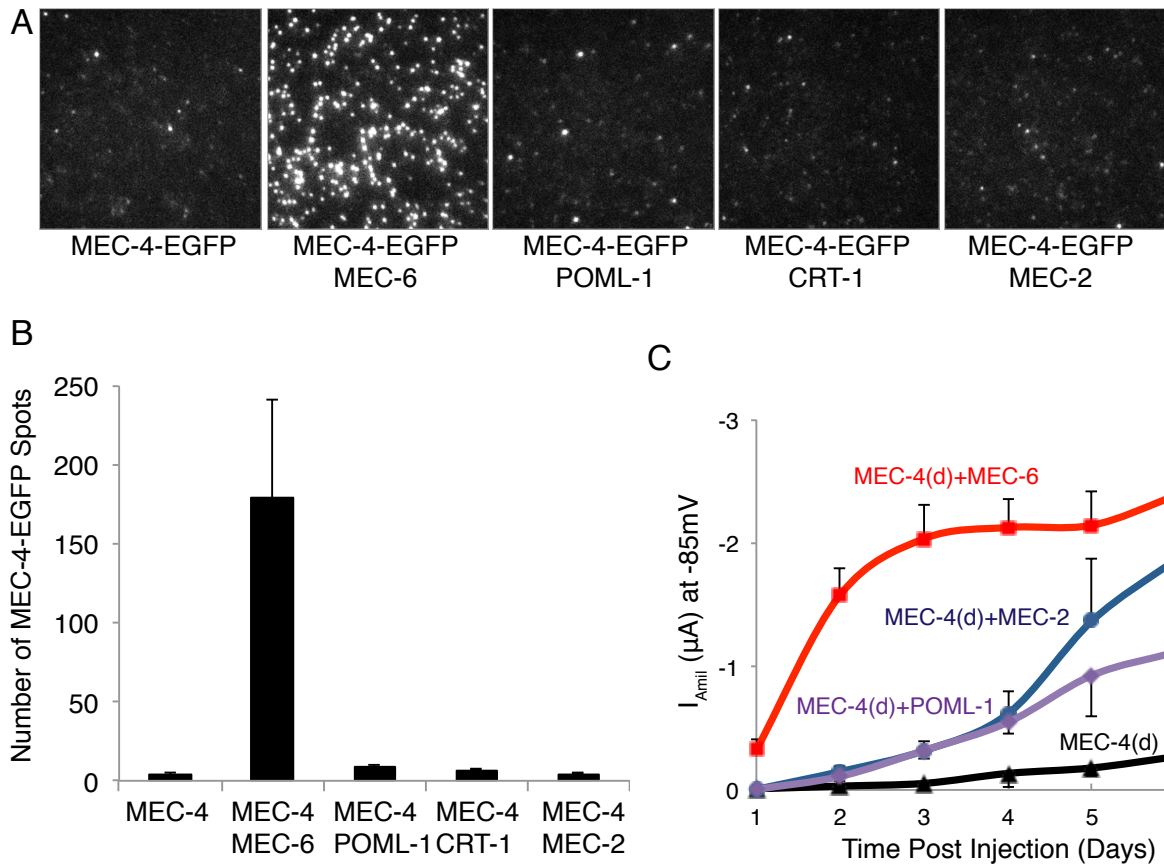


Figure 7 (II-7). The effect of MEC-6, POML-1 and CRT-1 on MEC-4 surface expression. Images (A) and quantification (B) of MEC-4::EGFP fluorescent spots on the *Xenopus* oocytes surface by TIRF imaging (mean  $\pm$  SEM,  $n = 9-12$  patches). 7-10 cells from two different batches were examined. The field dimensions are  $13 \mu m \times 13 \mu m$ . *Xenopus* oocytes were injected with 3.75 ng MEC-4 cRNA, 1 ng MEC-6 cRNA, 3.75 and 7.5 ng MEC-2 cRNA, 3.75 and 5 ng cRNA of POML-1, and 3.75 ng CRT-1. (C) The amiloride-sensitive MEC-4(d) current at  $-85 mV$  (mean  $\pm$  SEM; from 6-10 oocytes of two batches) on its own and in the presence of MEC-2, MEC-6, and POML-1 at various times post injection. *Xenopus* oocytes were injected with 3.75 ng MEC-4 cRNA, 1 ng MEC-6 cRNA, 7.5 ng MEC-2 cRNA, 5 ng cRNA of POML-1.

## **Stoichiometry and co-localization of the MEC-4/MEC-10 channel complex**

We examined the association and stoichiometry of the proteins of the MEC-4/10 channel complex using single molecule optical imaging (Ulbrich and Isacoff, 2007, 2008) in *Xenopus* oocytes. The tagged proteins used in these experiments retained their normal function, as they rescued touch sensitivity in *C. elegans* mutants and produced similar currents as untagged protein when expressed in *Xenopus* oocytes (Figure 8A). When expressed alone in *Xenopus* oocytes, MEC-4 formed homotrimers (Figure 8B). The stoichiometry of MEC-10 expressed on its own could not be determined because of its continuous mobility on the oocytes surface (Movie S1). In contrast, coexpression of MEC-10 and MEC-4 produced stable, colocalized complexes containing two molecules of MEC-4 and one of MEC-10 (Figures 8C, 8D, and 8E). These results are consistent with the stoichiometry of ASIC1, a chicken DEG/ENaC homotrimeric protein (Jasti et al., 2007).

The lack of visible MEC-10::GFP puncta in the TRNs, although previously observed (Chatzigeorgiou et al., 2010), is nonetheless surprising given the association of MEC-4 and MEC-10 in the oocyte and the appearance of MEC-4 puncta in the TRNs. Even eliminating endogenous MEC-10 using the *mec-10(ok1104)* mutation did not result in MEC-10::GFP puncta (data not shown). Interestingly, we did see MEC-10::GFP puncta, which colocalized with MEC-4::TagRFP in puncta in the TRN process, but only when animals expressed both fusion proteins (Figure 8F). MEC-10::GFP puncta were also seen when multiple copies of untagged MEC-4 was expressed (Figure 8F). Previous studies showed that the formation of MEC-4::GFP puncta did not require MEC-10 (Arnadóttir et al., 2011). These results suggest

that MEC-10 is not a major component of the puncta, except, perhaps, when MEC-4 is overexpressed.

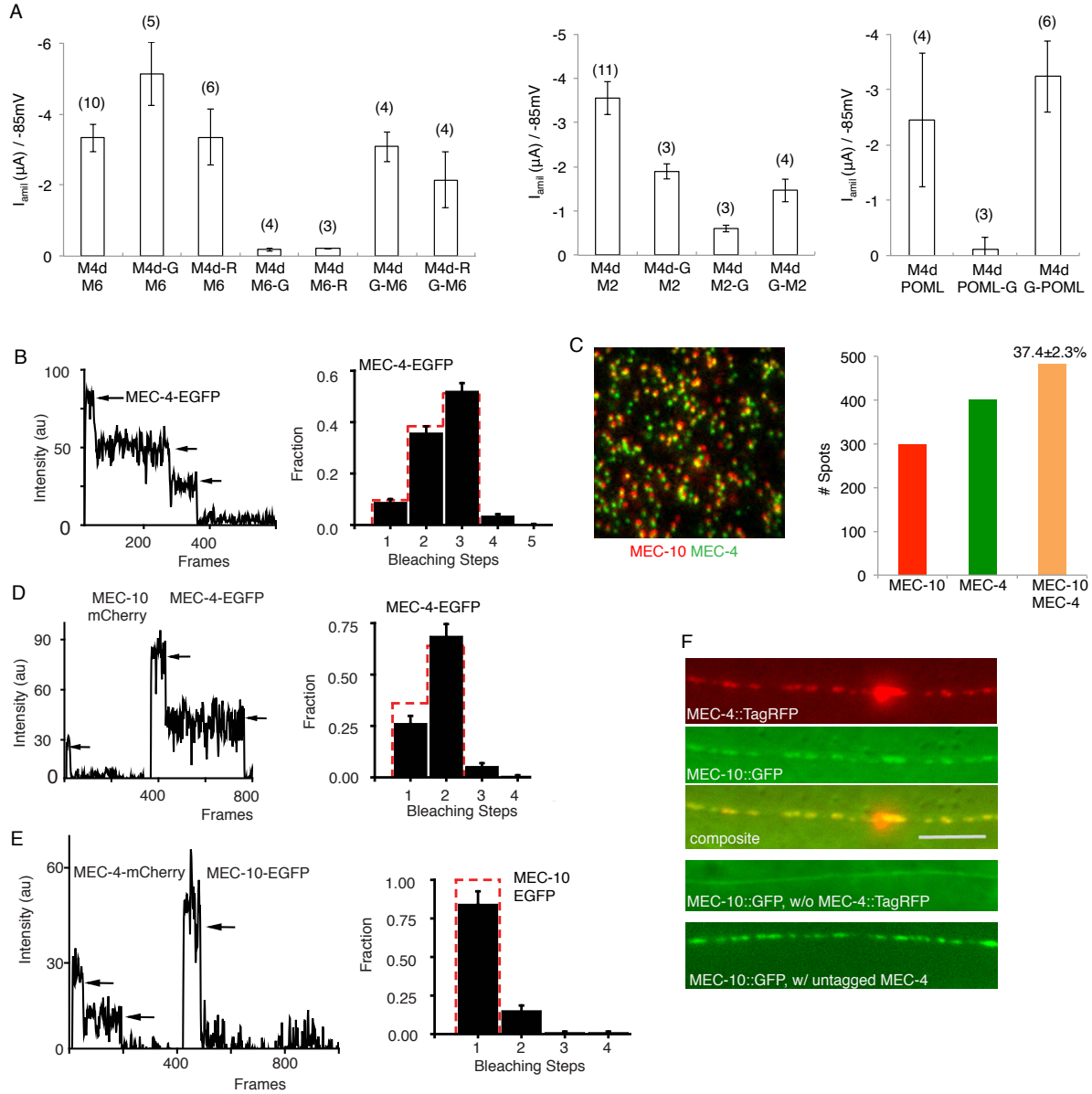


Figure 8 (II-8). The stoichiometry and co-localization of the MEC-4/MEC-10 channel complex. (A) The effect of N or C-terminal EGFP/mCherry-tagged MEC-4(d), MEC-2, MEC-6 and POML-1 on the amiloride-sensitive current at -85mV in frog oocytes (mean  $\pm$  SEM). G indicates EGFP; R indicates mCherry. The number of tested oocytes is given in parenthesis. B-E display results from experiments examining expression on the plasma membrane of *Xenopus* oocytes; F shows expression in the TRNs in vivo. (B) MEC-4::EGFP forms trimers on its own. Left panel shows an example of a MEC-4::EGFP complex with three bleaching steps (arrows). The right panel (here and in Figures 8E, 9A and 9C) gives the observed number of bleaching steps (black bars) as well as predicted pattern (red dotted bars). The error bars in the subunit counting data show counting errors and are given by  $I/N*\sqrt{n}$  ( $n$ = total number of spots for each step;  $N$ = total number of spots for all steps). (C) The co-localization of MEC-4-EGFP and MEC-10-mCherry. The left panel shows a representative image; the right panel shows the number of spots with MEC-4 alone (green), MEC-10 alone (red), and both proteins (orange). The co-localization fraction (here and in Figures 9B and 9D) is given as mean  $\pm$  SEM. (D and E) An example (left panel) and quantification (right panel) of the photobleaching of a MEC-4<sub>2</sub>MEC-10 heterotrimer. (F) MEC-10::GFP puncta form only in the presence of MEC-4::TagRFP puncta, with which they colocalize in the TRN process. Scale bar = 5  $\mu$ m.

Although we had previously thought that MEC-6 was also part of the TRN channel complex (Chelur et al., 2002), single molecule imaging in *Xenopus* oocytes showed that MEC-6 (N or C-terminally tagged) existed as a stable monomer (Figure 9A) that did not bind to MEC-4 (with or without MEC-10, Figure 9B and data not shown) or change MEC-4 stoichiometry (Figure 9C). These results argue against MEC-6 being part of the channel complex. In addition the MEC-6 monomers did not appear to co-localize with POML-1 (Figure 9D), a result consistent with the weak physical interaction between these two proteins (Figure 3C). Because these proteins appeared to co-localize in the TRNs (Figures 1D and 1F), the colocalization may reflect their existence in the same domain within the cell.

We also asked whether MEC-2 colocalized with MEC-4. The stoichiometry of MEC-2 could not be determined because the molecules moved on the surface of frog oocytes even in the presence of MEC-4 and did not seem to co-localize with MEC-4 (Movie S2). In addition, MEC-2 did not change the stoichiometry of the MEC-4 trimer (Figure 9E). In

contrast, MEC-2 (detected by an anti-MEC-2 antibody) often colocalized with MEC-4::TagRFP puncta in TRN processes (Figure 9F) as reported previously (Zhang et al., 2004). These results could indicate that MEC-2 and MEC-4 are loosely associated in the TRNs (a weak interaction would not be detected at the low density expression in the single molecule imaging experiments) or that their association needs other factors present in the TRNs but not in *Xenopus* oocytes.

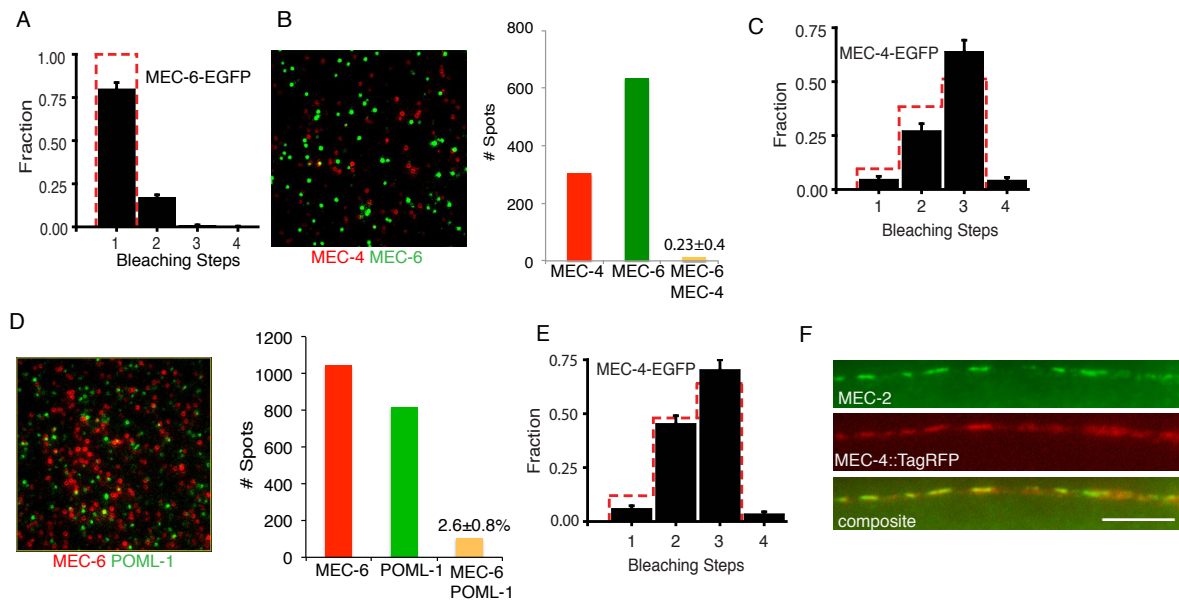


Figure 9 (II-9). MEC-2, MEC-6, POML-1, and MEC-4 do not colocalize on the plasma membrane of *Xenopus* oocytes. (A) Quantification of bleaching steps indicating that MEC-6-EGFP is monomeric. (B) MEC-4-mCherry and EGFP-MEC-6 fail to colocalize in the presence of untagged MEC-10. (C and E) Bleaching steps indicate that MEC-4::EGFP forms trimers in the presence of MEC-6 (C) and MEC-2 (E). The observed number of bleaching steps (black bars) and the predicted pattern (red dotted bars) are indicated. (D) MEC-6-mCherry and EGFP-POML-1 fail to colocalize. (F) MEC-2 (detected with an anti-MEC-2 antibody) co-localizes with MEC-4::TagRFP. Scale bar = 5 μm.



## Discussion

### **MEC-6 and POML-1 may be DEG/ENaC-specific chaperones**

The experiments presented here provide a very different view of MEC-6 (and POML-1) activity than we hypothesized previously (Chelur et al., 2002). By examining MEC-6 action in frog oocytes at earlier times, the TIRF and electrophysiological experiments correct these previous results and show that MEC-6 is needed for rapid accumulation of MEC-4 at the plasma membrane. The ER localization of MEC-6 and POML-1 in the TRN cell body, their absence from the plasma membrane of TRN processes in culture, their failure to colocalize with MEC-4 or MEC-2 in vivo and in frog oocytes, and their effect on MEC-4 surface expression in vivo and in frog oocytes suggest that these proteins are more important for the production of the channel complex than for its function. Furthermore MEC-6 does not affect the amiloride-binding affinity and single channel conductance of the MEC-4(d) channel expressed in frog oocytes, whereas MEC-2 and MEC-10 do (Brown et al., 2008; Goodman et al., 2002). Moreover, only slight binding is seen between MEC-6 and MEC-4 and between POML-1 and MEC-4.

The results with MEC-6 and POML-1 suggest a role in the production and transport of MEC-4, perhaps as chaperones. This hypothesis is supported by the similarity in the action of *mec-6* and *poml-1* mutations to that of *crt-1* mutations, which affect a Ca<sup>2+</sup> binding chaperone (Park et al., 2001), on MEC-4(d)-induced deaths, MEC-4 distribution, and MEC-4 folding.

The three proteins do not act identically. For example, the mutant phenotypes of *poml-1* and *crt-1*, but not *mec-6*, were partially rescued by over-expression of SEC-24. Although all these three proteins affect MEC-4 folding in the TRNs, only MEC-6 demonstrably shortened the time required for MEC-4 to reach the surface and become active in *Xenopus* oocytes. These data suggest that MEC-6 may have additional functions from the other two proteins. In contrast, POML-1 may play a different or minor role, which cannot be detected by the TIRF experiment; other proteins in *Xenopus* oocytes may compensate for CRT-1.

In contrast to CRT-1, which has more general functions in cells, e.g., facilitating glycoprotein folding and regulating Ca<sup>2+</sup> homeostasis in the ER (Michalak et al., 2009), MEC-6 and POML-1 seem to act specifically on DEG/ENaC protein. MEC-6, which is expressed in many neurons and muscles, is needed for the action of gain-of-function (d) mutations affecting several DEG-ENaC proteins (DEG-1, UNC-8, and UNC-105) and ectopically-expressed MEC-4(d), but not a gain-of-function, degeneration-causing mutation affecting the nicotinic acetylcholine receptor protein DEG-3 (Chalfie and Wolinsky, 1990; García-Añoveros et al., 1995; Shreffler et al., 1995; Harbinder et al., 1997). POML-1 is more narrowly expressed. In addition mutations in *mec-6* and *poml-1* do not affect the expression of each other or other TRN proteins, such as MEC-2 and MEC-18 (data not shown), and their loss did not generally disrupt TRN development or affect light induced activation of TRN-expressed channelrhodopsin-2.

Because POML-1 increased MEC-4d channel activity in *Xenopus* oocytes with MEC-2 or with MEC-2 and MEC-6 together, but not with MEC-6 on its own, we hypothesize that either the larger current reveals an additional effect of POML-1 or that POML-1 may affect

MEC-2 activity. The finding that both MEC-6 (Chelur et al., 2002) and POML-1 (this work) can produce an amiloride-resistant current in *Xenopus* oocytes hints that they may act on other proteins. Unfortunately, we could not test directly the effect of POML-1 on MEC-2 surface expression in *Xenopus* oocytes because of the continuous mobility of MEC-2 at the surface. Nonetheless, because the loss of *poml-1* did not affect the distribution of MEC-2 puncta in the TRN process, any potential effect of POML-1 on MEC-2 expression may be relatively minor.

MEC-6 and POML-1 and the human PONs are ~27% identical (over the C-terminal 260 residues), and all have an N-terminal hydrophobic region (Sorenson et al., 1999). Interestingly, two of the three mammalian PONs, PON2 and PON3 are found in the ER (Horke et al., 2007; Schweikert et al., 2012). The characterization of MEC-6 and POML-1 in *C. elegans* suggests a novel function of this protein family: ER chaperones that facilitate the maturation and export of DEG/ENaC and, perhaps in mammalian cells, other proteins.

The requirement for these proteins for the production of DEG/ENaC channels need not be absolute. Functional MEC-4 channels are made, albeit slower, in *Xenopus* oocytes without MEC-6. Moreover, although *Drosophila melanogaster* has 25 genes encoding DEG/ENaC proteins (Liu et al., 2003), it has no genes encoding proteins that are obviously similar to MEC-6, POML-1, or the mammalian PON proteins (Hicks et al., 2011). Presumably the function of these PON-like proteins has been assumed by other proteins in *Drosophila*.

### **The MEC-4/MEC-10 channel is heterotrimeric**

MEC-4 and MEC-10 formed MEC-4<sub>3</sub> and MEC-4<sub>2</sub>MEC-10 trimers in frog oocytes. This arrangement is consistent with the crystal structure of the chicken DEG/ENaC protein ASIC1 channel (Jasti et al., 2007) and immunoelectron microscopy, which suggested that half of the membrane-associated MEC-4 existed as doublets (Cueva et al., 2007). In contrast to MEC-4, which formed immobile homotrimers on the oocyte surface, MEC-10 was very mobile on its own, so we could not determine its stoichiometry. Since MEC-10(d) does not form a functional channel in frog oocytes (Goodman et al., 2002), it may not be able to form trimers on its own. The differences between MEC-4 and MEC-10 may explain several genetic results: 1) loss of MEC-4 causes complete touch insensitivity (Chalfie and Sulston, 1981), whereas loss of MEC-10 does not (Arnadóttir et al., 2011); 2) MEC-4(d) causes nearly 100% TRN cell death and its toxicity does not require MEC-10, whereas MEC-10(d) only causes about 30% TRN cell death and its toxicity requires MEC-4 (Huang and Chalfie, 1994); and 3) MEC-10::GFP localization needs MEC-4::TagRFP whereas MEC-4::TagRFP localization as puncta does not need MEC-10.

Several other DEG/ENaC proteins cannot form functional homomeric channels. The mammalian epithelial sodium channel has three subunits ( $\alpha$ -,  $\beta$ -, and  $\gamma$ -ENaC), but only  $\alpha$ -ENaC forms a functional channel on its own (Canessa et al., 1994). In contrast, ASIC channels (including ASIC1, ASIC2 and ASIC3) can form functional homomeric and heterotrimer channels with distinct physiological properties (Benson et al., 2002). We could not predict the interacting residues of MEC-4 and MEC-10 based on those of the chick ASIC1 channel, because most of the prominent interacting residues in ASIC1 are not conserved in MEC-4 or MEC-10.

The formation of MEC-4<sub>2</sub>MEC-10 trimers brings into question the role of the MEC-4 puncta and whether they are the sites of mechanically-gated channels. Electrophysiological evidence predicts that the number of functional channels is about the same as the number of puncta (O'Hagan et al., 2005), yet such trimeric channels should not be visible with either fluorescent protein tags or with antibodies. Therefore, most channels in the puncta are probably inactive. Indeed, MEC-10::GFP puncta did not form unless MEC-4::TagRFP was present. In addition, *poml-1* mutants are touch sensitive, but have no obvious MEC-4 puncta in their processes. Presumably, these animals have functional trimers. Since MEC-4 puncta can be seen with anti-MEC-4 antibodies (Cueva et al., 2007), they are not artifacts of fluorescent protein expression. One possibility is that the puncta may be intracellular reservoirs for MEC-4 (and possibly other proteins). Indeed, Cueva et al. (2007) found about half of the MEC-4 immunogold labeling in electron micrographs to be associated with the plasma membrane of TRNs; and the rest are associated with 15-protofilament microtubules. Butterworth et al. (2005) have suggested that mammalian ENaC channels can enter the plasma membrane from a recycling pool.

### **A simplified mechanosensory channel complex**

The data presented here simplify the model of the mechanotransduction complex in the TRNs. We have confirmed the high affinity and stable association of MEC-4 and MEC-10, but suggest that the other membrane proteins, MEC-2 (and perhaps UNC-24, which we did not test), MEC-6, and POML-1 have very low affinity and/or transient interactions with MEC-4 and MEC-10. MEC-2 binds cholesterol and we have hypothesized that it may be

necessary for touch sensitivity because it modulates the lipid microenvironment of the MEC-4<sub>2</sub>MEC-10 channel (Huber et al., 2006). The finding that MEC-2 and a similar protein, podocin, form multimeric complexes in HEK293T1/2 cells (Huber et al., 2006) may explain why a MEC-2 antibody identifies puncta that colocalize with MEC-4 puncta (Zhang et al., 2004; Cueva et al., 2007) even though we do not find evidence for a direct interaction. Our data suggest new, non-transduction roles for MEC-6, POML-1, and MEC-2, but cannot exclude the possibility that they also directly affect, albeit transiently, the transduction complex.

## Chapter III

### **MEC-10 and C49G9.1 reduce the neurotoxicity of the MEC-4(d) DEG/ENaC channel**

(The following manuscript will be submitted to *Genetics* with other authors, including Shashank Bharill, Robert O'Hagan, Ehud Y. Isacoff, and Martin Chalfie. Shashank Bharill performed the single molecule imaging and the TRIF imaging experiment in *Xenopus* oocytes. Robert O'Hagan collected the in vivo electrophysiology data. I performed the remaining experiments.)

## Summary

The *C. elegans* DEG/ENaC proteins MEC-4 and MEC-10 transduce gentle touch in the six touch receptor neurons (TRNs). Gain-of-function mutations of *mec-4*, *mec-4(d)*, result in a hyperactive channel and neurodegeneration in vivo. Loss of MEC-6, a putative DEG/ENaC-specific chaperone, or the similar protein POML-1 suppress the neurodegeneration caused by *mec-4(d)* mutations. We find that mutation of two genes, *mec-10* and C49G9.1 prevent this action of POML-1, allowing the TRNs to die in *poml-1 mec-4(d)* animals. The proteins encoded by these genes affect *mec-4(d)* neurotoxicity through different mechanisms. MEC-10 inhibits MEC-4(d) activities, without affecting MEC-4 expression. In contrast, C49G9.1, a membrane protein specific to nematodes, inhibits MEC-4(d), at least in part, by reducing MEC-4 surface expression.



## Introduction

Degenerin and epithelial Na<sup>+</sup> channel (DEG/ENaC) proteins form sodium-selective, amiloride-sensitive channels in invertebrate and vertebrate. These channels can be constitutively active (the ENaC channels; Canessa et al., 1993; Lingueglia et al., 1993) or they can be gated mechanically (O'Hagan et al., 2005), by acid (Canessa et al., 1993; O'Hagan et al., 2005; Waldmann et al., 1997), or by small peptides (FMRFamide peptide-gated Na<sup>+</sup> channel (Lingueglia et al., 1995). DEG/ENaC channels serve a wide range of functions, including mechanosensation, sour and sodium taste, peripheral pain, synaptic plasticity, learning and memory, and sodium homeostasis (Ben-Shahar, 2011; Schild, 2010; Wemmie et al., 2002).

Accumulation of high levels of constitutively-open ENaC channels or hyperactivation of gated DEG/ENaC channels can be very detrimental. For example, the excessive accumulation of ENaC channels in the kidney leads to increased sodium reabsorption and hypertension in Liddle syndrome in humans (Snyder, 2002). The hyperactivation of ASIC1 channel by local acidosis caused by ischemia and stroke in mouse brains causes massive neuronal death (Xiong et al., 2004). Gain-of-function mutations affecting *C. elegans* DEG/ENaC proteins produce hyperactive channels that cause neuronal lysis and degeneration (Chalfie and Wolinsky, 1990; Goodman et al., 2002; Shreffler et al., 1995; Tavernarakis et al., 1997) or hypercontraction of muscle (UNC-105; Liu et al., 1996; Park and Horvitz, 1986). Therefore, studying molecular mechanisms that regulate hyperactive DEG/ENaCs will better our understanding of both hyperactivation-induced toxicity and the normal channel physiology.

In the DEG/ENaC family, *C. elegans* DEG/ENaC proteins MEC-4 is best characterized at genetic details. MEC-4 is essential for touch sensitivity, and together with MEC-10, comprise the pore of the mechanotransduction complex in the six touch receptor neurons (Arnadottir et al., 2011; O'Hagan et al., 2005). The *mec-4(d)* gain-of-function mutation results in an A713T substitution that causes constitutive channel activation and thus neurodegeneration (Brown et al., 2007; Driscoll and Chalfie, 1991; Goodman et al., 2002). The *mec-4(d)* induced cell death requires three proteins with chaperone activities: MEC-6 (paraoxonase-like protein), CRT-1/calreticulin (calcium binding chaperone), and POML-1, which encodes a MEC-6 and paraoxonase like protein in *C. elegans* (Chalfie and Wolinsky, 1990; Xu et al., 2001; Y.C and M.C, submitted). However, it remains unknown what factors inhibit *mec-4(d)* neurotoxicity.

Here we performed a genetic screening for enhancers of *mec-4(d)*-induced TRNs cell death in *poml-1 mec-4(d)* genetic background, and found loss of *mec-10* or C49G9.1 make *mec-4(d)* more toxic. Their protein products, MEC-10 and C49G9.1 reduced MEC-4(d) activities through different mechanism: MEC-10 dampened MEC-4(d) activities without affecting MEC-4 expression. By contrast, C49G9.1, a novel membrane protein expressed in TRN, inhibited MEC-4(d), at least partly through reducing MEC-4 surface expression.

## **Experimental procedures**

### ***C. elegans* procedures**

Unless otherwise indicated, strains were maintained and studied at 20°C according to Brenner (1974) on the OP50 strain of *E. coli*. The strains used in this study are given in Table

4. Strains with the *poml-1(ok2266)*, *mec-10(ok1104)*, *C49G9.1(ok2504)*, *crt-1(ok948)* mutations were obtained from the *C. elegans* Genetic Center. *mec-4(d)(e1611)*, *mec-4(u45)*, *mec-6(u450)* (Chalfie and Au, 1989; Driscoll and Chalfie, 1991; Huang and Chalfie, 1994; Zheng et al., 2013) have been described previously. *C49G9.1(u898)* was obtained by ethyl methanesulfonate mutagenesis as described below. Double or triple mutants were created by standard genetics procedures and verified either phenotypically or by PCR.

Ethyl methanesulphonate mutagenesis was performed according to (Brenner, 1974) to identify suppressors of the *poml-1* suppression of *mec-4(d)* degeneration. We mutagenized TU3871 [*uls152 (Pmec-3::tagrfp)*; *uls31(mec-17::gfp)*; *poml-1(ok2266) mec-4(d)(e1611)*] animals and screened F2 progeny for animals missing RFP and GFP in the TRNs, but expressing RFP in the FLPs. Normally in TU3871 animals TagRFP labels both the TRNs and the FLP neurons and MEC-17::GFP labels only the TRNs.

We assayed for gentle touch sensitivity in blind tests as described (Chalfie and Sulston, 1981). We quantified the response by counting the number of response to 10 touches delivered alternately near the head and tail in 30 animals (Hobert et al., 1999)

We performed in vivo electrophysiology as previously described (O'Hagan et al., 2005).

Table 4 (III-1). Strains used in these studies.

Strain	Genotype
TU3871	<i>uls152(Pmec-3::tagrfp); uIs31; poml-1(ok2266) mec-4(e1611)</i>
TU3964	<i>mec-10(ok1104) poml-1(ok2266)</i> , TU3965 [ <i>mec-10(ok1104) poml-1(u882)</i>
TU3966	<i>mec-6(u450); uIs152; uIs31; mec-10(ok1104) poml-1(ok2266) mec-4(e1611)</i>
TU3968	<i>uls152; uIs31; mec-10(ok1104) poml-1(ok2266) mec-4(e1611)</i>
TU4013	<i>mec-6(u450) C49G9.1(u898); uIs152; uIs31; poml-1(ok2266) mec-4(e1611)</i>
TU4270	<i>C49G9.1(ok2504); uIs152; uIs31; poml-1(ok2266) mec-4(e1611)</i>
TU4360	<i>uIs146; uEx869[C49G9.1(+), Pmyo2::mCherry)</i>
TU4355	<i>C49G9.1(u898); uIs146</i> , TU4394 [ <i>uIs31; mec-4d(e1611); uEx869</i>
TU4327	<i>C49G9.1(u898); uIs31; poml-1(ok2266)</i>
TU4328	<i>C49G9.1(u898); uIs31</i>
TU4243	<i>uEx851(Pmec-4::mec-4::tagrfp); C49G9.1(u898); poml-1(ok2266)</i>

### Plasmids and Microinjection

*C49G9.1::gfp* and has been described (Topalidou and Chalfie, 2011).

*Pmyo2::mCherry* (PCFJ90) was obtained from Addgene ([www.addgene.org](http://www.addgene.org)). *mec-4::tagrfp* (TU#1175) was generated by removing *yfp::unc-54* 3'UTR from *mec-4::yfp* (Chelur et al., 2002) using *KpnI* and *ApaI* and replacing it with *tagrfp::unc-54* 3'UTR. *Pmec-4::aman-2::tagrfp* (TU#1181) was made by using the Three-Fragment Vector Construction Kit (Invitrogen). *mec-4* promoter and start codon of 1023 bp was cloned into pDONRP4P1R. *aman-2* coding sequence of 300bp (Rolls et al., 2002) was cloned into pDONR221. *tagrfp* and *unc-54* 3'UTR was cloned into pDONRP2RP3.

We microinjected 5-10 ng/μl of the relevant plasmid, 2 ng/μl *Pmyo2::mCherry* (PCFJ90) and 40 ng/μl of the *lin-15(+)* plasmid and pBluescript SK plasmid to make up to 100 ng/μl DNA in total. For complex array microinjection, we injected 0.2-2 ng/μl of PCR product or linearized plasmids, 10ng/μl *Pinx-20::gfp* as a marker and 125 ng/μl linearized *E. coli* OP50 genomic DNA.

## **Microscopy and Immunofluorescence**

Fluorescence and immunofluorescence were observed using a Zeiss Axio Observer Z1 inverted microscope and a Zeiss Axioskop II. Confocal images were acquired using Confocal ZEISS LSM700. Live animals were anesthetized using 0.1 mM 2-3 butanedione monoxime in 10 mM HEPES, pH 7.4.

MEC-4::TagRFP intensity in the cell body was determined by measuring the mean intensity of the entire cell body (20-30  $\mu\text{m}^2$ ) and subtracting the mean intensity of nearby background of the same size using Image J ([rsbweb.nih.gov/ij/](http://rsbweb.nih.gov/ij/)). The intensity of the MEC-4::TagRFP puncta in TRN processes was measured in the best focused image of six images taken at different depths through the TRNs using the Puncta Analysis Toolkit beta developed by Dr. Mei Zhen (Samuel Lunenfeld Research Institute, Toronto, Canada). Puncta were examined over a region approximately equivalent to ten cell body lengths starting near the cell body.

We performed single molecule fluorescence *in situ* hybridization (SM-FISH) as previously described (Topalidou et al., 2011). For imaging of individual protein complex in *Xenopus* oocyte membrane by total internal reflection fluorescence (TIRF) microscopy was performed as previously described (Abuin et al., 2011; Ulbrich and Isacoff, 2007, 2008).

Immunostaining was performed according to Miller and Shakes (1995) using antibodies against MEC-4 (mouse, Abcam ab22184) diluted 1:200 and Alex Fluor 488/555 goat anti-mouse (Invitrogen, Carlsbad, CA) diluted 1:1000.

## **Oocyte Experiments**

cRNA expression and electrophysiology in *Xenopus laevis* oocytes followed the procedures and used the plasmids described in Goodman et al. (2002). C49G9.1 cDNA of 390 bp was obtained by RT-PCR from cDNA library (generated by reverse-transcription using wild-type mRNA), and was cloned in pGEM-HE (Liman et al., 1992). 10 ng cRNA of *mec-4(d)*, 1 ng *mec-6*, and 1 ng C49G9.1 were injected to *Xenopus laevis* oocytes unless noted (Xenopus I, Dexter, MI or Nasco, Fort Atkinson, WI). Oocytes were maintained as previously describe by Arnadottir et al. (2011). Membrane current was measured 4-6 days after RNA injection using a two-electrode voltage clamp as previously described by Goodman et al. (2002).

C-terminally HA-tagged C49G9.1 and N-terminally Myc-tagged MEC-4(d) were expressed in oocytes as described previously (Goodman et al., 2002). Immunoprecipitation were performed 5-6 days after cRNA injection and detected by using antibodies against the Myc and HA tags (Sigma) and horse radish peroxidase-conjugated secondary antibodies (Jackson ImmunoResearch Laboratories, West Grove, PA).

## **Statistics**

Statistical analysis was done using the Student t-test unless otherwise noted.

## **Results**

### **Loss of *mec-10* or C49G9.1 enhances TRN cell death in *poml-1 mec-4(d)* animals**

Loss of *poml-1* (e.g. with the *ok2266* mutation) lowers MEC-4 protein levels and suppresses *mec-4(d)*-induced TRN degeneration (90% of the TRNs live; Y.C and M.C,

submitted). To identify components that may act downstream of POML-1 to allow the deaths and/or genes that normally reduce MEC-4 activity, we screened for mutations that increased TRN cell death in *poml-1(ok2266) mec-4(d)* animals. The starting strain also contained *mec-3p::tagrfp* to label the TRNs and the FLP neurons and *mec-17p::gfp* to label the TRNs. Mutations that allowed TRN deaths would lack the TRN label but not the FLP label.

Seventeen such mutations were found among 20,000 haploid genomes after ethyl methanesulfonate mutagenesis (Table 2; one mutation was a *mec-3* missense mutation (F33Y), which gave the phenotype by causing *mec-3* expression in the FLP neurons, but not in the TRNs). Fifteen of the mutations affected *mec-10*; these mutations included nonsense alleles, missense alleles, a deletion allele, and several splice junction alleles. Several of these *mec-10* mutations acted semi-dominantly. The *mec-10(ok1104)* allele, which is considered to be a loss-of-function deletion (Arnadóttir et al., 2011), also enhanced the TRN cell death in *poml-1(ok2266) mec-4(d)* animals semi-dominantly (Figure 1A). Addition of a wild-type copy of the gene rescued the effects of the *mec-10* mutations (Figure 1A).

The inhibitory effect of MEC-10 on MEC-4(d)-induced TRN neurodegeneration is consistent with our previous finding that MEC-10 decreased MEC-4(d) activity in *Xenopus* oocytes (Goodman et al., 2002). Thus, both the in vivo and in vitro data suggest that MEC-10(+) inhibits MEC-4(d) channel activity. Paradoxically, null alleles of *mec-10* cause a modest loss of the touch sensitivity (Arnadóttir et al., 2011), which was significantly enhanced by *poml-1* null mutations (*ok2266* and *u882*; Figure 1B). These data suggest that MEC-10 and POML-1 act additively in touch sensitivity, but against each other with regard to MEC-4(d) channel activity.

Table 2 (III-2). *poml-1* suppression of *mec-4d* requires *mec-10* and C49G9.1

Gene	Allele	Mutation	D/R*	% ALM	% PLM
<i>mec-10</i>	<i>u883</i>	TGG>TGA, 95W>Stop	semi-D	0	0
	<i>u884</i>	CAG>TAG, 147Q>Stop	semi-D	0	4
	<i>u885</i>	TGG>TGA, 618W>Stop	R	0	2
	<i>u886</i>	TGC>TAC, 170C>Y	R	0	3
	<i>u887</i>	TCC>TTC, 471S>F	R	2	12
	<i>u888</i>	CGC>TGC, 507R>C	R	1	6
	<i>u889</i>	TGC>TAC, 557C>Y	R	2	13
	<i>u890</i>	GTG>ATG, 573V>M	R	5	17
	<i>u891</i>	G>A splicing junction, 2nd exon	R	1	5
	<i>u892</i>	G>A splicing junction, 6th exon	R	2	11
	<i>u893</i>	A>T 3rd nucleotide, 6th intron	R	2	8
	<i>u894</i>	G>A splicing junction, 9th exon	semi-D	2	2
	<i>u895</i>	G>A splicing junction, 14th exon	semi-D	1	4
	<i>u896</i>	G>A, 6th nucleotide, 16th intron	R	2	1
	<i>u897</i>	deletion**	semi-D	6	18
C49G9.1	<i>u898</i>	deletion of the first exon	R	1	2
<i>mec-3</i>	<i>u899</i>	TTT>TAT, 33F>Y	R	0	1

\*D, dominant; R, recessive. \*\*DNA from *u897* animals could not be amplified using primers that were 120 bp upstream of the start ATG and 80 bp downstream of the stop codon.



The remaining mutation deleted a 288 bp sequence containing 19 bp upstream of start codon, the first exon and part of first intron from C49G9.1. The effect on *mec-4(d)* degeneration was shown to be caused by the C49G9.1 mutation, because it could be rescued by the wild-type gene (Figure 1A). Given the nature of the deletion, this mutation is probably a null; it enhanced *mec-4(d)* recessively. We also tested the effect of C49G9.1 deletion on the suppression of *mec-4(d)* by *crt-1* and *mec-6* mutation. Loss of C49G9.1 also enhanced cell death in *crt-1; mec-4(d)* animals, but to a lesser extent (Figure 1A), suggesting that CRT-1 acts differently from POML-1. However, *mec-10* and C49G9.1 mutations has no effect on *mec-4(d)* degeneration when *mec-6* is lost (Figure 1A), probably due to a more broader role of *mec-6* in *mec-4(d)* function (Y.C. and M.C., submitted).

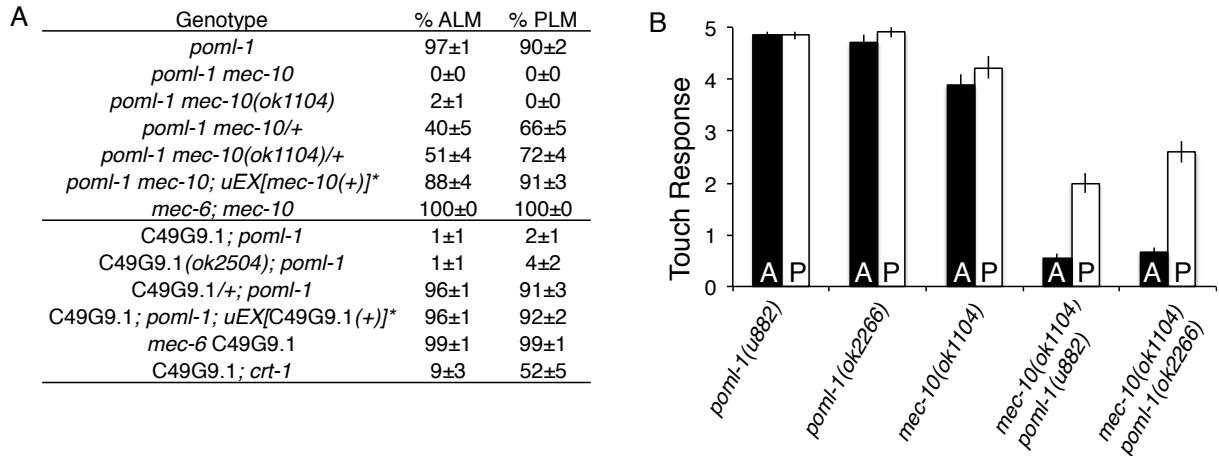


Figure 1 (III-1). *mec-10* and C49G9 on *mec-4(d)* degeneration and touch sensitivity. (A) Loss of *mec-10* and C49G9.1 enhanced TRNs degeneration in *poml-1 mec-4(d)*.  $n > 50$ . All experiments used *poml-1(ok2266)*, *mec-6(u450)*, *crt-1(ok948)*, *mec-10(u883)*, and C49G9.1(*u898*) unless noted. \**mec-10* rescue was examined in two stable lines ( $n > 50$  animals); C49G9.1 rescue was examined in four stable lines ( $n > 100$  animals). (B) *mec-10(ok1104)* further reduced the touch sensitivity of two *poml-1* null mutations (mean  $\pm$  SEM,  $n = 30$ ). A = anterior touch response; P = posterior touch response.

### C49G9.1 reduces MEC-4 surface expression in the TRN

C49G9.1 encodes a novel membrane protein of 129 amino acids with one predicted transmembrane domain near its N-terminus (Figure 2A). Similar proteins are found in nematodes but not in other organisms (Table 3 and Table 4). The gene is expressed in the TRNs, FLP neurons, and PVD neurons (Topalidou and Chalfie, 2011). A C49G9.1::GFP translational fusion was found throughout the TRN process and also on the plasma membrane of the TRN cell body (Figures 2B and 2C); it also forms puncta within the cell body. C49G9.1::GFP expression overlapped somewhat with MEC-4 (Figure 2B) and MEC-2 (Topalidou and Chalfie, 2011) in the proximal process and cell body. In the cell body, C49G9.1 puncta also overlap somewhat with the Golgi marker AMAN-2::TagRFP (Figure 2C).

Loss of C49G9.1 increased MEC-4 in the TRN processes by 70% in wild-type (Figures 2D and 2E) and *poml-1* animals (Figure 2F). C49G9.1; *poml-1* also expressed 40% less MEC-4 in their cell bodies than *poml-1* animals (Figure 2F), but a similar effect was not observed in wild type (Figure 2E). In contrast, loss of *mec-10* did not increase MEC-4 levels (Figure 2F). The increased MEC-4 was not due to an increase in the amount of steady state *mec-4* mRNA as measured by SM-FISH ( $8.2 \pm 0.3$  mRNA molecules/PLM for C49G9.1(*u898*),  $8.6 \pm 0.3$  for C49G9.1(*ok2504*), and  $8.7 \pm 0.4$  for wild type, mean  $\pm$  SEM, n=20).

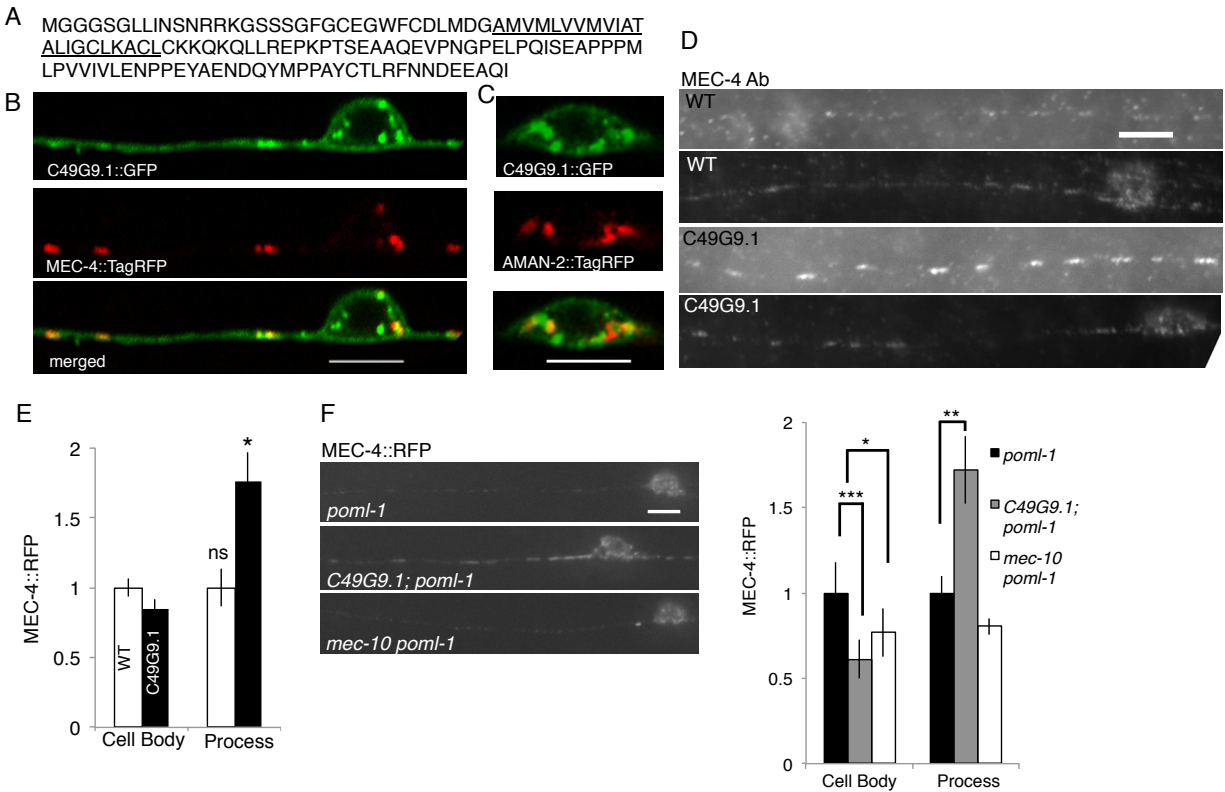


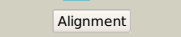
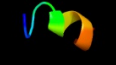
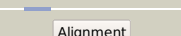

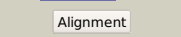
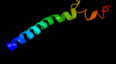


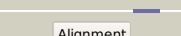
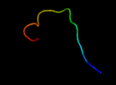
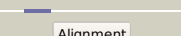

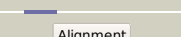

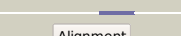
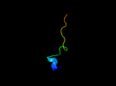
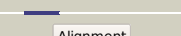

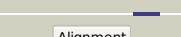



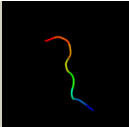
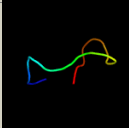
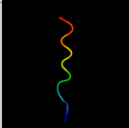
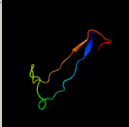
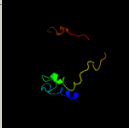
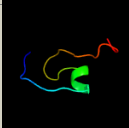
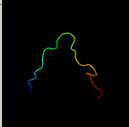

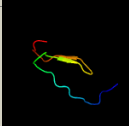
Figure 2 (III-2). C49G9.1 sequence, expression and effect on MEC-4 expression. (A) The deduced amino acid sequence of C49G9.1. The predicted transmembrane is underlined. (B, C) Confocal images showing the partial overlap of C49G9.1::GFP with MEC-4::TagRFP (B) in cell body and proximal process and the Golgi marker (AMAN-2::TagRFP) (C) in the cell body. Scale bar = 5  $\mu$ m. (D) MEC-4 labeling with an anti-MEC-4 antibody in the TRN of wild-type animals and C49G9.1(*u898*) mutants. Each pair of panels shows the TRN process (upper) and cell body (lower). (E) Normalized MEC-4::TagRFP fluorescence intensity (mean  $\pm$  SEM) in the TRN process of WT and C49G9.1(*u898*).  $n=10$ , \*  $p=0.01$ . (F) Images (left panel) and quantification (right panel) of MEC-4::TagRFP fluorescence intensity (mean  $\pm$  SEM) in TRNs of *poml-1(ok2266)*, *C49G9.1(u898); poml-1(ok2266)* or *C49G9.1(u898); mec-10(ok1104)* animals. Fluorescence intensity was normalized to that of *poml-1*.  $n>40$ . \*  $p=0.01$ , \*\* $p=0.002$ , \*\*\* $p=0.001$ .

Table 3 (III-3). C49G9.1 homology identified by BLASTP

BLAST e-value	Species	Description	Identities	Positives	Gaps
9e-49	<i>C. brenneri</i>	hypothetical protein CAEBREN_22708	82/132(62%)	101/132(76%)	5/132(3%)
2e-42	<i>C. remanei</i>	hypothetical protein CRE_14224	78/133(59%)	99/133(74%)	11/133(8%)
8e-34	<i>C. briggsae</i>	Hypothetical protein CBG08708	74/139(53%)	89/139(64%)	27/139(19%)
2.6	<i>Thiomicrospira arctica</i>	hypothetical protein	21/64(33%)	32/64(50%)	0/64(0%)
2.7	<i>Vibrio metschnikovii</i>	glutaminyl-tRNA synthetase	21/57(37%)	29/57(50%)	4/57(7%)
3.7	<i>Calescamantes bacterium</i> SCGC AAA471-M6	flagellar M-ring protein FliF	18/40(45%)	22/40(55%)	1/40(2%)
5.8	<i>Amphimedon queenslandica</i>	hypothetical protein LOC100635484	16/43(37%)	24/43(55%)	2/43(4%)
6.5	<i>Acyrtosiphon pisum</i>	phosphorylase b kinase gamma catalytic chain, skeletal muscle isoform-like	34/113(30%)	50/113(44%)	23/113(20%)

Table 4 (III-4). C49G9.1 homology recognized by Phyre2 (Kelley and Sternberg, 2009)

#	Template	Alignment Coverage	3D Model	Confidence	% i.d.	Template Information
1	<a href="#">c1yk1E</a>	 Alignment		32.2	64	<b>PDB header:</b> hormone/growth factor receptor <b>Chain:</b> E; <b>PDB Molecule:</b> natriuretic peptides b; <b>PDBTitle:</b> structure of natriuretic peptide receptor-c complexed with brain2 natriuretic peptide
2	<a href="#">c1tujA</a>	 Alignment		32.1	64	<b>PDB header:</b> transport protein <b>Chain:</b> A; <b>PDB Molecule:</b> odorant binding protein asp2; <b>PDBTitle:</b> solution structure of the honey bee general odorant binding2 protein asp2 in complex with trimethylsilyl-d4 propionate
3	<a href="#">c1q01A</a>	 Alignment		28.3	70	<b>PDB header:</b> blood clotting <b>Chain:</b> A; <b>PDB Molecule:</b> lebetin 2 isoform alpha; <b>PDBTitle:</b> lebetin peptides, a new class of potent aggregation2 inhibitors
4	<a href="#">c2jp3A</a>	 Alignment		16.9	16	<b>PDB header:</b> transcription <b>Chain:</b> A; <b>PDB Molecule:</b> fxyd domain-containing ion transport regulator 4; <b>PDBTitle:</b> solution structure of the human fxyd4 (chif) protein in sds2 micelles
5	<a href="#">c1yk0E</a>	 Alignment		14.6	46	<b>PDB header:</b> hormone/growth factor receptor <b>Chain:</b> E; <b>PDB Molecule:</b> atrial natriuretic factor; <b>PDBTitle:</b> structure of natriuretic peptide receptor-c complexed with atrial2 natriuretic peptide
6	<a href="#">c2v3mF</a>	 Alignment		13.8	13	<b>PDB header:</b> ribosomal protein <b>Chain:</b> F; <b>PDB Molecule:</b> naf1; <b>PDBTitle:</b> structure of the gar1 domain of naf1
7	<a href="#">c1t34H</a>	 Alignment		12.5	46	<b>PDB header:</b> signaling protein,membrane protein <b>Chain:</b> H; <b>PDB Molecule:</b> atrial natriuretic peptide factor; <b>PDBTitle:</b> rotation mechanism for transmembrane signaling by the atrial2 natriuretic peptide receptor
8	<a href="#">c2p5xB</a>	 Alignment		10.3	20	<b>PDB header:</b> cell cycle <b>Chain:</b> B; <b>PDB Molecule:</b> n-acetylserotonin o-methyltransferase-like protein; <b>PDBTitle:</b> crystal structure of maf domain of human n-acetylserotonin o-2 methyltransferase-like protein
9	<a href="#">c3s7xC</a>	 Alignment		10.1	35	<b>PDB header:</b> viral protein <b>Chain:</b> C; <b>PDB Molecule:</b> major capsid protein vp1; <b>PDBTitle:</b> unassembled washington university polyomavirus vp1 pentamer r198k2 mutant
10	<a href="#">d1zvfa1</a>	 Alignment		9.9	21	<b>Fold:</b> Double-stranded beta-helix <b>Superfamily:</b> RmlC-like cupins <b>Family:</b> 3-hydroxyanthranilic acid dioxygenase-like
11	<a href="#">d1wjpa2</a>	 Alignment		9.2	60	<b>Fold:</b> beta-beta-alpha zinc fingers <b>Superfamily:</b> beta-beta-alpha zinc fingers <b>Family:</b> Classic zinc finger, C2H2

12	<a href="#">c1zfuA_</a>	Alignment		8.6	63	<b>PDB header:</b> antimicrobial protein <b>Chain:</b> A; <b>PDB Molecule:</b> plectasin; <b>PDBTitle:</b> plectasin:a peptide antibiotic with therapeutic potential2 from a saprophytic fungus
13	<a href="#">c2lr3A_</a>	Alignment		8.2	47	<b>PDB header:</b> antimicrobial protein <b>Chain:</b> A; <b>PDB Molecule:</b> pelovaterin; <b>PDBTitle:</b> antibacterial peptide from eggshell matrix: structure and2 self-assembly of beta-defensin like peptide from the3 chinese soft-shelled turtle eggshell
14	<a href="#">d2hh8a1</a>	Alignment		7.9	20	<b>Fold:</b> YdfO-like <b>Superfamily:</b> YdfO-like <b>Family:</b> YdfO-like
15	<a href="#">d1y5oa1</a>	Alignment		7.7	15	<b>Fold:</b> PH domain-like barrel <b>Superfamily:</b> PH domain-like <b>Family:</b> TFIIH domain
16	<a href="#">c2i0eB_</a>	Alignment		7.3	16	<b>PDB header:</b> transferase <b>Chain:</b> B; <b>PDB Molecule:</b> protein kinase c-beta ii; <b>PDBTitle:</b> structure of catalytic domain of human protein kinase c2 beta ii complexed with a bisindolylmaleimide inhibitor
17	<a href="#">c2jvmA_</a>	Alignment		6.5	21	<b>PDB header:</b> structural genomics, unknown function <b>Chain:</b> A; <b>PDB Molecule:</b> uncharacterized protein; <b>PDBTitle:</b> solution nmr structure of rhodobacter sphaeroides protein2 rhos4_26430. northeast structural genomics consortium3 target rhr95
18	<a href="#">d1yfua1</a>	Alignment		6.3	42	<b>Fold:</b> Double-stranded beta-helix <b>Superfamily:</b> RmlC-like cupins <b>Family:</b> 3-hydroxyanthranilic acid dioxygenase-like
19	<a href="#">c2yrmA_</a>	Alignment		6.3	41	<b>PDB header:</b> gene regulation <b>Chain:</b> A; <b>PDB Molecule:</b> b-cell lymphoma 6 protein; <b>PDBTitle:</b> solution structure of the 1st zf-c2h2 domain from human b-2 cell lymphoma 6 protein
20	<a href="#">c2jrrA_</a>	Alignment		6.1	13	<b>PDB header:</b> structural genomics, unknown function <b>Chain:</b> A; <b>PDB Molecule:</b> uncharacterized protein; <b>PDBTitle:</b> solution nmr structure of q5l1s5 from silicibacter2 pomeroyi. northeast structural genomics consortium target3 sir90

We next tested whether C49G9.1 loss affected touch sensitivity and the mechanoreceptor current (MRC). The C49G9.1 mutation did not detectably change touch sensitivity either with or without *poml-1* mutations, but it increased the touch sensitivity of *mec-4ts* animals (Gu et al., 1996) at various temperatures (Figure 3A). Surprisingly, the C49G9.1 TRNs were slightly less sensitive than that wild-type TRNs to pressure as seen in

changes in the MRC (C49G9.1  $P_{1/2} = 7.0 \pm 1.2 \text{ nN}/\mu\text{m}^2$  versus wild type  $P_{1/2} = 4.5 \pm 0.7 \text{ nN}/\mu\text{m}^2$ ; Figures 3B); the peak MRC at the saturating stimuli, however, was not changed (Figure 3C). These data suggest that although C49G9.1 mutation increased MEC-4 expression in the TRN process, it had only modest effect on touch sensitivity and the MRC.

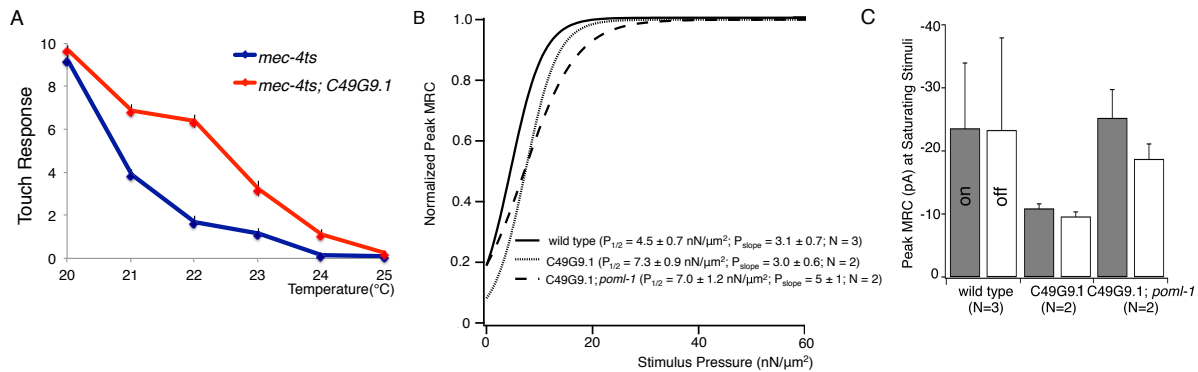


Figure 3 (III-3). The effect of C49G9.1 mutation on touch sensitivity and the MRC. (A) C49G9.1 (*u898*) increases touch sensitivity of *mec-4ts* animals (mean  $\pm$  SEM, n=30). (B) C49G9.1 (*u898*) produced a small but significant change on I vs P of MRC responses to varied pressure stimuli (wild type versus C49G9.1,  $p=0.05$ ; C49G9.1 versus C49G9.1; *poml-1*,  $p<0.0001$ , F test; N indicates the number of cells tested). (C) C49G9.1 (*u898*) does not affect the maximum peak amplitude of MRC recorded from PLM (at -74mV) at the onset (gray bars) and offset (white bars) of a response to saturating mechanical stimulus in the presence of either wild type or *poml-1(ok2266)* (mean  $\pm$  SEM, N indicates the number of cells tested).

Overexpressing C49G9.1 reduced the amount of MEC-4 in the process by 30% without affecting the amount or distribution of MEC-4 in the cell body (data not shown), reduced animal touch sensitivity by 50%, and suppressed 50% of the *mec-4(d)* TRN deaths (Figures 4A-4C). Most of the TRNs surviving with *mec-4(d)* had morphological defects (wavy process, overgrowth of PLM anterior process, multiple neurites on the process), which also appear, albeit to a lesser extent, in wild-type animals overexpressing C49G9.1. By contrast,



*mec-10* overexpression did not dramatically affect *mec-4(d)* degenerations (Figure 4C) or cause any morphological defects (data not shown).

Thus, C49G9.1 affects MEC-4 surface expression. The increase in cell deaths in C49G9.1; *poml-1 mec-4(d)* animals could be due, at least in part, to elevated levels of surface MEC-4(d). In contrast, *mec-10* does not seem to affect MEC-4 protein levels and presumably enhanced *mec-4(d)* cell deaths through a different mechanism.

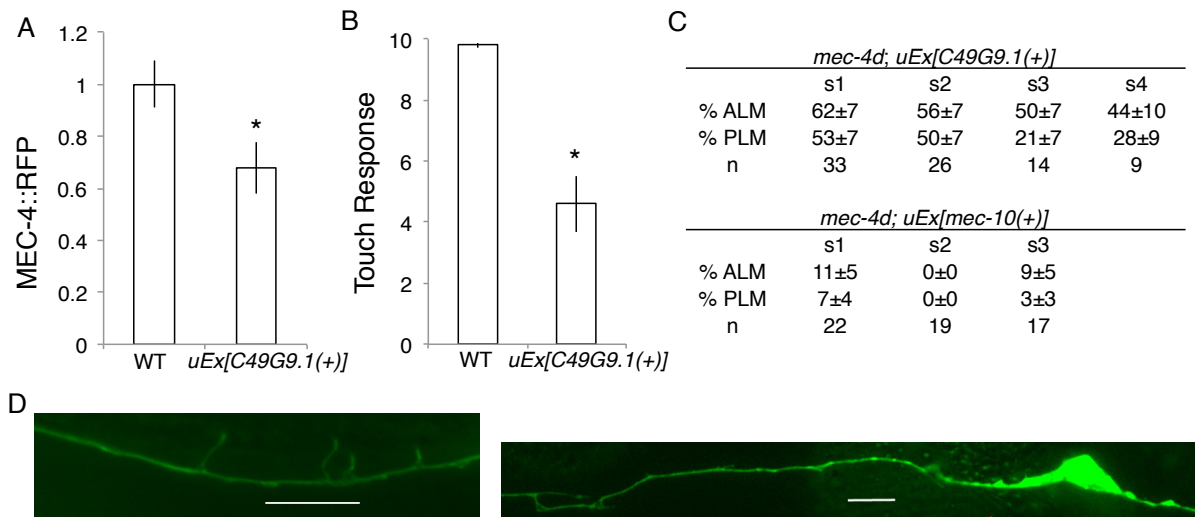


Figure 4 (III-4). The effect of overexpression of C49G9.1(+). (A) Overexpression of C49G9.1(+) reduces the amount of MEC-4::TagRFP in the TRN process (two stable lines, n=21, p=0.02). (B) Overexpression of C49G9.1(+) reduces touch sensitivity (two stable lines, n=25, p<0.0001) and causes morphological defects in the TRNs. Scale bars = 5  $\mu$ m. (C) Overexpression of C49G9.1(+) and to a lesser extent *mec-10* (+) prevents *mec-4(d)*-induced TRN deaths. All cells die in *mec-4(d)* animals. Stable lines are labeled as s1, s2, etc. (D) The morphological defects of surviving TRNs in *mec-4(d)* animals that overexpressed C49G9.1(+). Scale bars represent 5  $\mu$ m.

### **C49G9.1 reduces MEC-4 activity and surface expression in *Xenopus* oocytes**

We next tested the effect of C49G9.1 on MEC-4 currents in *Xenopus* oocytes.

C49G9.1 dramatically reduced the amiloride-sensitive current of MEC-4(d) coexpressed with MEC-6, POML-1, or MEC-2 by approximately 80% (Figure 5A) [C49G9.1 alone produced amiloride-resistant current when expressed at higher concentration in *Xenopus* oocytes (Figures 5B and 5C)]. Thus, both in vivo and in vitro experiments suggest that wild-type C49G9.1 inhibits MEC-4(d) channel activity. Part or all of this inhibition could have resulted from the loss of surface MEC-4 in the frog oocytes, which was seen using TIRF 2 days post-injection (Figures 5D and 5E). Even in the presence of MEC-6, C49G9.1 still reduced MEC-4 surface expression by 50% (Figure 5D and 5E). The action of C49G9.1 on MEC-4(d) could be direct, since C49G9.1 and MEC-4(d) from frog oocytes co-immunoprecipitated each other (Figure 5F).

Because the expression of C49G9.1 overlapped with that of MEC-4 and MEC-2 in the TRNs and co-immunoprecipitated with MEC-4 in the frog oocytes, we asked whether it is part of the MEC-4/MEC-10 channel. We tagged C49G9.1 with EGFP/mCherry at its C termini, and expressed them in *Xenopus* oocytes. [The tagged protein retains their normal function because it acted like the untagged protein in rescuing the C49G9.1 enhancement of TRN cell death in *poml-1 mec-4(d)*, and reducing the MEC-4(d) current amplitude in *Xenopus* oocytes (Figure 5G)]. The stoichiometry of C49G9.1 could not be determined because the molecules moved on the surface of frog oocytes even in the presence of MEC-4; they did not seem to co-localize with MEC-4 (Video S1). In addition, C49G9.1 did not change the stoichiometry of the MEC-4 trimer (Figure 5H), which indicates that this protein is not incorporated into the MEC-4 channel. C49G9.1 may interact with MEC-4 transiently.

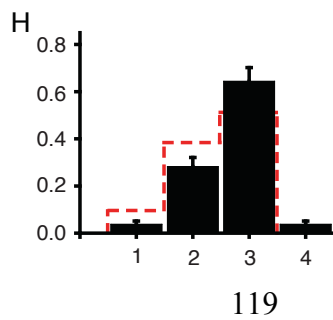
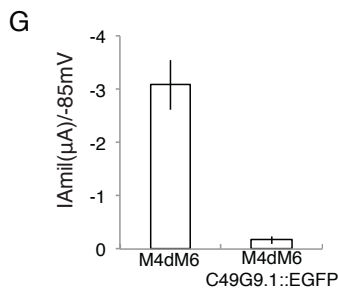
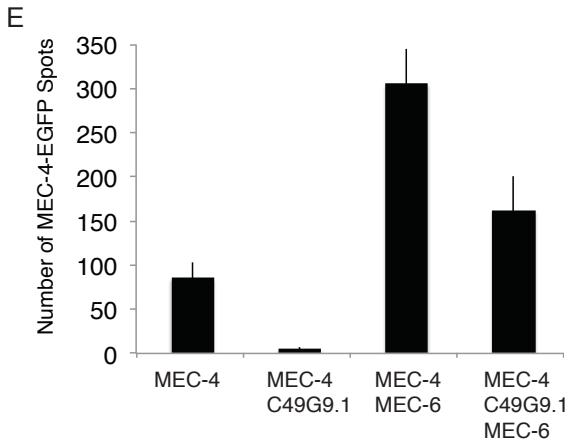
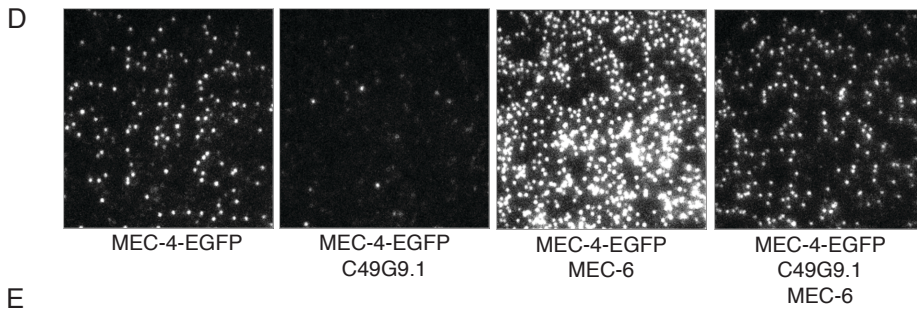
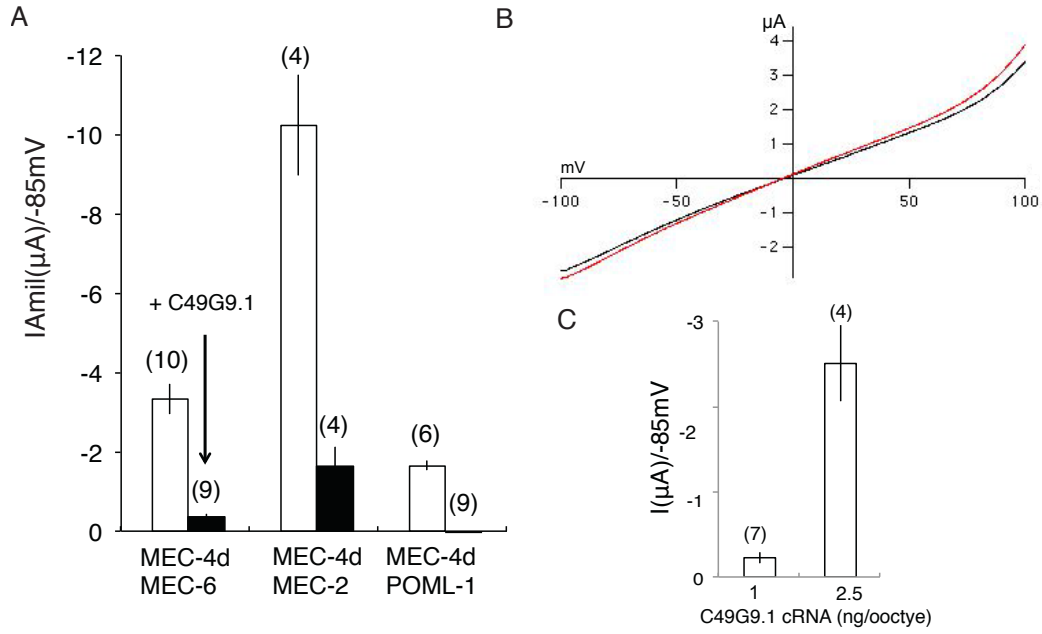


Figure 5 (III-5). C49G9.1 and MEC-4 in *Xenopus* oocytes. (A) The effect of C49G9.1 on the MEC-4(d) amiloride-sensitive current in the presence of MEC-6, MEC-2 or POML-1. The number of oocytes from at least two individual frogs is given in parentheses. (B and C) Amiloride-resistant current produced by expressing C49G9.1 alone in *Xenopus* oocytes. (B) Steady-state current-voltage relation in the control saline (black line) and saline with 300  $\mu$ M amiloride (red line). (C) Dependence of current amplitude on the concentration of C49G9.1 cRNA (mean  $\pm$  SEM). The number of tested oocytes was indicated in parenthesis. Injecting more than 2.5 ng cRNA killed the majority of *Xenopus* oocytes. Images (D) and quantification (E) of MEC-4-EGFP spots by TIRF imaging in the presence of C49G9.1 and MEC-6 (mean  $\pm$  SEM, n=8-15 patches from 7-10 cells of two different batches. 10 ng cRNA of MEC-4-EGFP, 1 ng MEC-6 and 0.5 ng C49G9.1 were injected to *Xenopus* oocytes. (F) Immunoprecipitation (IP) of Myc::MEC-4d by C49G9.1. IB = immunoblot probe. (G) C49G9.1::EGFP reduced the amiloride current produced by MEC-4(d) and MEC-6. (H) Bleaching steps indicate that MEC-4::EGFP forms trimers in the presence of C49G9.1. The observed number of bleaching steps (black bars) and the predicted pattern (red dotted bars) are indicated. The error bars in the subunit counting data show counting errors and are given by  $I/N\sqrt{n}$  (n= total number of spots for each step; N= total number of spots for all steps).

## Discussion

The *poml-1 mec-4(d)* double mutant provides a sensitized background in which to screen for genes that normally inhibit *mec-4(d)* degeneration. Using this mutant, we identified two inhibitors, MEC-10 and C49G9.1, that function downstream of POML-1, because POML-1 acts as a chaperone for MEC-4 folding and transport (Y.C. and M.C. submitted); whereas C49G9.1 is localized on the plasma membrane and partially overlap with the Golgi. MEC-10 is part of MEC-4<sub>2</sub>MEC-10 trimer, and inhibits MEC-4(d) both in vivo and in vitro. In contrast, C49G9.1 is not part of MEC-4 channel complex, though it may transiently interact with MEC-4. C49G9.1 appears to act by reducing MEC-4 surface expression, although it could presumably also inhibit MEC-4(d) or MEC-4 channel activity directly. The suppression of *poml-1* by the loss of C49G9.1 is likely to result from the increase in MEC-4(d) channels on the surface of the TRNs.

The effect of MEC-10 is more difficult to understand, since it seems to have opposite effect on MEC-4 and MEC-4(d) channels. In vivo MEC-10 loss decreases the mechanoreceptor current amplitude by 25% and modestly decreases touch sensitivity (Arnadóttir et al., 2011), but it increases *mec-4(d)* toxicity in *poml-1* mutants. Moreover, MEC-10 decreases the macroscopic MEC-4(d) current amplitude in the frog oocytes (Goodman et al., 2002). These differences may result because these channel function differently. Specifically, the wild type MEC-4<sub>3</sub> channel may need MEC-10 to allow it to be maximally gated, whereas the MEC-4(d)<sub>3</sub> channel, which is constitutively open, allows more current when MEC-10 is absent. Because MEC-10 does not affect MEC-4(d) surface expression (Arnadóttir et al., 2011), single channel conductance, or open probability (Brown et al., 2008) in *Xenopus* oocytes, it may act by inactivating some MEC4(d) channels, making them unable to be opened.

MEC-4 surface expression can be reduced by C49G9.1, though the mechanism remains obscure. Given its localization on the plasma membrane and its negative effect on MEC-4 expression on the membrane, one possible hypothesis is that C49G9.1 may regulate the removal of the transduction channel from the plasma membrane, though we cannot rule out the possibility that it inhibits the insertion of channel to the membrane.

## **Chapter IV**

### **Summary and Future Directions**

## Summary

My doctoral research combined genetics, molecular biology, electrophysiology, and single molecule imaging to redefine the MEC-4/MEC-10 mechanotransduction complex in *C. elegans*, and found that the complex adopts a simpler model than previously proposed (Figure IV-1). In particular, the channel complex consists of two MEC-4 and one MEC-10. Neither MEC-2 nor MEC-6 tightly associate with the channel complex, and thus, they may not be part of the channel. MEC-2 often co-localizes with MEC-4 in vivo and can bind to cholesterol, and therefore, may regulate the lipid microenvironment of the MEC-4<sub>2</sub>MEC-10 channel. MEC-6 and a similar protein POML-1 are required for MEC-4 expression and localization, and likely act as chaperones and/or assembly factors for MEC-4 folding and transport.

I also used the *poml-1* mutation as a sensitized background to screen for genes that normally inhibit the neurotoxicity of *mec-4(d)*, and found the loss of *mec-10* and C49G9.1 make *mec-4(d)* more toxic. C49G9.1 encodes a novel membrane protein found in nematode, which can reduce MEC-4 surface expression.

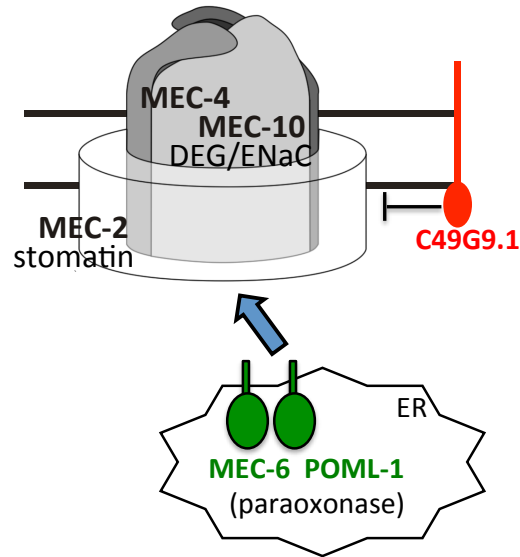


Figure IV. A new model of the DEG/ENaC mechanotransduction complex.

### The MEC-4<sub>2</sub>MEC-10 mechanosensory channel complex

After figuring out how the transduction channel organizes, one important open question is, how does the MEC-4<sub>2</sub>MEC-10 channel transduce mechanical stimuli into electrical signal? The genetic and electrophysiological methods have identified many residues crucial for the channel function, but have limits in probing the gating mechanism. A high-resolution structure is needed to further address this question. Expressing MEC-4 and MEC-10 proteins in bacteria is problematic, because the *mec-4* and *mec-10* genes, both the cDNA and the coding sequence that contains introns and exons, are toxic to bacteria, making bacteria grow very slowly. Therefore, it is difficult to express the full-length protein of MEC-4 and MEC-10 in bacteria. Future work involves trying eukaryotic expression systems, such as yeast or insect cells Sf9, which have been successfully used to produce chick ASIC1 proteins (Jasti



et al., 2007). Moreover, because MEC-6 is needed for MEC-4 folding and transport, co-expression of MEC-4 and MEC-6 may be a good strategy.

The MEC-4 puncta also need further characterization. Previous work has suggested that most proteins in MEC-4 puncta may not be active (O'Hagan et al., 2005) and MEC-4 puncta do not appear to be essential for touch sensitivity (Chapter II). Future work needs to study whether the proteins in MEC-4 puncta reside on the plasma membrane or intracellular vesicles by fusing the MEC-4 proteins to pH-sensitive fluorescence proteins, such as superecliptic phluorin (Miesenbock et al., 1998). Additionally, the physiological role of the MEC-4 puncta also needs to be explored. MEC-4 puncta may function as reservoirs of MEC-4 proteins and affect the modulation and/or habituation of mechanosensation.

### **MEC-6 and POML-1 in MEC-4 folding and transport**

Future work needs to study the chaperone activities of MEC-6 and POML-1 in the ER. The molecular mechanism of MEC-6 and POML-1 in MEC-4 folding and transport is not understood. As I mentioned in Chapter I, calnexin and calreticulin constitute the crucial step of folding glycoproteins into their native state. [MEC-4 has also been shown to be glycosylated (Lai et al., 1996)]. Whether MEC-6 and POML-1 are also involved in the calnexin/calreticulin folding cycle needs further investigation. However, the additive effects of *poml-1* and *crt-1* in touch sensitivity suggest that POML-1 and/or MEC-6 may participate in other folding pathways in parallel to calnexin/calreticulin. One previous experiment hinted that MEC-6 and POML-1 may specifically bind to unfolded MEC-4 proteins or MEC-4 folding intermediates and release the properly folded MEC-4, because MEC-6 mutant

proteins can bind to MEC-4 more strongly than the MEC-6 wild type protein (B.C and M.C, unpublished result). One experiment to test this possibility is to examine whether MEC-6 and POML-1 can pull down more misfolded MEC-4 proteins than folded MEC-4 proteins. To do this experiment, we need a *mec-4* missense mutation that can specifically disrupt MEC-4 folding, we can then test whether the mutant MEC-4 proteins can bind more strongly to MEC-6 than the wild type MEC-4 proteins.

Assaying MEC-6 chaperone activities has several difficulties. First, we cannot express and purify MEC-6 proteins from heterologous systems; MEC-6 expression in bacteria produced merely insoluble proteins (Y.C. and M.C., unpublished work). The lack of purified MEC-6 prohibits us from examining its effect on protein aggregation induced by heat and protein refolding. Second, MEC-4 is only weakly expressed in the six TRNs out of 1000 somatic cells in worms. Low protein abundance makes collecting sufficient amounts of MEC-4 proteins for biochemical assays very difficult. Third, there is no good heterologous system to test their chaperone activities, because MEC-4 alone can also reach the surface of frog oocytes and *Drosophila* S2 cells (Y.C. and M.C., unpublished data), which do not have any MEC-6 or human paraoxonase like proteins (Hicks et al., 2011), indicating other proteins in the heterologous system can also do the similar job, and thus, obscure the roles of MEC-6 and POML-1.

The role of calreticulin (CRT-1) in storing  $\text{Ca}^{2+}$  in the ER raises the possibility that MEC-6 and POML-1 may also affect the ER  $\text{Ca}^{2+}$  homeostasis. CRT-1, a  $\text{Ca}^{2+}$ -binding chaperone, plays dual roles in regulating the ER  $\text{Ca}^{2+}$  homeostasis and protein folding. Xu et al. (2001) suggested the loss of *crt-1* suppresses *mec-4(d)* induced cell death, at least in part, through disrupting the release of  $\text{Ca}^{2+}$  from the ER. However, because MEC-6 and POML-1

have no sequence or structural similarity to CRT-1, and do not have any known  $\text{Ca}^{2+}$ -binding motifs, it is unlikely that MEC-6 and POML-1 facilitate  $\text{Ca}^{2+}$  storage in the ER, and affect the ER  $\text{Ca}^{2+}$  level and/or release, though we cannot rule out the possibility that they may indirectly affect the  $\text{Ca}^{2+}$  level in the ER.

To test whether MEC-6 and POML-1 affect the ER  $\text{Ca}^{2+}$  level, I have used cameleon proteins, D1ER (Palmer et al., 2004) and split-YC 7.3er (Ishii et al., 2006), to measure the free ER  $\text{Ca}^{2+}$  level in the TRNs. I have found that the free ER  $\text{Ca}^{2+}$  level appears to be very similar among the TRNs of wild-type, *mec-6(u450);poml-1(ok2266)*, and *crt-1(ok948)* animals. Moreover, I have also tried to use chemicals to induce the release of  $\text{Ca}^{2+}$  from the ER of TRNs isolated from embryos and cultured on cover glass, using GCaMP3 to monitor the cytosolic  $\text{Ca}^{2+}$  increase (Suzuki et al., 2003). However, ATP and histamine (Riach et al., 1995) did not produce any cytosolic  $\text{Ca}^{2+}$  increase, perhaps due to the absence of H1 and P2u receptors in *C. elegans*. Neither thapsigargin (sarco / endoplasmic reticulum  $\text{Ca}^{2+}$  ATPase inhibitor) nor caffeine (ryanodine receptor agonist) resulted in any intracellular  $\text{Ca}^{2+}$  increase. Application of 5mM 4-Chloro-*m*-cresol (potential ryanodine receptor agonist; Al-Mousa and Michelangeli, 2009; Higure et al., 2006) caused substantial intracellular  $\text{Ca}^{2+}$  increase, followed by cell swelling and death. The rate of  $\text{Ca}^{2+}$  increase and peak intracellular  $\text{Ca}^{2+}$  level varied among different TRNs. No significant difference was observed in TRNs of wild type, *mec-6*; *poml-1*, and *crt-1* (Y.C. and M.C., unpublished data). All of the above experiments raise the doubt about whether *crt-1* and *mec-6* mutations have significant effects on the  $\text{Ca}^{2+}$  level in the ER of TRNs. Indeed, calreticulin knock-out reduced the total cellular  $\text{Ca}^{2+}$  content by approximately 45% in mouse cells (measured by  $^{45}\text{Ca}^{2+}$ ), but did not affect the free ER  $\text{Ca}^{2+}$  concentration (measured by a cameleon based  $\text{Ca}^{2+}$  indicator), or the  $\text{InsP}_3$

induced  $\text{Ca}^{2+}$  release from the ER (Nakamura et al., 2001). To study the effect of *crt-1* or *mec-6* on the ER  $\text{Ca}^{2+}$  homeostasis, future work needs to find better ways to monitor the ER  $\text{Ca}^{2+}$  level and induce the release of  $\text{Ca}^{2+}$  from the ER in *C. elegans*.

Additionally, the potential role of MEC-6 in the production of other degenerin proteins (UNC-8 and DEG-1) needs further study. Like MEC-4, their hyperactivation induced cell death requires MEC-6, suggesting a role for MEC-6 in producing these proteins. Future work needs to examine their expression and localization in *mec-6(u450)* mutants by using their translational GFP fusion (no antibody is available for UNC-8 or DEG-1). Because the *deg-1* gene contains large introns, construction of entire coding sequence fusion is difficult; GFP fusion with the *deg-1* cDNA sequence is an alternative.

### **The function of other paraoxonase-like proteins**

The role of MEC-6 and POML-1 as ER chaperones suggests that mammalian PONs may also have chaperone activities. Indeed, PON2 and PON3 are expressed in the ER and can reduce the cell death caused by the unfolded protein stress. Their potential chaperone activities need to be further studied. Human PON1, PON2, and PON3 have no effect on MEC-4(d) activities when expressed in *Xenopus* oocytes (Y.C and M.C., unpublished data) [whereas MEC-6 (Chelur et al., 2002) and POML-1 can increase MEC-4(d) activities (Chapter II)], suggesting these PONs may act on other substrate proteins, if they have any chaperone activities.

I also studied the expression pattern and the loss of function phenotypes of the other three PONs-like proteins in *C. elegans* (more details in Appendix II). POML-2 is expressed in

DA motor neurons, intestinal-rectal valve, and rectal glands. POML-3 and POML-4 are expressed in hypodermis. As with MEC-6 and POML-1, protein fusions of POML-2, 3, and 4 form the mesh-like structure, and perhaps are localized in the ER of the cell body. Animals with the deletion of each gene exhibit no obvious phenotypes, except that *poml-2(ok1886)* mutants have smaller brood size compared to the wild-type animals.

The function of *C. elegans* PONs-like proteins remains largely unknown, except in the TRNs. Although MEC-6 is widely expressed in many neurons, muscles, and the excretory canal (Chelur et al., 2002), animals with *mec-6* null mutation exhibited no other obvious abnormality besides touch insensitivity. Several double mutants among the five genes produced no obvious phenotypes besides the defects mentioned above. Either these genes are dispensable for worms, or they are highly redundant. Future work needs to make triple, quadruple, and quintuple mutants to study their functions.

### **Inhibition of the MEC-4(d) neurotoxicity**

Mutation of *poml-1(ok2266) mec-4(d)* provides a sensitized background for identifying genes that inhibit the MEC-4(d) neurotoxicity. These genes may negatively regulate MEC-4 activities or surface expression, as shown by the two identified inhibitors, C49G9.1 and MEC-10. The genetic screens described in this thesis only searched for nearly healthy mutants, and thus, missed all the lethal genes. To identify the potential MEC-4(d) inhibitors among the lethal genes, particularly those that may be involved in protein secretory, endocytic, and degradation pathways, a good strategy is to perform neuronal or TRN specific feeding RNAi using the strain with enhanced efficiency on neuronal RNAi (Calixto et al.,

2010). Before the screens, the RNAi efficacy needs to be tested by feeding double-stranded RNA of MEC-10 and C49G9.1 to the enhanced strains with the *mec-4(d) poml-1* mutation.

How MEC-10 inhibits MEC-4(d) remains elusive. In *Xenopus* oocytes, MEC-10 reduces the amplitude of macroscopic MEC-4(d) current by 40%, but has no effect on single channel conductance, single channel open probability, or the surface expression of MEC-4(d), suggesting that MEC-10 may prevent a fraction of channels from opening (Brown et al., 2008; Goodman et al., 2002). Recently, we found that MEC-10 S118 phosphorylation may regulate the MEC-4/MEC-10 channel activity: animals expressing the phospho-mimetic MEC-10 (S118E) did not habituate after sustained mechanical vibration, whereas animals expressing phosphorylation-deficient MEC-10 (S118A) exhibited touch defects.

One hypothesis is that the inhibitory effect of MEC-10 depends on its phosphorylation status: unphosphorylated MEC-10 is inhibitory, while phosphorylated MEC-10 has no inhibitory effect. Perhaps in frog oocytes and the TRNs that express MEC-4(d), most MEC-10 proteins are unphosphorylated, and thus, inhibit MEC-4(d) activities. Future work needs to test this hypothesis by examining the effect MEC-10(S118A) and MEC-10(S118E) on MEC-4(d) activities both in frog oocytes and in worms. If the hypothesis is correct, I expect the following results: MEC-10(S118A) will inhibit the MEC-4(d) in frog oocytes, and suppress the TRN degeneration in *poml-1 mec-4(d) mec-10* animals; whereas MEC-10(S118E) will not have these inhibitory effects.

C49G9.1 needs to be further characterized. I have demonstrated that C49G9.1 reduces MEC-4 surface expression both in vivo and in vitro, but its molecular mechanism and physiological role is not understood. Because C49G9.1 sequence is not obviously similar to that of any known proteins, it is impossible to speculate its function based on its homology.

However, recently, we found that C49G9.1 is needed for mechanosensory habituation after sustained vibration (X.C., Y.C. and M.C., unpublished data), suggesting that its function can be further investigated in the context of habituation.

## References

- Abuin, L., Bargeton, B., Ulbrich, M.H., Isacoff, E.Y., Kellenberger, S., and Benton, R. (2011). Functional architecture of olfactory ionotropic glutamate receptors. *Neuron* *69*, 44-60.
- Adams, C.M., Anderson, M.G., Motto, D.G., Price, M.P., Johnson, W.A., and Welsh, M.J. (1998). Ripped pocket and pickpocket, novel *Drosophila* DEG/ENaC subunits expressed in early development and in mechanosensory neurons. *The Journal of cell biology* *140*, 143-152.
- Al-Mousa, F., and Michelangeli, F. (2009). Commonly used ryanodine receptor activator, 4-chloro-m-cresol (4CmC), is also an inhibitor of SERCA Ca<sup>2+</sup> pumps. *Pharmacological reports* : PR *61*, 838-842.
- Alagramam, K.N., Goodyear, R.J., Geng, R., Furness, D.N., van Aken, A.F., Marcotti, W., Kros, C.J., and Richardson, G.P. (2011). Mutations in protocadherin 15 and cadherin 23 affect tip links and mechanotransduction in mammalian sensory hair cells. *PloS one* *6*, e19183.
- Alloui, A., Zimmermann, K., Mamet, J., Duprat, F., Noel, J., Chemin, J., Guy, N., Blondeau, N., Voilley, N., Rubat-Coudert, C., *et al.* (2006). TREK-1, a K<sup>+</sup> channel involved in polymodal pain perception. *The EMBO journal* *25*, 2368-2376.
- Altenhofer, S., Witte, I., Teiber, J.F., Wilgenbus, P., Pautz, A., Li, H., Daiber, A., Witan, H., Clement, A.M., Forstermann, U., *et al.* (2010). One enzyme, two functions: PON2 prevents mitochondrial superoxide formation and apoptosis independent from its lactonase activity. *The Journal of biological chemistry* *285*, 24398-24403.
- Altier, C., Garcia-Caballero, A., Simms, B., You, H., Chen, L., Walcher, J., Tedford, H.W., Hermosilla, T., and Zamponi, G.W. (2011). The Cavbeta subunit prevents RFP2-mediated ubiquitination and proteasomal degradation of L-type channels. *Nature neuroscience* *14*, 173-180.
- Anantharam, A., Tian, Y., and Palmer, L.G. (2006). Open probability of the epithelial sodium channel is regulated by intracellular sodium. *The Journal of physiology* *574*, 333-347.
- Andersson, H., and von Heijne, G. (1994). Membrane protein topology: effects of delta mu H<sup>+</sup> on the translocation of charged residues explain the 'positive inside' rule. *The EMBO journal* *13*, 2267-2272.
- Appenzeller-Herzog, C., and Hauri, H.P. (2006). The ER-Golgi intermediate compartment (ERGIC): in search of its identity and function. *Journal of cell science* *119*, 2173-2183.
- Arnadottir, J., and Chalfie, M. (2010). Eukaryotic mechanosensitive channels. *Annual review of biophysics* *39*, 111-137.



- Arnadottir, J., O'Hagan, R., Chen, Y., Goodman, M.B., and Chalfie, M. (2011). The DEG/ENaC protein MEC-10 regulates the transduction channel complex in *Caenorhabditis elegans* touch receptor neurons. *The Journal of neuroscience : the official journal of the Society for Neuroscience* *31*, 12695-12704.
- Aviram, M., and Rosenblat, M. (2004). Paraoxonases 1, 2, and 3, oxidative stress, and macrophage foam cell formation during atherosclerosis development. *Free radical biology & medicine* *37*, 1304-1316.
- Baconguis, I., Bohlen, C.J., Goehring, A., Julius, D., and Gouaux, E. (2014). X-ray structure of acid-sensing ion channel 1-snake toxin complex reveals open state of a Na(+)-selective channel. *Cell* *156*, 717-729.
- Baconguis, I., and Gouaux, E. (2012). Structural plasticity and dynamic selectivity of acid-sensing ion channel-spider toxin complexes. *Nature* *489*, 400-405.
- Bang, H., Kim, Y., and Kim, D. (2000). TREK-2, a new member of the mechanosensitive tandem-pore K<sup>+</sup> channel family. *The Journal of biological chemistry* *275*, 17412-17419.
- Barlowe, C., Orci, L., Yeung, T., Hosobuchi, M., Hamamoto, S., Salama, N., Rexach, M.F., Ravazzola, M., Amherdt, M., and Schekman, R. (1994). COPII: a membrane coat formed by Sec proteins that drive vesicle budding from the endoplasmic reticulum. *Cell* *77*, 895-907.
- Barlowe, C., and Schekman, R. (1993). SEC12 encodes a guanine-nucleotide-exchange factor essential for transport vesicle budding from the ER. *Nature* *365*, 347-349.
- Bass, R.B., Strop, P., Barclay, M., and Rees, D.C. (2002). Crystal structure of *Escherichia coli* MscS, a voltage-modulated and mechanosensitive channel. *Science* *298*, 1582-1587.
- Bassilana, F., Champigny, G., Waldmann, R., de Weille, J.R., Heurteaux, C., and Lazdunski, M. (1997). The acid-sensitive ionic channel subunit ASIC and the mammalian degenerin MDEG form a heteromultimeric H<sup>+</sup>-gated Na<sup>+</sup> channel with novel properties. *The Journal of biological chemistry* *272*, 28819-28822.
- Ben-Shahar, Y. (2011). Sensory functions for degenerin/epithelial sodium channels (DEG/ENaC). *Advances in genetics* *76*, 1-26.
- Benson, C.J., Xie, J., Wemmie, J.A., Price, M.P., Henss, J.M., Welsh, M.J., and Snyder, P.M. (2002). Heteromultimers of DEG/ENaC subunits form H<sup>+</sup>-gated channels in mouse sensory neurons. *Proceedings of the National Academy of Sciences of the United States of America* *99*, 2338-2343.
- Bi, X., Corpina, R.A., and Goldberg, J. (2002). Structure of the Sec23/24-Sar1 pre-budding complex of the COPII vesicle coat. *Nature* *419*, 271-277.

Bianchi, L., Gerstbrein, B., Frokjaer-Jensen, C., Royal, D.C., Mukherjee, G., Royal, M.A., Xue, J., Schafer, W.R., and Driscoll, M. (2004). The neurotoxic MEC-4(d) DEG/ENaC sodium channel conducts calcium: implications for necrosis initiation. *Nature neuroscience* 7, 1337-1344.

Bize, V., and Horisberger, J.D. (2007). Sodium self-inhibition of human epithelial sodium channel: selectivity and affinity of the extracellular sodium sensing site. *American journal of physiology Renal physiology* 293, F1137-1146.

Bonewald, L.F. (2006). Mechanosensation and Transduction in Osteocytes. *BoneKey osteovision* 3, 7-15.

Bounoutas, A., and Chalfie, M. (2007). Touch sensitivity in *Caenorhabditis elegans*. *Pflügers Archiv : European journal of physiology* 454, 691-702.

Bounoutas, A., Kratz, J., Emtage, L., Ma, C., Nguyen, K.C., and Chalfie, M. (2011). Microtubule depolymerization in *Caenorhabditis elegans* touch receptor neurons reduces gene expression through a p38 MAPK pathway. *Proceedings of the National Academy of Sciences of the United States of America* 108, 3982-3987.

Bounoutas, A., O'Hagan, R., and Chalfie, M. (2009a). The multipurpose 15-protofilament microtubules in *C. elegans* have specific roles in mechanosensation. *Current biology : CB* 19, 1362-1367.

Bounoutas, A., Zheng, Q., Nonet, M.L., and Chalfie, M. (2009b). *mec-15* encodes an F-box protein required for touch receptor neuron mechanosensation, synapse formation and development. *Genetics* 183, 607-617, 601SI-604SI.

Braakman, I., and Hebert, D.N. (2013). Protein folding in the endoplasmic reticulum. *Cold Spring Harbor perspectives in biology* 5, a013201.

Brenner, S. (1974). The genetics of *Caenorhabditis elegans*. *Genetics* 77, 71-94.

Brockie, P.J., Jensen, M., Mellem, J.E., Jensen, E., Yamasaki, T., Wang, R., Maxfield, D., Thacker, C., Hoerndli, F., Dunn, P.J., *et al.* (2013). Cornichons control ER export of AMPA receptors to regulate synaptic excitability. *Neuron* 80, 129-142.

Brown, A.L., Fernandez-Illescas, S.M., Liao, Z., and Goodman, M.B. (2007). Gain-of-function mutations in the MEC-4 DEG/ENaC sensory mechanotransduction channel alter gating and drug blockade. *The Journal of general physiology* 129, 161-173.

Brown, A.L., Liao, Z., and Goodman, M.B. (2008). MEC-2 and MEC-6 in the *Caenorhabditis elegans* sensory mechanotransduction complex: auxiliary subunits that enable channel activity. *The Journal of general physiology* 131, 605-616.

- Butterworth, M.B., Edinger, R.S., Johnson, J.P., and Frizzell, R.A. (2005). Acute ENaC stimulation by cAMP in a kidney cell line is mediated by exocytic insertion from a recycling channel pool. *The Journal of general physiology* 125, 81-101.
- Calixto, A., Chelur, D., Topalidou, I., Chen, X., and Chalfie, M. (2010). Enhanced neuronal RNAi in *C. elegans* using SID-1. *Nature methods* 7, 554-559.
- Cameron, P., Hiroi, M., Ngai, J., and Scott, K. (2010). The molecular basis for water taste in *Drosophila*. *Nature* 465, 91-95.
- Canessa, C.M., Horisberger, J.D., and Rossier, B.C. (1993). Epithelial sodium channel related to proteins involved in neurodegeneration. *Nature* 361, 467-470.
- Canessa, C.M., Schild, L., Buell, G., Thorens, B., Gautschi, I., Horisberger, J.D., and Rossier, B.C. (1994). Amiloride-sensitive epithelial Na<sup>+</sup> channel is made of three homologous subunits. *Nature* 367, 463-467.
- Carattino, M.D., Hughey, R.P., and Kleyman, T.R. (2008). Proteolytic processing of the epithelial sodium channel gamma subunit has a dominant role in channel activation. *The Journal of biological chemistry* 283, 25290-25295.
- Chalfie, M. (2009). Neurosensory mechanotransduction. *Nature reviews Molecular cell biology* 10, 44-52.
- Chalfie, M., and Au, M. (1989). Genetic control of differentiation of the *Caenorhabditis elegans* touch receptor neurons. *Science* 243, 1027-1033.
- Chalfie, M., and Sulston, J. (1981). Developmental genetics of the mechanosensory neurons of *Caenorhabditis elegans*. *Developmental biology* 82, 358-370.
- Chalfie, M., and Wolinsky, E. (1990). The identification and suppression of inherited neurodegeneration in *Caenorhabditis elegans*. *Nature* 345, 410-416.
- Chandrashekar, J., Kuhn, C., Oka, Y., Yarmolinsky, D.A., Hummler, E., Ryba, N.J., and Zuker, C.S. (2010). The cells and peripheral representation of sodium taste in mice. *Nature* 464, 297-301.
- Chandrashekar, J., Yarmolinsky, D., von Buchholtz, L., Oka, Y., Sly, W., Ryba, N.J., and Zuker, C.S. (2009). The taste of carbonation. *Science* 326, 443-445.
- Chang, G., Spencer, R.H., Lee, A.T., Barclay, M.T., and Rees, D.C. (1998). Structure of the MscL homolog from *Mycobacterium tuberculosis*: a gated mechanosensitive ion channel. *Science* 282, 2220-2226.

Chatzigeorgiou, M., Grundy, L., Kindt, K.S., Lee, W.H., Driscoll, M., and Schafer, W.R. (2010). Spatial asymmetry in the mechanosensory phenotypes of the *C. elegans* DEG/ENaC gene *mec-10*. *Journal of neurophysiology* *104*, 3334-3344.

Chelur, D.S., and Chalfie, M. (2007). Targeted cell killing by reconstituted caspases. *Proceedings of the National Academy of Sciences of the United States of America* *104*, 2283-2288.

Chelur, D.S., Ernstrom, G.G., Goodman, M.B., Yao, C.A., Chen, L., R, O.H., and Chalfie, M. (2002). The mechanosensory protein MEC-6 is a subunit of the *C. elegans* touch-cell degenerin channel. *Nature* *420*, 669-673.

Chen, C.C., and Wong, C.W. (2013). Neurosensory mechanotransduction through acid-sensing ion channels. *Journal of cellular and molecular medicine* *17*, 337-349.

Chen, Z., Wang, Q., and Wang, Z. (2010). The amiloride-sensitive epithelial Na<sup>+</sup> channel PPK28 is essential for drosophila gustatory water reception. *The Journal of neuroscience : the official journal of the Society for Neuroscience* *30*, 6247-6252.

Chun, C.K., Ozer, E.A., Welsh, M.J., Zabner, J., and Greenberg, E.P. (2004). Inactivation of a *Pseudomonas aeruginosa* quorum-sensing signal by human airway epithelia. *Proceedings of the National Academy of Sciences of the United States of America* *101*, 3587-3590.

Colbert, H.A., Smith, T.L., and Bargmann, C.I. (1997). OSM-9, a novel protein with structural similarity to channels, is required for olfaction, mechanosensation, and olfactory adaptation in *Caenorhabditis elegans*. *The Journal of neuroscience : the official journal of the Society for Neuroscience* *17*, 8259-8269.

Consortium, C.e.S. (1998). Genome sequence of the nematode *C. elegans*: a platform for investigating biology. *Science* *282*, 2012-2018.

Copeland, C.S., Zimmer, K.P., Wagner, K.R., Healey, G.A., Mellman, I., and Helenius, A. (1988). Folding, trimerization, and transport are sequential events in the biogenesis of influenza virus hemagglutinin. *Cell* *53*, 197-209.

Copic, A., Latham, C.F., Horlbeck, M.A., D'Arcangelo, J.G., and Miller, E.A. (2012). ER cargo properties specify a requirement for COPII coat rigidity mediated by Sec13p. *Science* *335*, 1359-1362.

Corey, D.P., and Hudspeth, A.J. (1979). Response latency of vertebrate hair cells. *Biophysical journal* *26*, 499-506.

Coscoy, S., Lingueglia, E., Lazdunski, M., and Barbry, P. (1998). The Phe-Met-Arg-Phe-amide-activated sodium channel is a tetramer. *The Journal of biological chemistry* *273*, 8317-8322.

Coste, B., Mathur, J., Schmidt, M., Earley, T.J., Ranade, S., Petrus, M.J., Dubin, A.E., and Patapoutian, A. (2010). Piezo1 and Piezo2 are essential components of distinct mechanically activated cation channels. *Science* 330, 55-60.

Coste, B., Xiao, B., Santos, J.S., Syeda, R., Grandl, J., Spencer, K.S., Kim, S.E., Schmidt, M., Mathur, J., Dubin, A.E., *et al.* (2012). Piezo proteins are pore-forming subunits of mechanically activated channels. *Nature* 483, 176-181.

Cueva, J.G., Mulholland, A., and Goodman, M.B. (2007). Nanoscale organization of the MEC-4 DEG/ENaC sensory mechanotransduction channel in *Caenorhabditis elegans* touch receptor neurons. *The Journal of neuroscience : the official journal of the Society for Neuroscience* 27, 14089-14098.

Davies, H.G., Richter, R.J., Keifer, M., Broomfield, C.A., Sowalla, J., and Furlong, C.E. (1996). The effect of the human serum paraoxonase polymorphism is reversed with diazoxon, soman and sarin. *Nature genetics* 14, 334-336.

Deppe, U., Schierenberg, E., Cole, T., Krieg, C., Schmitt, D., Yoder, B., and von Ehrenstein, G. (1978). Cell lineages of the embryo of the nematode *Caenorhabditis elegans*. *Proceedings of the National Academy of Sciences of the United States of America* 75, 376-380.

Deval, E., Gasull, X., Noel, J., Salinas, M., Baron, A., Diochot, S., and Lingueglia, E. (2010). Acid-sensing ion channels (ASICs): pharmacology and implication in pain. *Pharmacology & therapeutics* 128, 549-558.

Diakov, A., and Korbmayer, C. (2004). A novel pathway of epithelial sodium channel activation involves a serum- and glucocorticoid-inducible kinase consensus motif in the C terminus of the channel's alpha-subunit. *The Journal of biological chemistry* 279, 38134-38142.

Dinudom, A., Fotia, A.B., Lefkowitz, R.J., Young, J.A., Kumar, S., and Cook, D.I. (2004). The kinase Grk2 regulates Nedd4/Nedd4-2-dependent control of epithelial Na<sup>+</sup> channels. *Proceedings of the National Academy of Sciences of the United States of America* 101, 11886-11890.

Draganov, D.I., Teiber, J.F., Speelman, A., Osawa, Y., Sunahara, R., and La Du, B.N. (2005). Human paraoxonases (PON1, PON2, and PON3) are lactonases with overlapping and distinct substrate specificities. *Journal of lipid research* 46, 1239-1247.

Drew, L.J., Rohrer, D.K., Price, M.P., Blaver, K.E., Cockayne, D.A., Cesare, P., and Wood, J.N. (2004). Acid-sensing ion channels ASIC2 and ASIC3 do not contribute to mechanically activated currents in mammalian sensory neurones. *The Journal of physiology* 556, 691-710.

Driscoll, M., and Chalfie, M. (1991). The *mec-4* gene is a member of a family of *Caenorhabditis elegans* genes that can mutate to induce neuronal degeneration. *Nature* 349, 588-593.

Duden, R. (2003). ER-to-Golgi transport: COP I and COP II function (Review). *Molecular membrane biology* 20, 197-207.

Eisenhoffer, G.T., Loftus, P.D., Yoshigi, M., Otsuna, H., Chien, C.B., Morcos, P.A., and Rosenblatt, J. (2012). Crowding induces live cell extrusion to maintain homeostatic cell numbers in epithelia. *Nature* 484, 546-549.

Emtage, L., Gu, G., Hartweg, E., and Chalfie, M. (2004). Extracellular proteins organize the mechanosensory channel complex in *C. elegans* touch receptor neurons. *Neuron* 44, 795-807.

Eskandari, S., Snyder, P.M., Kreman, M., Zampighi, G.A., Welsh, M.J., and Wright, E.M. (1999). Number of subunits comprising the epithelial sodium channel. *The Journal of biological chemistry* 274, 27281-27286.

Estin, M.L., Stoltz, D.A., and Zabner, J. (2010). Paraoxonase 1, quorum sensing, and *P. aeruginosa* infection: a novel model. *Advances in experimental medicine and biology* 660, 183-193.

Firsov, D., Gautschi, I., Merillat, A.M., Rossier, B.C., and Schild, L. (1998). The heterotetrameric architecture of the epithelial sodium channel (ENaC). *The EMBO journal* 17, 344-352.

Franks, N.P., and Honore, E. (2004). The TREK K2P channels and their role in general anaesthesia and neuroprotection. *Trends in pharmacological sciences* 25, 601-608.

Frokjaer-Jensen, C., Davis, M.W., Ailion, M., and Jorgensen, E.M. (2012). Improved Mos1-mediated transgenesis in *C. elegans*. *Nature methods* 9, 117-118.

Frokjaer-Jensen, C., Davis, M.W., Hollopeter, G., Taylor, J., Harris, T.W., Nix, P., Lofgren, R., Prestgard-Duke, M., Bastiani, M., Moerman, D.G., *et al.* (2010). Targeted gene deletions in *C. elegans* using transposon excision. *Nature methods* 7, 451-453.

Furukawa, Y., Miyawaki, Y., and Abe, G. (2006). Molecular cloning and functional characterization of the *Aplysia* FMRFamide-gated Na<sup>+</sup> channel. *Pflugers Archiv : European journal of physiology* 451, 646-656.

García-Añoveros, J. (1995). Genetic analysis of degenerin proteins in *Caenorhabditis elegans* (New York, NY: Columbia University).

Garcia-Anoveros, J., Garcia, J.A., Liu, J.D., and Corey, D.P. (1998). The nematode degenerin UNC-105 forms ion channels that are activated by degeneration- or hypercontraction-causing mutations. *Neuron* 20, 1231-1241.

Garcia-Anoveros, J., Ma, C., and Chalfie, M. (1995). Regulation of *Caenorhabditis elegans* degenerin proteins by a putative extracellular domain. *Current biology : CB* 5, 441-448.

Geffeney, S.L., Cueva, J.G., Glauser, D.A., Doll, J.C., Lee, T.H., Montoya, M., Karania, S., Garakani, A.M., Pruitt, B.L., and Goodman, M.B. (2011). DEG/ENaC but not TRP channels are the major mechanoelectrical transduction channels in a *C. elegans* nociceptor. *Neuron* 71, 845-857.

Geffeney, S.L., and Goodman, M.B. (2012). How we feel: ion channel partnerships that detect mechanical inputs and give rise to touch and pain perception. *Neuron* 74, 609-619.

Goodman, M.B. (2006). Mechanosensation. *WormBook : the online review of C elegans biology*, 1-14.

Goodman, M.B., Ernstrom, G.G., Chelur, D.S., O'Hagan, R., Yao, C.A., and Chalfie, M. (2002). MEC-2 regulates *C. elegans* DEG/ENaC channels needed for mechanosensation. *Nature* 415, 1039-1042.

Gopfert, M.C., Albert, J.T., Nadrowski, B., and Kamikouchi, A. (2006). Specification of auditory sensitivity by *Drosophila* TRP channels. *Nature neuroscience* 9, 999-1000.

Goulet, C.C., Volk, K.A., Adams, C.M., Prince, L.S., Stokes, J.B., and Snyder, P.M. (1998). Inhibition of the epithelial Na<sup>+</sup> channel by interaction of Nedd4 with a PY motif deleted in Liddle's syndrome. *The Journal of biological chemistry* 273, 30012-30017.

Gu, C., Zhou, W., Puthenveedu, M.A., Xu, M., Jan, Y.N., and Jan, L.Y. (2006). The microtubule plus-end tracking protein EB1 is required for Kv1 voltage-gated K<sup>+</sup> channel axonal targeting. *Neuron* 52, 803-816.

Gu, G., Caldwell, G.A., and Chalfie, M. (1996). Genetic interactions affecting touch sensitivity in *Caenorhabditis elegans*. *Proceedings of the National Academy of Sciences of the United States of America* 93, 6577-6582.

Hall, D.H., Gu, G., Garcia-Anoveros, J., Gong, L., Chalfie, M., and Driscoll, M. (1997). Neuropathology of degenerative cell death in *Caenorhabditis elegans*. *The Journal of neuroscience : the official journal of the Society for Neuroscience* 17, 1033-1045.

Hansson, J.H., Nelson-Williams, C., Suzuki, H., Schild, L., Shimkets, R., Lu, Y., Canessa, C., Iwasaki, T., Rossier, B., and Lifton, R.P. (1995a). Hypertension caused by a truncated epithelial sodium channel gamma subunit: genetic heterogeneity of Liddle syndrome. *Nature genetics* 11, 76-82.

Hansson, J.H., Schild, L., Lu, Y., Wilson, T.A., Gautschi, I., Shimkets, R., Nelson-Williams, C., Rossier, B.C., and Lifton, R.P. (1995b). A de novo missense mutation of the beta subunit of the epithelial sodium channel causes hypertension and Liddle syndrome, identifying a proline-rich segment critical for regulation of channel activity. *Proceedings of the National Academy of Sciences of the United States of America* 92, 11495-11499.

- Hao, J., Padilla, F., Dandonneau, M., Lavebratt, C., Lesage, F., Noel, J., and Delmas, P. (2013). Kv1.1 channels act as mechanical brake in the senses of touch and pain. *Neuron* *77*, 899-914.
- Harbinder, S., Tavernarakis, N., Herndon, L.A., Kinnell, M., Xu, S.Q., Fire, A., and Driscoll, M. (1997). Genetically targeted cell disruption in *Caenorhabditis elegans*. *Proceedings of the National Academy of Sciences of the United States of America* *94*, 13128-13133.
- Harel, M., Aharoni, A., Gaidukov, L., Brumshtein, B., Khersonsky, O., Meged, R., Dvir, H., Ravelli, R.B., McCarthy, A., Toker, L., *et al.* (2004). Structure and evolution of the serum paraoxonase family of detoxifying and anti-atherosclerotic enzymes. *Nature structural & molecular biology* *11*, 412-419.
- Haswell, E.S., and Meyerowitz, E.M. (2006). MscS-like proteins control plastid size and shape in *Arabidopsis thaliana*. *Current biology : CB* *16*, 1-11.
- Haswell, E.S., Peyronnet, R., Barbier-Brygoo, H., Meyerowitz, E.M., and Frachisse, J.M. (2008). Two MscS homologs provide mechanosensitive channel activities in the *Arabidopsis* root. *Current biology : CB* *18*, 730-734.
- Hebert, D.N., and Molinari, M. (2007). In and out of the ER: protein folding, quality control, degradation, and related human diseases. *Physiological reviews* *87*, 1377-1408.
- Helms, J.B., and Zurzolo, C. (2004). Lipids as targeting signals: lipid rafts and intracellular trafficking. *Traffic* *5*, 247-254.
- Hicks, M.A., Barber, A.E., 2nd, Giddings, L.A., Caldwell, J., O'Connor, S.E., and Babbitt, P.C. (2011). The evolution of function in strictosidine synthase-like proteins. *Proteins* *79*, 3082-3098.
- Figure, Y., Shimazaki, Y., and Nohmi, M. (2006). Can 4-chloro-m-cresol be substituted for caffeine as an activator of calcium oscillation in bullfrog sympathetic ganglion cells? *Cell calcium* *39*, 467-470.
- Hobert, O., Moerman, D.G., Clark, K.A., Beckerle, M.C., and Ruvkun, G. (1999). A conserved LIM protein that affects muscular adherens junction integrity and mechanosensory function in *Caenorhabditis elegans*. *The Journal of cell biology* *144*, 45-57.
- Hong, K., Mano, I., and Driscoll, M. (2000). In vivo structure-function analyses of *Caenorhabditis elegans* MEC-4, a candidate mechanosensory ion channel subunit. *The Journal of neuroscience : the official journal of the Society for Neuroscience* *20*, 2575-2588.
- Horke, S., Witte, I., Wilgenbus, P., Kruger, M., Strand, D., and Forstermann, U. (2007). Paraoxonase-2 reduces oxidative stress in vascular cells and decreases endoplasmic reticulum stress-induced caspase activation. *Circulation* *115*, 2055-2064.



- Hou, J.C., and Pessin, J.E. (2007). Ins (endocytosis) and outs (exocytosis) of GLUT4 trafficking. *Current opinion in cell biology* 19, 466-473.
- Huang, A.L., Chen, X., Hoon, M.A., Chandrashekar, J., Guo, W., Trankner, D., Ryba, N.J., and Zuker, C.S. (2006). The cells and logic for mammalian sour taste detection. *Nature* 442, 934-938.
- Huang, M., and Chalfie, M. (1994). Gene interactions affecting mechanosensory transduction in *Caenorhabditis elegans*. *Nature* 367, 467-470.
- Huang, M., Gu, G., Ferguson, E.L., and Chalfie, M. (1995). A stomatin-like protein necessary for mechanosensation in *C. elegans*. *Nature* 378, 292-295.
- Huber, T.B., Schermer, B., Muller, R.U., Hohne, M., Bartram, M., Calixto, A., Haggmann, H., Reinhardt, C., Koos, F., Kunzelmann, K., *et al.* (2006). Podocin and MEC-2 bind cholesterol to regulate the activity of associated ion channels. *Proceedings of the National Academy of Sciences of the United States of America* 103, 17079-17086.
- Hughey, R.P., Carattino, M.D., and Kleyman, T.R. (2007). Role of proteolysis in the activation of epithelial sodium channels. *Current opinion in nephrology and hypertension* 16, 444-450.
- Huque, T., Cowart, B.J., Dankulich-Nagrudny, L., Pribitkin, E.A., Bayley, D.L., Spielman, A.I., Feldman, R.S., Mackler, S.A., and Brand, J.G. (2009). Sour ageusia in two individuals implicates ion channels of the ASIC and PKD families in human sour taste perception at the anterior tongue. *PloS one* 4, e7347.
- Ihara, Y., Cohen-Doyle, M.F., Saito, Y., and Williams, D.B. (1999). Calnexin discriminates between protein conformational states and functions as a molecular chaperone in vitro. *Molecular cell* 4, 331-341.
- Ishii, K., Hirose, K., and Iino, M. (2006). Ca<sup>2+</sup> shuttling between endoplasmic reticulum and mitochondria underlying Ca<sup>2+</sup> oscillations. *EMBO reports* 7, 390-396.
- Jasti, J., Furukawa, H., Gonzales, E.B., and Gouaux, E. (2007). Structure of acid-sensing ion channel 1 at 1.9 Å resolution and low pH. *Nature* 449, 316-323.
- Ji, H.L., Su, X.F., Kedar, S., Li, J., Barbry, P., Smith, P.R., Matalon, S., and Benos, D.J. (2006). Delta-subunit confers novel biophysical features to alpha beta gamma-human epithelial sodium channel (ENaC) via a physical interaction. *The Journal of biological chemistry* 281, 8233-8241.
- Jones, D., Crowe, E., Stevens, T.A., and Candido, E.P. (2002). Functional and phylogenetic analysis of the ubiquitylation system in *Caenorhabditis elegans*: ubiquitin-conjugating enzymes, ubiquitin-activating enzymes, and ubiquitin-like proteins. *Genome biology* 3, RESEARCH0002.

- Josse, D., Xie, W., Renault, F., Rochu, D., Schopfer, L.M., Masson, P., and Lockridge, O. (1999). Identification of residues essential for human paraoxonase (PON1) arylesterase/organophosphatase activities. *Biochemistry* 38, 2816-2825.
- Kamikouchi, A., Inagaki, H.K., Effertz, T., Hendrich, O., Fiala, A., Gopfert, M.C., and Ito, K. (2009). The neural basis of *Drosophila* gravity-sensing and hearing. *Nature* 458, 165-171.
- Kang, L., Gao, J., Schafer, W.R., Xie, Z., and Xu, X.Z. (2010). *C. elegans* TRP family protein TRP-4 is a pore-forming subunit of a native mechanotransduction channel. *Neuron* 67, 381-391.
- Kataoka, S., Yang, R., Ishimaru, Y., Matsunami, H., Seigny, J., Kinnamon, J.C., and Finger, T.E. (2008). The candidate sour taste receptor, PKD2L1, is expressed by type III taste cells in the mouse. *Chemical senses* 33, 243-254.
- Kawashima, Y., Geleoc, G.S., Kurima, K., Labay, V., Lelli, A., Asai, Y., Makishima, T., Wu, D.K., Della Santina, C.C., Holt, J.R., *et al.* (2011). Mechanotransduction in mouse inner ear hair cells requires transmembrane channel-like genes. *The Journal of clinical investigation* 121, 4796-4809.
- Kelley, L.A., and Sternberg, M.J. (2009). Protein structure prediction on the Web: a case study using the Phyre server. *Nature protocols* 4, 363-371.
- Kernan, M., Cowan, D., and Zuker, C. (1994). Genetic dissection of mechanosensory transduction: mechanoreception-defective mutations of *Drosophila*. *Neuron* 12, 1195-1206.
- Khersonsky, O., and Tawfik, D.S. (2005). Structure-reactivity studies of serum paraoxonase PON1 suggest that its native activity is lactonase. *Biochemistry* 44, 6371-6382.
- Kim, K.X., Beurg, M., Hackney, C.M., Furness, D.N., Mahendrasingam, S., and Fettiplace, R. (2013). The role of transmembrane channel-like proteins in the operation of hair cell mechanotransducer channels. *The Journal of general physiology* 142, 493-505.
- Kim, S.E., Coste, B., Chadha, A., Cook, B., and Patapoutian, A. (2012). The role of *Drosophila* Piezo in mechanical nociception. *Nature* 483, 209-212.
- Kindt, K.S., Viswanath, V., Macpherson, L., Quast, K., Hu, H., Patapoutian, A., and Schafer, W.R. (2007). *Caenorhabditis elegans* TRPA-1 functions in mechanosensation. *Nature neuroscience* 10, 568-577.
- Kleyman, T.R., Carattino, M.D., and Hughey, R.P. (2009). ENaC at the cutting edge: regulation of epithelial sodium channels by proteases. *The Journal of biological chemistry* 284, 20447-20451.
- Kung, C. (2005). A possible unifying principle for mechanosensation. *Nature* 436, 647-654.

- Kung, C., and Blount, P. (2004). Channels in microbes: so many holes to fill. *Molecular microbiology* 53, 373-380.
- Kung, C., Martinac, B., and Sukharev, S. (2010). Mechanosensitive channels in microbes. *Annual review of microbiology* 64, 313-329.
- Lai, C.C., Hong, K., Kinnell, M., Chalfie, M., and Driscoll, M. (1996). Sequence and transmembrane topology of MEC-4, an ion channel subunit required for mechanotransduction in *Caenorhabditis elegans*. *The Journal of cell biology* 133, 1071-1081.
- Laitko, U., Juranka, P.F., and Morris, C.E. (2006). Membrane stretch slows the concerted step prior to opening in a Kv channel. *The Journal of general physiology* 127, 687-701.
- Laitko, U., and Morris, C.E. (2004). Membrane tension accelerates rate-limiting voltage-dependent activation and slow inactivation steps in a Shaker channel. *The Journal of general physiology* 123, 135-154.
- Leach, M.R., Cohen-Doyle, M.F., Thomas, D.Y., and Williams, D.B. (2002). Localization of the lectin, ERp57 binding, and polypeptide binding sites of calnexin and calreticulin. *The Journal of biological chemistry* 277, 29686-29697.
- Lee, I.H., Dinudom, A., Sanchez-Perez, A., Kumar, S., and Cook, D.I. (2007). Akt mediates the effect of insulin on epithelial sodium channels by inhibiting Nedd4-2. *The Journal of biological chemistry* 282, 29866-29873.
- Lee, M.C., Orci, L., Hamamoto, S., Futai, E., Ravazzola, M., and Schekman, R. (2005). Sar1p N-terminal helix initiates membrane curvature and completes the fission of a COPII vesicle. *Cell* 122, 605-617.
- Levina, N., Totemeyer, S., Stokes, N.R., Louis, P., Jones, M.A., and Booth, I.R. (1999). Protection of *Escherichia coli* cells against extreme turgor by activation of MscS and MscL mechanosensitive channels: identification of genes required for MscS activity. *The EMBO journal* 18, 1730-1737.
- Li, W., Feng, Z., Sternberg, P.W., and Xu, X.Z. (2006). A *C. elegans* stretch receptor neuron revealed by a mechanosensitive TRP channel homologue. *Nature* 440, 684-687.
- Liedtke, W., and Friedman, J.M. (2003). Abnormal osmotic regulation in *trpv4*<sup>-/-</sup> mice. *Proceedings of the National Academy of Sciences of the United States of America* 100, 13698-13703.
- Liedtke, W., Tobin, D.M., Bargmann, C.I., and Friedman, J.M. (2003). Mammalian TRPV4 (VR-OAC) directs behavioral responses to osmotic and mechanical stimuli in *Caenorhabditis elegans*. *Proceedings of the National Academy of Sciences of the United States of America* 100 Suppl 2, 14531-14536.

- Liman, E.R., Tytgat, J., and Hess, P. (1992). Subunit stoichiometry of a mammalian K<sup>+</sup> channel determined by construction of multimeric cDNAs. *Neuron* 9, 861-871.
- Lin, W., Laitko, U., Juranka, P.F., and Morris, C.E. (2007). Dual stretch responses of mHCN2 pacemaker channels: accelerated activation, accelerated deactivation. *Biophysical journal* 92, 1559-1572.
- Lin, W., Ogura, T., and Kinnamon, S.C. (2002). Acid-activated cation currents in rat vallate taste receptor cells. *Journal of neurophysiology* 88, 133-141.
- Lingueglia, E., Champigny, G., Lazdunski, M., and Barbry, P. (1995). Cloning of the amiloride-sensitive FMRFamide peptide-gated sodium channel. *Nature* 378, 730-733.
- Lingueglia, E., de Weille, J.R., Bassilana, F., Heurteaux, C., Sakai, H., Waldmann, R., and Lazdunski, M. (1997). A modulatory subunit of acid sensing ion channels in brain and dorsal root ganglion cells. *The Journal of biological chemistry* 272, 29778-29783.
- Lingueglia, E., Voilley, N., Waldmann, R., Lazdunski, M., and Barbry, P. (1993). Expression cloning of an epithelial amiloride-sensitive Na<sup>+</sup> channel. A new channel type with homologies to *Caenorhabditis elegans* degenerins. *FEBS letters* 318, 95-99.
- Liu, J., Schrank, B., and Waterston, R.H. (1996). Interaction between a putative mechanosensory membrane channel and a collagen. *Science* 273, 361-364.
- Liu, L., Leonard, A.S., Motto, D.G., Feller, M.A., Price, M.P., Johnson, W.A., and Welsh, M.J. (2003). Contribution of *Drosophila* DEG/ENaC genes to salt taste. *Neuron* 39, 133-146.
- Loffing, J., and Korbmayer, C. (2009). Regulated sodium transport in the renal connecting tubule (CNT) via the epithelial sodium channel (ENaC). *Pflugers Archiv : European journal of physiology* 458, 111-135.
- Loffing, J., Zecevic, M., Feraille, E., Kaissling, B., Asher, C., Rossier, B.C., Firestone, G.L., Pearce, D., and Verrey, F. (2001). Aldosterone induces rapid apical translocation of ENaC in early portion of renal collecting system: possible role of SGK. *American journal of physiology Renal physiology* 280, F675-682.
- Lu, Y., Ma, X., Sabharwal, R., Snitsarev, V., Morgan, D., Rahmouni, K., Drummond, H.A., Whiteis, C.A., Costa, V., Price, M., *et al.* (2009). The ion channel ASIC2 is required for baroreceptor and autonomic control of the circulation. *Neuron* 64, 885-897.
- Lund-Katz, S., Liu, L., Thuahnai, S.T., and Phillips, M.C. (2003). High density lipoprotein structure. *Frontiers in bioscience : a journal and virtual library* 8, d1044-1054.
- Mackness, M.I., Arrol, S., Abbott, C., and Durrington, P.N. (1993). Protection of low-density lipoprotein against oxidative modification by high-density lipoprotein associated paraoxonase. *Atherosclerosis* 104, 129-135.

Maingret, F., Fosset, M., Lesage, F., Lazdunski, M., and Honore, E. (1999). TRAAK is a mammalian neuronal mechano-gated K<sup>+</sup> channel. *The Journal of biological chemistry* 274, 1381-1387.

Mano, I., and Driscoll, M. (1999). DEG/ENaC channels: a touchy superfamily that watches its salt. *BioEssays : news and reviews in molecular, cellular and developmental biology* 21, 568-578.

Merzlyak, E.M., Goedhart, J., Shcherbo, D., Bulina, M.E., Shcheglov, A.S., Fradkov, A.F., Gaintzeva, A., Lukyanov, K.A., Lukyanov, S., Gadella, T.W., *et al.* (2007). Bright monomeric red fluorescent protein with an extended fluorescence lifetime. *Nature methods* 4, 555-557.

Michalak, M., Groenendyk, J., Szabo, E., Gold, L.I., and Opas, M. (2009). Calreticulin, a multi-process calcium-buffering chaperone of the endoplasmic reticulum. *The Biochemical journal* 417, 651-666.

Miesenbock, G., De Angelis, D.A., and Rothman, J.E. (1998). Visualizing secretion and synaptic transmission with pH-sensitive green fluorescent proteins. *Nature* 394, 192-195.

Miller, D.M., and Shakes, D.C. (1995). Immunofluorescence microscopy. *Methods in cell biology* 48, 365-394.

Miller, E., Antony, B., Hamamoto, S., and Schekman, R. (2002). Cargo selection into COPII vesicles is driven by the Sec24p subunit. *The EMBO journal* 21, 6105-6113.

Miller, E.A., Beilharz, T.H., Malkus, P.N., Lee, M.C., Hamamoto, S., Orci, L., and Schekman, R. (2003). Multiple cargo binding sites on the COPII subunit Sec24p ensure capture of diverse membrane proteins into transport vesicles. *Cell* 114, 497-509.

Miyawaki, A., Llopis, J., Heim, R., McCaffery, J.M., Adams, J.A., Ikura, M., and Tsien, R.Y. (1997). Fluorescent indicators for Ca<sup>2+</sup> based on green fluorescent proteins and calmodulin. *Nature* 388, 882-887.

Mogil, J.S., Breese, N.M., Witty, M.F., Ritchie, J., Rainville, M.L., Ase, A., Abbadi, N., Stucky, C.L., and Seguela, P. (2005). Transgenic expression of a dominant-negative ASIC3 subunit leads to increased sensitivity to mechanical and inflammatory stimuli. *The Journal of neuroscience : the official journal of the Society for Neuroscience* 25, 9893-9901.

Montell, C. (2005). The TRP superfamily of cation channels. *Science's STKE : signal transduction knowledge environment* 2005, re3.

Montell, C., Jones, K., Hafen, E., and Rubin, G. (1985). Rescue of the *Drosophila* phototransduction mutation *trp* by germline transformation. *Science* 230, 1040-1043.

Montell, C., and Rubin, G.M. (1989). Molecular characterization of the *Drosophila* trp locus: a putative integral membrane protein required for phototransduction. *Neuron* 2, 1313-1323.

Nagel, G., Szellas, T., Huhn, W., Kateriya, S., Adeishvili, N., Berthold, P., Ollig, D., Hegemann, P., and Bamberg, E. (2003). Channelrhodopsin-2, a directly light-gated cation-selective membrane channel. *Proceedings of the National Academy of Sciences of the United States of America* 100, 13940-13945.

Nakamura, K., Zuppini, A., Arnaudeau, S., Lynch, J., Ahsan, I., Krause, R., Papp, S., De Smedt, H., Parys, J.B., Muller-Esterl, W., *et al.* (2001). Functional specialization of calreticulin domains. *The Journal of cell biology* 154, 961-972.

Nelson, T.M., Lopezjimenez, N.D., Tessarollo, L., Inoue, M., Bachmanov, A.A., and Sullivan, S.L. (2010). Taste function in mice with a targeted mutation of the *pkd113* gene. *Chemical senses* 35, 565-577.

Ng, C.J., Wadleigh, D.J., Gangopadhyay, A., Hama, S., Grijalva, V.R., Navab, M., Fogelman, A.M., and Reddy, S.T. (2001). Paraoxonase-2 is a ubiquitously expressed protein with antioxidant properties and is capable of preventing cell-mediated oxidative modification of low density lipoprotein. *The Journal of biological chemistry* 276, 44444-44449.

O'Hagan, R., Chalfie, M., and Goodman, M.B. (2005). The MEC-4 DEG/ENaC channel of *Caenorhabditis elegans* touch receptor neurons transduces mechanical signals. *Nature neuroscience* 8, 43-50.

Olzmann, J.A., Kopito, R.R., and Christianson, J.C. (2013). The mammalian endoplasmic reticulum-associated degradation system. *Cold Spring Harbor perspectives in biology* 5.

Palmer, A.E., Jin, C., Reed, J.C., and Tsien, R.Y. (2004). Bcl-2-mediated alterations in endoplasmic reticulum Ca<sup>2+</sup> analyzed with an improved genetically encoded fluorescent sensor. *Proceedings of the National Academy of Sciences of the United States of America* 101, 17404-17409.

Pan, B., Geleoc, G.S., Asai, Y., Horwitz, G.C., Kurima, K., Ishikawa, K., Kawashima, Y., Griffith, A.J., and Holt, J.R. (2013). TMC1 and TMC2 are components of the mechanotransduction channel in hair cells of the mammalian inner ear. *Neuron* 79, 504-515.

Paquet, M.E., Leach, M.R., and Williams, D.B. (2005). In vitro and in vivo assays to assess the functions of calnexin and calreticulin in ER protein folding and quality control. *Methods* 35, 338-347.

Park, B.J., Lee, D.G., Yu, J.R., Jung, S.K., Choi, K., Lee, J., Lee, J., Kim, Y.S., Lee, J.I., Kwon, J.Y., *et al.* (2001). Calreticulin, a calcium-binding molecular chaperone, is required for stress response and fertility in *Caenorhabditis elegans*. *Molecular biology of the cell* 12, 2835-2845.

- Park, E.C., and Horvitz, H.R. (1986). *C. elegans* unc-105 mutations affect muscle and are suppressed by other mutations that affect muscle. *Genetics* 113, 853-867.
- Patel, A.J., Honore, E., Maingret, F., Lesage, F., Fink, M., Duprat, F., and Lazdunski, M. (1998). A mammalian two pore domain mechano-gated S-like K<sup>+</sup> channel. *The EMBO journal* 17, 4283-4290.
- Peng, R., Grabowski, R., De Antoni, A., and Gallwitz, D. (1999). Specific interaction of the yeast cis-Golgi syntaxin Sed5p and the coat protein complex II component Sec24p of endoplasmic reticulum-derived transport vesicles. *Proceedings of the National Academy of Sciences of the United States of America* 96, 3751-3756.
- Philipps, B., Hennecke, J., and Glockshuber, R. (2003). FRET-based in vivo screening for protein folding and increased protein stability. *Journal of molecular biology* 327, 239-249.
- Pickles, J.O., and Corey, D.P. (1992). Mechanoelectrical transduction by hair cells. *Trends in neurosciences* 15, 254-259.
- Poole, K., Herget, R., Lapatsina, L., Ngo, H.D., and Lewin, G.R. (2014). Tuning Piezo ion channels to detect molecular-scale movements relevant for fine touch. *Nature communications* 5, 3520.
- Prabakaran, D., Kim, P.S., Dixit, V.M., and Arvan, P. (1996). Oligomeric assembly of thrombospondin in the endoplasmic reticulum of thyroid epithelial cells. *European journal of cell biology* 70, 134-141.
- Presley, J.F., Cole, N.B., Schroer, T.A., Hirschberg, K., Zaal, K.J., and Lippincott-Schwartz, J. (1997). ER-to-Golgi transport visualized in living cells. *Nature* 389, 81-85.
- Price, M.P., McIlwrath, S.L., Xie, J., Cheng, C., Qiao, J., Tarr, D.E., Sluka, K.A., Brennan, T.J., Lewin, G.R., and Welsh, M.J. (2001). The DRASIC cation channel contributes to the detection of cutaneous touch and acid stimuli in mice. *Neuron* 32, 1071-1083.
- Primo-Parmo, S.L., Sorenson, R.C., Teiber, J., and La Du, B.N. (1996). The human serum paraoxonase/arylesterase gene (PON1) is one member of a multigene family. *Genomics* 33, 498-507.
- Rapoport, T.A. (2007). Protein translocation across the eukaryotic endoplasmic reticulum and bacterial plasma membranes. *Nature* 450, 663-669.
- Rapoport, T.A., Goder, V., Heinrich, S.U., and Matlack, K.E. (2004). Membrane-protein integration and the role of the translocation channel. *Trends in cell biology* 14, 568-575.
- Reddy, S.T., Wadleigh, D.J., Grijalva, V., Ng, C., Hama, S., Gangopadhyay, A., Shih, D.M., Lusis, A.J., Navab, M., and Fogelman, A.M. (2001). Human paraoxonase-3 is an HDL-

associated enzyme with biological activity similar to paraoxonase-1 protein but is not regulated by oxidized lipids. *Arteriosclerosis, thrombosis, and vascular biology* 21, 542-547.

Riach, R.A., Duncan, G., Williams, M.R., and Webb, S.F. (1995). Histamine and ATP mobilize calcium by activation of H1 and P2u receptors in human lens epithelial cells. *The Journal of physiology* 486 ( Pt 2), 273-282.

Richter, T.A., Dvoryanchikov, G.A., Roper, S.D., and Chaudhari, N. (2004). Acid-sensing ion channel-2 is not necessary for sour taste in mice. *The Journal of neuroscience : the official journal of the Society for Neuroscience* 24, 4088-4091.

Riddle, D.L. (1997). *C. elegans II* (Plainview, N.Y.: Cold Spring Harbor Laboratory Press).

Roberts, B., Clucas, C., and Johnstone, I.L. (2003). Loss of SEC-23 in *Caenorhabditis elegans* causes defects in oogenesis, morphogenesis, and extracellular matrix secretion. *Molecular biology of the cell* 14, 4414-4426.

Rodrigo, L., Gil, F., Hernandez, A.F., Lopez, O., and Pla, A. (2003). Identification of paraoxonase 3 in rat liver microsomes: purification and biochemical properties. *The Biochemical journal* 376, 261-268.

Rolls, M.M., Hall, D.H., Victor, M., Stelzer, E.H., and Rapoport, T.A. (2002). Targeting of rough endoplasmic reticulum membrane proteins and ribosomes in invertebrate neurons. *Molecular biology of the cell* 13, 1778-1791.

Rosenblat, M., Draganov, D., Watson, C.E., Bisgaier, C.L., La Du, B.N., and Aviram, M. (2003). Mouse macrophage paraoxonase 2 activity is increased whereas cellular paraoxonase 3 activity is decreased under oxidative stress. *Arteriosclerosis, thrombosis, and vascular biology* 23, 468-474.

Rosenblat, M., Gaidukov, L., Khersonsky, O., Vaya, J., Oren, R., Tawfik, D.S., and Aviram, M. (2006). The catalytic histidine dyad of high density lipoprotein-associated serum paraoxonase-1 (PON1) is essential for PON1-mediated inhibition of low density lipoprotein oxidation and stimulation of macrophage cholesterol efflux. *The Journal of biological chemistry* 281, 7657-7665.

Roza, C., Puel, J.L., Kress, M., Baron, A., Diochot, S., Lazdunski, M., and Waldmann, R. (2004). Knockout of the ASIC2 channel in mice does not impair cutaneous mechanosensation, visceral mechanonociception and hearing. *The Journal of physiology* 558, 659-669.

Saito, Y., Ihara, Y., Leach, M.R., Cohen-Doyle, M.F., and Williams, D.B. (1999). Calreticulin functions in vitro as a molecular chaperone for both glycosylated and non-glycosylated proteins. *The EMBO journal* 18, 6718-6729.

Shekman, R. (2002). Lasker Basic Medical Research Award. SEC mutants and the secretory apparatus. *Nature medicine* 8, 1055-1058.



- Schild, L. (2010). The epithelial sodium channel and the control of sodium balance. *Biochimica et biophysica acta* *1802*, 1159-1165.
- Schweikert, E.M., Devarajan, A., Witte, I., Wilgenbus, P., Amort, J., Forstermann, U., Shabazian, A., Grijalva, V., Shih, D.M., Farias-Eisner, R., *et al.* (2012). PON3 is upregulated in cancer tissues and protects against mitochondrial superoxide-mediated cell death. *Cell death and differentiation* *19*, 1549-1560.
- Sherwood, T.W., Frey, E.N., and Askwith, C.C. (2012). Structure and activity of the acid-sensing ion channels. *American journal of physiology Cell physiology* *303*, C699-710.
- Shi, H., Asher, C., Chigaev, A., Yung, Y., Reuveny, E., Seger, R., and Garty, H. (2002a). Interactions of beta and gamma ENaC with Nedd4 can be facilitated by an ERK-mediated phosphorylation. *The Journal of biological chemistry* *277*, 13539-13547.
- Shi, H., Asher, C., Yung, Y., Kligman, L., Reuveny, E., Seger, R., and Garty, H. (2002b). Casein kinase 2 specifically binds to and phosphorylates the carboxy termini of ENaC subunits. *European journal of biochemistry / FEBS* *269*, 4551-4558.
- Shih, D.M., Xia, Y.R., Yu, J.M., and Lusic, A.J. (2010). Temporal and tissue-specific patterns of Pon3 expression in mouse: in situ hybridization analysis. *Advances in experimental medicine and biology* *660*, 73-87.
- Shimkets, R.A., Lifton, R., and Canessa, C.M. (1998). In vivo phosphorylation of the epithelial sodium channel. *Proceedings of the National Academy of Sciences of the United States of America* *95*, 3301-3305.
- Shimkets, R.A., Warnock, D.G., Bositis, C.M., Nelson-Williams, C., Hansson, J.H., Schambelan, M., Gill, J.R., Jr., Ulick, S., Milora, R.V., Findling, J.W., *et al.* (1994). Liddle's syndrome: heritable human hypertension caused by mutations in the beta subunit of the epithelial sodium channel. *Cell* *79*, 407-414.
- Shimoni, Y., Kurihara, T., Ravazzola, M., Amherdt, M., Orci, L., and Schekman, R. (2000). Lst1p and Sec24p cooperate in sorting of the plasma membrane ATPase into COPII vesicles in *Saccharomyces cerevisiae*. *The Journal of cell biology* *151*, 973-984.
- Shreffler, W., Magardino, T., Shekdar, K., and Wolinsky, E. (1995). The *unc-8* and *sup-40* genes regulate ion channel function in *Caenorhabditis elegans* motoneurons. *Genetics* *139*, 1261-1272.
- Sidi, S., Friedrich, R.W., and Nicolson, T. (2003). NompC TRP channel required for vertebrate sensory hair cell mechanotransduction. *Science* *301*, 96-99.
- Smolen, A., Eckerson, H.W., Gan, K.N., Hailat, N., and La Du, B.N. (1991). Characteristics of the genetically determined allozymic forms of human serum paraoxonase/arylesterase. *Drug metabolism and disposition: the biological fate of chemicals* *19*, 107-112.

Snyder, P.M. (2002). The epithelial Na<sup>+</sup> channel: cell surface insertion and retrieval in Na<sup>+</sup> homeostasis and hypertension. *Endocrine reviews* 23, 258-275.

Snyder, P.M., Cheng, C., Prince, L.S., Rogers, J.C., and Welsh, M.J. (1998). Electrophysiological and biochemical evidence that DEG/ENaC cation channels are composed of nine subunits. *The Journal of biological chemistry* 273, 681-684.

Snyder, P.M., Olson, D.R., Kabra, R., Zhou, R., and Steines, J.C. (2004). cAMP and serum and glucocorticoid-inducible kinase (SGK) regulate the epithelial Na<sup>(+)</sup> channel through convergent phosphorylation of Nedd4-2. *The Journal of biological chemistry* 279, 45753-45758.

Sorenson, R.C., Bisgaier, C.L., Aviram, M., Hsu, C., Billecke, S., and La Du, B.N. (1999). Human serum Paraoxonase/Arylesterase's retained hydrophobic N-terminal leader sequence associates with HDLs by binding phospholipids : apolipoprotein A-I stabilizes activity. *Arteriosclerosis, thrombosis, and vascular biology* 19, 2214-2225.

Springer, S., and Schekman, R. (1998). Nucleation of COPII vesicular coat complex by endoplasmic reticulum to Golgi vesicle SNAREs. *Science* 281, 698-700.

Stanley, P. (2011). Golgi glycosylation. *Cold Spring Harbor perspectives in biology* 3.

Staruschenko, A., Adams, E., Booth, R.E., and Stockand, J.D. (2005). Epithelial Na<sup>+</sup> channel subunit stoichiometry. *Biophysical journal* 88, 3966-3975.

Staruschenko, A., Pochynyuk, O., Vandewalle, A., Bugaj, V., and Stockand, J.D. (2007). Acute regulation of the epithelial Na<sup>+</sup> channel by phosphatidylinositide 3-OH kinase signaling in native collecting duct principal cells. *Journal of the American Society of Nephrology : JASN* 18, 1652-1661.

Staub, O., Dho, S., Henry, P., Correa, J., Ishikawa, T., McGlade, J., and Rotin, D. (1996). WW domains of Nedd4 bind to the proline-rich PY motifs in the epithelial Na<sup>+</sup> channel deleted in Liddle's syndrome. *The EMBO journal* 15, 2371-2380.

Straub, C., and Tomita, S. (2012). The regulation of glutamate receptor trafficking and function by TARPs and other transmembrane auxiliary subunits. *Current opinion in neurobiology* 22, 488-495.

Stronge, V.S., Saito, Y., Ihara, Y., and Williams, D.B. (2001). Relationship between calnexin and BiP in suppressing aggregation and promoting refolding of protein and glycoprotein substrates. *The Journal of biological chemistry* 276, 39779-39787.

Sukharev, S.I., Blount, P., Martinac, B., Blattner, F.R., and Kung, C. (1994). A large-conductance mechanosensitive channel in *E. coli* encoded by *mscL* alone. *Nature* 368, 265-268.

Suzuki, H., Kerr, R., Bianchi, L., Frokjaer-Jensen, C., Slone, D., Xue, J., Gerstbrein, B., Driscoll, M., and Schafer, W.R. (2003). In vivo imaging of *C. elegans* mechanosensory neurons demonstrates a specific role for the MEC-4 channel in the process of gentle touch sensation. *Neuron* 39, 1005-1017.

Tadeo, I., Berbegall, A.P., Escudero, L.M., Alvaro, T., and Noguera, R. (2014). Biotensegrity of the Extracellular Matrix: Physiology, Dynamic Mechanical Balance, and Implications in Oncology and Mechanotherapy. *Frontiers in oncology* 4, 39.

Tavernarakis, N., Shreffler, W., Wang, S., and Driscoll, M. (1997). *unc-8*, a DEG/ENaC family member, encodes a subunit of a candidate mechanically gated channel that modulates *C. elegans* locomotion. *Neuron* 18, 107-119.

Tobin, D., Madsen, D., Kahn-Kirby, A., Peckol, E., Moulder, G., Barstead, R., Maricq, A., and Bargmann, C. (2002). Combinatorial expression of TRPV channel proteins defines their sensory functions and subcellular localization in *C. elegans* neurons. *Neuron* 35, 307-318.

Topalidou, I., and Chalfie, M. (2011). Shared gene expression in distinct neurons expressing common selector genes. *Proceedings of the National Academy of Sciences of the United States of America* 108, 19258-19263.

Topalidou, I., Keller, C., Kalebic, N., Nguyen, K.C., Somhegyi, H., Politi, K.A., Heppenstall, P., Hall, D.H., and Chalfie, M. (2012). Genetically separable functions of the MEC-17 tubulin acetyltransferase affect microtubule organization. *Current biology : CB* 22, 1057-1065.

Topalidou, I., van Oudenaarden, A., and Chalfie, M. (2011). *Caenorhabditis elegans* *aristaless/Arx* gene *alr-1* restricts variable gene expression. *Proceedings of the National Academy of Sciences of the United States of America* 108, 4063-4068.

Traub, L.M., and Kornfeld, S. (1997). The trans-Golgi network: a late secretory sorting station. *Current opinion in cell biology* 9, 527-533.

Turnheim, K. (1991). Intrinsic regulation of apical sodium entry in epithelia. *Physiological reviews* 71, 429-445.

Ugawa, S. (2003). Identification of sour-taste receptor genes. *Anatomical science international* 78, 205-210.

Ugawa, S., Minami, Y., Guo, W., Saishin, Y., Takatsuji, K., Yamamoto, T., Tohyama, M., and Shimada, S. (1998). Receptor that leaves a sour taste in the mouth. *Nature* 395, 555-556.

Ugawa, S., Ueda, T., Ishida, Y., Nishigaki, M., Shibata, Y., and Shimada, S. (2002). Amiloride-blockable acid-sensing ion channels are leading acid sensors expressed in human nociceptors. *The Journal of clinical investigation* 110, 1185-1190.

Ulbrich, M.H., and Isacoff, E.Y. (2007). Subunit counting in membrane-bound proteins. *Nature methods* 4, 319-321.

Ulbrich, M.H., and Isacoff, E.Y. (2008). Rules of engagement for NMDA receptor subunits. *Proceedings of the National Academy of Sciences of the United States of America* 105, 14163-14168.

Vembar, S.S., and Brodsky, J.L. (2008). One step at a time: endoplasmic reticulum-associated degradation. *Nature reviews Molecular cell biology* 9, 944-957.

Venkatachalam, K., and Montell, C. (2007). TRP channels. *Annual review of biochemistry* 76, 387-417.

Volk, T., Konstas, A.A., Bassalay, P., Ehmke, H., and Korbmayer, C. (2004). Extracellular Na<sup>+</sup> removal attenuates rundown of the epithelial Na<sup>+</sup>-channel (ENaC) by reducing the rate of channel retrieval. *Pflügers Archiv : European journal of physiology* 447, 884-894.

Waithe, D., Ferron, L., Page, K.M., Chaggar, K., and Dolphin, A.C. (2011). Beta-subunits promote the expression of Ca<sub>v</sub>2.2 channels by reducing their proteasomal degradation. *The Journal of biological chemistry* 286, 9598-9611.

Waldmann, R., Champigny, G., Bassilana, F., Heurteaux, C., and Lazdunski, M. (1997). A proton-gated cation channel involved in acid-sensing. *Nature* 386, 173-177.

Waldmann, R., Champigny, G., Voilley, N., Lauritzen, I., and Lazdunski, M. (1996). The mammalian degenerin MDEG, an amiloride-sensitive cation channel activated by mutations causing neurodegeneration in *Caenorhabditis elegans*. *The Journal of biological chemistry* 271, 10433-10436.

Walker, R.G., Willingham, A.T., and Zuker, C.S. (2000). A *Drosophila* mechanosensory transduction channel. *Science* 287, 2229-2234.

Wang, Y., Apicella, A., Jr., Lee, S.K., Ezcurra, M., Slone, R.D., Goldmit, M., Schafer, W.R., Shaham, S., Driscoll, M., and Bianchi, L. (2008). A glial DEG/ENaC channel functions with neuronal channel DEG-1 to mediate specific sensory functions in *C. elegans*. *The EMBO journal* 27, 2388-2399.

Wang, Y., and Bianchi, L. (2009). Insights into the molecular determinants of proton inhibition in an acid-inactivated degenerins and mammalian epithelial Na<sup>(+)</sup> channel. *Biochemistry* 48, 10005-10013.

Wang, Y., Matthewman, C., Han, L., Miller, T., Miller, D.M., 3rd, and Bianchi, L. (2013). Neurotoxic unc-8 mutants encode constitutively active DEG/ENaC channels that are blocked by divalent cations. *The Journal of general physiology* 142, 157-169.

Weisz, O.A., and Rodriguez-Boulan, E. (2009). Apical trafficking in epithelial cells: signals, clusters and motors. *Journal of cell science* 122, 4253-4266.

Wemmie, J.A., Askwith, C.C., Lamani, E., Cassell, M.D., Freeman, J.H., Jr., and Welsh, M.J. (2003). Acid-sensing ion channel 1 is localized in brain regions with high synaptic density and contributes to fear conditioning. *The Journal of neuroscience : the official journal of the Society for Neuroscience* 23, 5496-5502.

Wemmie, J.A., Chen, J., Askwith, C.C., Hruska-Hageman, A.M., Price, M.P., Nolan, B.C., Yoder, P.G., Lamani, E., Hoshi, T., Freeman, J.H., Jr., *et al.* (2002). The acid-activated ion channel ASIC contributes to synaptic plasticity, learning, and memory. *Neuron* 34, 463-477.

Wemmie, J.A., Price, M.P., and Welsh, M.J. (2006). Acid-sensing ion channels: advances, questions and therapeutic opportunities. *Trends in neurosciences* 29, 578-586.

Wemmie, J.A., Taugher, R.J., and Kreple, C.J. (2013). Acid-sensing ion channels in pain and disease. *Nature reviews Neuroscience* 14, 461-471.

Wetzel, C., Hu, J., Riethmacher, D., Benckendorff, A., Harder, L., Eilers, A., Moshourab, R., Kozlenkov, A., Labuz, D., Caspani, O., *et al.* (2007). A stomatin-domain protein essential for touch sensation in the mouse. *Nature* 445, 206-209.

White, J.G., Southgate, E., Thomson, J.N., and Brenner, S. (1986). The structure of the nervous system of the nematode *Caenorhabditis elegans*. *Philosophical transactions of the Royal Society of London Series B, Biological sciences* 314, 1-340.

Woo, S.H., Ranade, S., Weyer, A.D., Dubin, A.E., Baba, Y., Qiu, Z., Petrus, M., Miyamoto, T., Reddy, K., Lumpkin, E.A., *et al.* (2014). Piezo2 is required for Merkel-cell mechanotransduction. *Nature* 509, 622-626.

Xia, Z., and Liu, Y. (2001). Reliable and global measurement of fluorescence resonance energy transfer using fluorescence microscopes. *Biophysical journal* 81, 2395-2402.

Xiong, Z.G., Zhu, X.M., Chu, X.P., Minami, M., Hey, J., Wei, W.L., MacDonald, J.F., Wemmie, J.A., Price, M.P., Welsh, M.J., *et al.* (2004). Neuroprotection in ischemia: blocking calcium-permeable acid-sensing ion channels. *Cell* 118, 687-698.

Xu, K., Tavernarakis, N., and Driscoll, M. (2001). Necrotic cell death in *C. elegans* requires the function of calreticulin and regulators of Ca(2+) release from the endoplasmic reticulum. *Neuron* 31, 957-971.

Youvan, D.C., Silva, C. M., Bylina E. J., Coleman W. J., Dilworth M. R., Yang M. M (1997). Calibration of Fluorescence Resonance Energy Transfer in Microscopy Using Genetically Engineered GFP Derivatives on Nickel Chelating Beads. . *Biotechnology et alia* 3, 18.

Zha, X.M., Wemmie, J.A., Green, S.H., and Welsh, M.J. (2006). Acid-sensing ion channel 1a is a postsynaptic proton receptor that affects the density of dendritic spines. *Proceedings of the National Academy of Sciences of the United States of America* *103*, 16556-16561.

Zhang, S. (2004). *Stomatin gene family in Caenorhabditis elegans*. (New York, NY: Columbia University).

Zhang, S., Arnadottir, J., Keller, C., Caldwell, G.A., Yao, C.A., and Chalfie, M. (2004). MEC-2 is recruited to the putative mechanosensory complex in *C. elegans* touch receptor neurons through its stomatin-like domain. *Current biology* : *CB 14*, 1888-1896.

Zhang, X.F., Chen, J., Faltynek, C.R., Moreland, R.B., and Neelands, T.R. (2008). Transient receptor potential A1 mediates an osmotically activated ion channel. *The European journal of neuroscience* *27*, 605-611.

Zhang, Y., Ma, C., Delohery, T., Nasipak, B., Foat, B.C., Bounoutas, A., Bussemaker, H.J., Kim, S.K., and Chalfie, M. (2002). Identification of genes expressed in *C. elegans* touch receptor neurons. *Nature* *418*, 331-335.

Zheng, C., Karimzadegan, S., Chiang, V., and Chalfie, M. (2013). Histone Methylation Restrains the Expression of Subtype-Specific Genes during Terminal Neuronal Differentiation in *Caenorhabditis elegans*. *PLoS genetics* *9*, e1004017.

Zhong, L., Hwang, R.Y., and Tracey, W.D. (2010). Pickpocket is a DEG/ENaC protein required for mechanical nociception in *Drosophila* larvae. *Current biology* : *CB 20*, 429-434.

Zhou, X.L., Batiza, A.F., Loukin, S.H., Palmer, C.P., Kung, C., and Saimi, Y. (2003). The transient receptor potential channel on the yeast vacuole is mechanosensitive. *Proceedings of the National Academy of Sciences of the United States of America* *100*, 7105-7110.

Zimmermann, R., Eyrich, S., Ahmad, M., and Helms, V. (2011). Protein translocation across the ER membrane. *Biochimica et biophysica acta* *1808*, 912-924.

## Appendix I

### **The DEG/ENaC protein MEC-10 regulates the transduction channel complex in *Caenorhabditis elegans* touch receptor neurons**

(In the following paper published on *The Journal of Neuroscience* in August of 2011, Johanna Arnadottir and other authors confirmed the functional contribution of MEC-10 to the mechanotransduction complex by showing that several *mec-10* point mutations altered the ion selectivity of the channel and abolished touch responses, while a potential *mec-10* null mutation resulted in only modest touch defects and reduction of mechanoreceptor current amplitude. I performed touch test on the wild type worms and two strains with partial deletion of *mec-10*, and found that animals with *mec-10* deletions, compared to the wild type, did not show defects in responding to touch stimuli delivered near the cell bodies of the TRNs. The touch response is shown in Supplemental Figure 1C.)

# The DEG/ENaC Protein MEC-10 Regulates the Transduction Channel Complex in *Caenorhabditis elegans* Touch Receptor Neurons

Jóhanna Árnadóttir,<sup>1</sup> Robert O'Hagan,<sup>1</sup> Yushu Chen,<sup>1</sup> Miriam B. Goodman,<sup>2</sup> and Martin Chalfie<sup>1</sup>

<sup>1</sup>Department of Biological Sciences, Columbia University, New York, New York 10027, and <sup>2</sup>Department of Molecular and Cellular Physiology, Stanford University, Stanford, California 94025

Gentle touch sensation in *Caenorhabditis elegans* is mediated by the MEC-4/MEC-10 channel complex, which is expressed exclusively in six touch receptor neurons (TRNs). The complex contains two pore-forming subunits, MEC-4 and MEC-10, as well as the accessory subunits MEC-2, MEC-6, and UNC-24. MEC-4 is essential for channel function, but beyond its role as a pore-forming subunit, the functional contribution of MEC-10 to the channel complex and to touch sensation is unclear. We addressed this question using behavioral assays, *in vivo* electrophysiological recordings from TRNs, and heterologous expression of mutant MEC-10 isoforms. Animals with a deletion in *mec-10* showed only a partial loss of touch sensitivity and a modest decrease in the size of the mechanoreceptor current (MRC). In contrast, five previously identified *mec-10* alleles acted as recessive gain-of-function alleles that resulted in complete touch insensitivity. Each of these alleles produced a substantial decrease in MRC size and a shift in the reversal potential *in vivo*. The latter finding indicates that these *mec-10* mutations alter the ionic selectivity of the transduction channel *in vivo*. All *mec-10* mutant animals had properly localized channel complexes, indicating that the loss of MRCs was not attributable to a dramatic mislocalization of transduction channels. Finally, electrophysiological examination of heterologously expressed complexes suggests that mutant MEC-10 proteins may affect channel current via MEC-2.

## Introduction

The degenerin/epithelial Na<sup>+</sup> channel (DEG/ENaC) proteins comprise a diverse family of ion channel proteins found in invertebrates and vertebrates (for review, see Kellenberger and Schild, 2002). DEG/ENaC proteins are involved in diverse physiological processes, such as sodium transport, mechanosensation, and salt and water taste, but share a common structure with two transmembrane domains, intracellular termini, and a large extracellular loop. Both homomeric and heteromeric channels can be formed.

Mutations in the genes for two DEG/ENaC proteins, MEC-4 and MEC-10, disrupt gentle touch sensation in the nematode *Caenorhabditis elegans* (Chalfie and Sulston, 1981; Driscoll and Chalfie, 1991; Huang and Chalfie, 1994). These two proteins and at least three accessory subunits (the prohibitin-domain proteins MEC-2 and UNC-24 and the paraoxonase-like protein MEC-6)

form a channel complex that transduces touch (Huang et al., 1995; Chelur et al., 2002; Zhang et al., 2004; O'Hagan et al., 2005).

Regions of MEC-4 and MEC-10 both contribute to the pore of the channel complex, as evidenced by the ability of mutations in either protein to affect the ion selectivity of the mechanoreceptor current (MRC) (O'Hagan et al., 2005). The two proteins share extensive sequence similarity, yet the two genes encoding them show dramatically different genetics. This difference may reflect the different roles that the two proteins play in the mechanosensory channel complex. Saturation mutagenesis screens for touch-insensitive animals identified 59 *mec-4* mutant alleles compared with only six *mec-10* mutant alleles (Chalfie and Sulston, 1981; Chalfie and Au, 1989). Furthermore, although the different *mec-4* alleles have mutations scattered throughout the gene, all but one of five *mec-10* mutations are clustered within a 25 nt stretch (the defect in the sixth allele has not been identified; Huang and Chalfie, 1994). These observations suggest that MEC-10 may play a minor role in touch sensation. This idea is supported by the finding that no MRC is generated in *mec-4* null animals with a wild-type *mec-10* allele (O'Hagan et al., 2005), suggesting that MEC-10 is not sufficient for generation of MRCs in the absence of MEC-4. Furthermore, a gain-of-function mutation in *mec-10* that causes the degeneration of the touch receptor neurons (TRNs) requires wild-type *mec-4*, but similar mutations in *mec-4* do not require wild-type *mec-10* (Chalfie and Wolinsky, 1990; Huang and Chalfie, 1994). However, all six of the previously characterized *mec-10* mutations result in complete touch insensitivity. If these mutations cause the loss of MEC-10

Received Sept. 1, 2010; revised May 25, 2011; accepted July 5, 2011.

Author contributions: J.Á., R.O., Y.C., M.B.G., and M.C. designed research; J.Á., R.O., and Y.C. performed research; J.Á., R.O., Y.C., M.B.G., and M.C. analyzed data; J.Á., R.O., M.B.G., and M.C. wrote the paper.

This work was supported by National Institutes of Health Grants GM30997 (M.C.) and NS047715 (M.B.G.) and a Howard Hughes Medical Institute Predoctoral Fellowship (R.O.). We thank C. A. Yao for helpful comments on this manuscript, I. Topalidou for help with the touch sensitivity studies, and A. L. Eastwood for generating and providing the *mec-4 mec-10* double mutant.

Correspondence should be addressed to Martin Chalfie, Department of Biological Sciences, Columbia University, 1012 Fairchild Center, Mail Code 2446, New York, NY 10027. E-mail: mc21@columbia.edu.

R. O'Hagan's present address: Department of Genetics, Rutgers University, Piscataway, NJ 08854.

DOI:10.1523/JNEUROSCI.4580-10.2011

Copyright © 2011 the authors 0270-6474/11/3112695-10\$15.00/0



activity, this finding implies that MEC-10 plays a critical role in mechanosensation.

In this paper, we resolve the apparent paradox of MEC-10 function by showing that the protein is not required for a behavioral or electrophysiological response to touch. Instead, MEC-10 plays a regulatory role in the channel complex and is essential for full sensitivity to gentle touch. In addition, we show that five previously identified *mec-10* mutant alleles are not loss-of-function mutations but recessive gain-of-function alleles. Finally, by recording currents from heterologously expressed channel complexes, we show that the gain-of-function effect of the *mec-10* mutations may be mediated via the MEC-2 accessory subunit.

## Materials and Methods

**Worm strains.** Wild type (N2) and strains with the mutations *mec-3(e1338)*, *mec-4(u253)*, *mec-10(e1515)*, *mec-10(u20)*, *mec-10(u390)*, *mec-10(u332)*, *mec-10(e1715)*, *lin-35(n745)*, and *mec-4(u339)* have been described previously (Brenner, 1974; Chalfie and Au, 1989; Huang and Chalfie, 1994; Lu and Horvitz, 1998) or constructed genetically (Brenner, 1974). In addition, we used TU2769, a strain with an integrated array containing *mec-17::gfp* and *lin-15(+)* in a *lin-15(n765ts)* background (O'Hagan et al., 2005), to generate strains with labeled TRNs. *mec-10(ok1104)* was obtained from the *C. elegans* Gene Knockout Consortium at Oklahoma Medical Research Foundation (Oklahoma City, OK). *mec-10(tm1552)* was obtained from the National Bioresource Project for the Nematode at Tokyo Women's Medical University (Tokyo, Japan). For visualization of MEC-4::YFP, an extrachromosomal array of *P<sub>mec-4</sub> mec-4::yfpP<sub>mec-4</sub>cfp* (Chelur et al., 2002) was integrated using gamma irradiation (Mello and Fire, 1995) and outcrossed seven times to wild type before crossing into the *mec-10* backgrounds.

***mec-10(ok1104)* sequencing.** The following primer pairs were used for PCR amplification of overlapping 1–2 kb regions of the *mec-10* gene for sequencing (Genewiz): 5'-GAAGGAATTTTTGGGATGGGG and 5'-ACGGGTTCAAATTGCAAAGA; 5'-CACGGATATACAATTGAGTTTGAC and 5'-CACTATCGCCAAAGTATTCCC; 5'-GATCGGAACCAAGAAGGAG and 5'-CGACACTTGAATGATCCGTG; and 5'-GTTAGGAACATTTGATACGGTTTC and 5'-CAAAAAAAAAAATGCAAAAGTGTGTACCC. cDNA was sequenced from products amplified from mRNA isolated from *ok1104* animals by RT-PCR using the following primer pairs: 5'-CGTAGTCGCAGTCGATTTC and 5'-CGACACTTGAATGATCCGTG; and 5'-CGTAGTCGCAGTCGATTTC and 5'-CACTATCGCCAAAGTATTCCC.

**Touch assays.** Animals were assayed for response to gentle touch as described by Chalfie and Sulston (1981) and scored as described by Hober et al. (1999). Each animal was usually touched 10 times, alternating between touch to the anterior and the posterior part of the animal. In experiments to test whether *mec-10* mutations resulted in differential responses along the TRN processes, we touched individual animals at specific locations only once. All touch assays were performed as blind tests.

To determine the touch sensitivity of animals that had a *mec-10* mutant allele and the *mec-10(ok1104)* deletion allele, we mated *mec-10(ok1104)* hermaphrodites with males hemizygous for the *mec-10* mutations and homozygous for the *mec-17::gfp* transgene from TU2769. Animals with this transgene express GFP in the TRNs without any significant effect on the touch sensitivity of the animal (O'Hagan et al., 2005). GFP-positive F1 progeny were picked from the crosses and tested for response to touch as described above.

Harsh touch was tested by prodding 20 wild-type, *mec-4(u253)*, *mec-3(e1338)*, and *mec-10(tm1552)* *mec-4(u253)* animals near the vulva with a platinum wire.

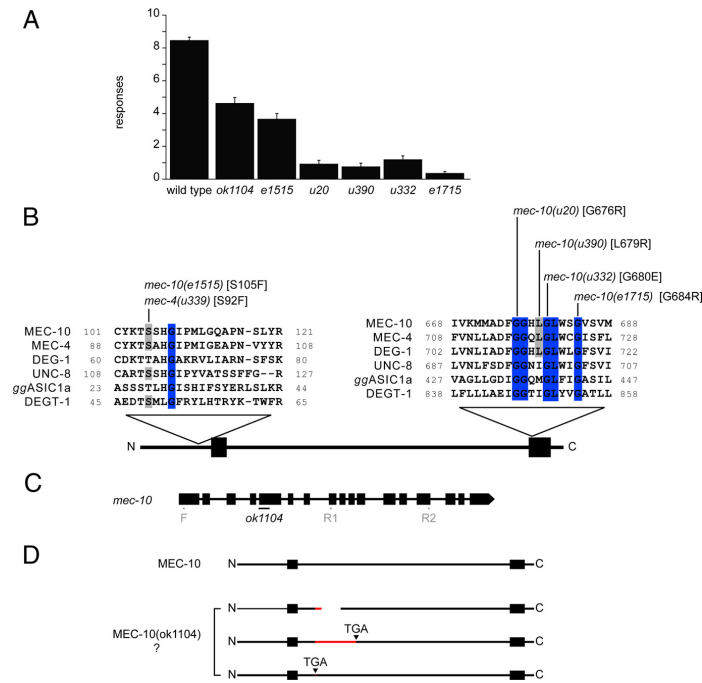
**RNA interference.** RNA interference (RNAi) was performed by feeding, essentially as described by Kamath and Ahringer (2003), using three different RNAi sensitizing backgrounds: *lin-35(n745)* (Lehner et al., 2006), *P<sub>unc-119</sub>sid-1P<sub>unc-119</sub>gfpP<sub>mec-6</sub>mec-6*; *lin-15b(n744)*, and *P<sub>unc-119</sub>sid-1P<sub>unc-119</sub>gfpP<sub>mec-6</sub>mec-6* (Calixto et al., 2010). The latter was used for knockdown of *mec-10* in *ok1104* animals, because *mec-10* and *lin-15b* are located in close proximity to each other on chromosome X. Worms were

fed *Escherichia coli* expressing double-stranded RNA against either *mec-10* or *mec-4* [Geneservice RNAi library, ID number X-4G16 (*mec-10*) or X-7D15 (*mec-4*) (Fraser et al., 2000); primer pairs for the *mec-10* clone: forward, ATCGGAAAACCAACTTGC and reverse, CGTAGTCGCAGTCGATTTC; and for the *mec-4* clone: forward, TACCTGCAACGGAAAGATCC and reverse, ATACAACGGAAAGACGCCAC]. To control for nonspecific effects of RNAi, we compared the touch response of test animals with that of animals fed bacteria expressing double-stranded RNA against GFP [pPD128.110 from the Fire Lab Vector kit, Addgene plasmid 1649 (Addgene); sequence available at <http://www.addgene.org>]. The bacteria was grown in liquid at 37°C for ~12 h before seeding onto nematode growth medium–isopropyl-thio-β-D-galactoside (NGM–IPTG) plates and then grown at room temperature for 24 h before use. Eggs were harvested by bleaching gravid adult animals in 0.1 M KOH, 10% bleach solution for 5 min. The eggs were washed three times in M9 buffer and then placed on seeded NGM–IPTG plates and grown at 20°C (*lin-35* background) or 15°C [*P<sub>unc-119</sub>sid-1P<sub>unc-119</sub>gfpP<sub>mec-6</sub>mec-6*; *lin-15b(n744)* and *P<sub>unc-119</sub>sid-1P<sub>unc-119</sub>gfpP<sub>mec-6</sub>mec-6* backgrounds]. Touch assays were as described above and were performed blind, with respect to both the strain and the bacteria on which it was raised.

**Whole-mount immunocytochemistry.** Animals were fixed with 1% formaldehyde for 30 min and permeabilized with β-mercaptoethanol, DTT, and H<sub>2</sub>O<sub>2</sub> for antibody staining as described (Miller and Shakes, 1995). Fixed animals were stained with a rabbit polyclonal antibody against the N terminus of MEC-2 (1:200) (Zhang et al., 2004) overnight at 4°C and Alexa Fluor 488-conjugated goat anti-rabbit antibody (1:2000) (Invitrogen) for 2 h at room temperature. Fluorescent micrographs were collected at 100× and used to compute inter-punctum intervals as follows: line segments tracing PLM neurons were straightened using the “straighten selection” function in Fiji (<http://pacific.mpi-cbg.de/wiki/index.php?title=Fiji&oldid=4701>), and straightened segments were used to compute intensity line scans from which inter-punctum intervals were measured from the distance between intensity peaks.

**In vivo electrophysiology.** Electrical responses to a mechanical stimulus were recorded at a holding potential of –74 mV from the cell body of a PLM touch receptor neuron that was exposed in the tail of an immobilized worm. Whole-cell recordings and data analysis were performed as described by O'Hagan et al. (2005), except data were collected using a HEKA EPC-10 amplifier. Recordings with a holding current of less than –15 pA and a series resistance of <100 MΩ were used for analysis (average series resistance was 64 MΩ). External saline contained the following (in mM): 145 NaCl, 5 KCl, 5 MgCl<sub>2</sub>, 1 CaCl<sub>2</sub>, 10 KHEPES, pH 7.2 (adjusted to ~320 mOsm with D-glucose). Internal saline contained the following (in mM): 125 Kgluconate, 22 NaCl, 1 MgCl<sub>2</sub>, 0.6 CaCl<sub>2</sub>, 10 NaHEPES, and 10 K<sub>2</sub>EGTA, pH 7.2. Sulforhodamine 101 (20 μM) was added to the internal saline to visualize the touch receptor neurite and confirm connection to the cell after recording. Holding potential was corrected for liquid junction potentials. For current–voltage relations, the membrane potential at the stimulus site was adjusted for attenuation because of the distance between the point of stimulus and the recording electrode ( $V_m$ ), using the following equation (O'Hagan et al., 2005):  $V_m = V_h \cosh(l_n/\lambda_n - d_e/\lambda_n) / \cosh(l_n/\lambda_n)$ , where  $V_h$  is the holding potential,  $l_n$  is the length of the neurite,  $\lambda_n$  is the length constant, and  $d_e$  is the distance between stimulus and electrode. The length of the neurite was estimated from the length of the body of the worm [measured from a video recording using NIH Image] (<http://rsbweb.nih.gov/ij/>) using the following relationship (O'Hagan et al., 2005):  $l_n = 123 + 0.34L$ , where  $L$  is the body length (in micrometers).  $d_e$  was measured from a video recording, and  $\lambda_n$  was estimated as described by O'Hagan et al. (2005).

Pressure dependence of MRCs was calculated as described by O'Hagan et al. (2005). The average  $P_{50}$  of wild-type MRCs we found in these experiments was similar but not identical to the previously published value. This difference is likely attributable to the errors associated with estimating the spring constants of the reference probe and the stimulus probe, as well as the area of stimulus probe that contacted the cuticle of the animal. However, this systematic difference had no effect on the



**Figure 1.** *mec-10* mutant alleles. **A**, Touch sensitivity of *mec-10* animals. Each animal was touched 10 times, as described in Materials and Methods (mean ± SEM,  $n = 30$  for each). **B**, Location of missense mutations in *mec-10* mutant alleles within conserved regions of DEG/ENaC proteins. Protein sequences were aligned using COBALT (Papadopoulos and Agarwal, 2007). Except ASIC1a (*Gallus gallus*), all sequences are from *C. elegans*. Gray shading indicates conserved residues at sites mutated in *mec-10*. Residues conserved among all the proteins are highlighted in blue. Transmembrane domains are represented by black boxes. **C**, The *ok1104* allele carries a 143 bp deletion (black bar) at the junction of the fourth intron and the fifth exon in the *mec-10* gene. Location of primer pairs used for RT-PCR amplification is indicated in gray (F, R1, and R2). **D**, Putative protein products in *ok1104* animals as derived from conceptual translation of three different RT-PCR products (see Results). Transmembrane domains are represented by black boxes, foreign amino acid residues by red bars, and a deletion by a white bar.

interpretation of results, as differences in  $P_{1/2}$  values between wild type and mutants were highly consistent.

Single-channel conductance of the mechanoreceptor channel in wild-type and *mec-10* deletion animals was determined using nonstationary noise analysis (Heinemann and Conti, 1992) as described by O'Hagan et al. (2005).

**Heterologous expression, electrophysiology, coimmunoprecipitation, and detection of surface-expressed channels.** Expression constructs for MEC-4d (A713T), MEC-2, MEC-6, MEC-10, myc::MEC-4d (A713T), and MEC-10::GFP have all been described previously (Chelur et al., 2002; Goodman et al., 2002). Point mutations corresponding to *mec-10* mutations were generated using the QuikChange site-directed mutagenesis kit (Stratagene).

cRNA was synthesized using the T7 mMESSAGE mMACHINE kit (Applied Biosystems/Ambion). Ten nanograms of MEC-4d, MEC-2, MEC-10 and 1 ng of MEC-6 cRNA were injected into *Xenopus laevis* oocytes. Oocytes were cultured in ND-96 with penicillin-streptomycin and 300  $\mu$ M amiloride at 17°C and recorded from or used for biochemical experiments, 5 d after injection. Two-electrode voltage-clamp recordings, coimmunoprecipitation, and surface expression experiments were performed as described previously (Chelur et al., 2002; Goodman et al., 2002).

For two-electrode voltage-clamp recordings, normal bath solution contained the following (in mM): 100 Na-gluconate, 2 KCl, 1 CaCl<sub>2</sub>, 2 MgCl<sub>2</sub>, and 10 NaHEPES, pH 7.2. Pipettes were filled with 3 M KCl.

Amiloride was added from a stock solution (0.1 M in DMSO) to a final concentration of 300  $\mu$ M to the bath solution to record amiloride-insensitive currents.

For coimmunoprecipitation experiments, oocytes were injected with cRNAs producing myc::MEC-4d, MEC-2, and wild-type or mutant forms of MEC-10::GFP. An agarose-conjugated polyclonal antibody against c-myc (A-14; Santa Cruz Biotechnology) was used to precipitate myc::MEC-4d from the lysate, followed by staining of Western blots with an HRP-conjugated monoclonal antibody against GFP (B-2; Santa Cruz Biotechnology) to detect GFP-tagged wild-type or mutant forms of MEC-10.

Surface expression was tested essentially as described (Goodman et al., 2002). In brief, oocytes were injected with cRNAs for myc::MEC-4d, MEC-2, and wild-type or mutant forms of MEC-10. Five days after injection, healthy and intact cells were selected and incubated in EZ-Link Sulfo-NHS-LC-Biotin (Thermo Scientific Pierce Protein Research Products). Unbound biotin was quenched with free glycine, and the oocytes were washed several times before lysis. Lysates were incubated with agarose-conjugated avidin beads to precipitate biotinylated surface proteins. Samples were then run on SDS-PAGE, and Western blots were stained with HRP-conjugated c-myc antibody (9E10; Santa Cruz Biotechnology) to detect surface-expressed myc::MEC-4d.

## Results

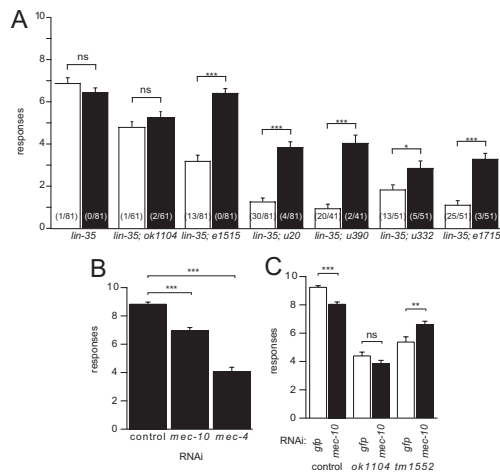
### Decreasing or eliminating *mec-10* results in a partial defect in touch sensation

Saturation mutagenesis screens for touch-insensitive animals identified five *mec-10* alleles (all recessive) with confirmed mutations: *e1515*, *u20*, *u390*, *u332*, and *e1715* (Chalfie and Sulston, 1981; Chalfie and Au, 1989). On average, *mec-10* mutant animals

respond only to 1–4 touches of 10, whereas wild-type animals respond to 9 touches of 10 (Fig. 1A). Each of the *mec-10* alleles has a single missense mutation (Huang and Chalfie, 1994) that affects a protein domain that is conserved within the DEG/ENaC protein family (Fig. 1B). Therefore, these mutations may affect critical functions not only of MEC-10 but also of DEG/ENaC channel proteins more generally.

To determine whether loss of *mec-10* also results in a touch-insensitive phenotype, we characterized a candidate null allele, *mec-10(ok1104)*. The *ok1104* allele was identified by PCR-based screening of a deletion library, rather than a phenotype-based screen. *ok1104* animals had a partial defect in response to gentle touch, a phenotype that was weaker than any of the five previously identified *mec-10* alleles (Fig. 1A).

*ok1104* animals have a 143 bp deletion in the *mec-10* gene starting at the junction between the fourth intron and the fifth exon. To learn how this deletion affects MEC-10 expression, we used two primer pairs for RT-PCR to compare *mec-10* mRNA in wild-type and *ok1104* animals (Fig. 1C). One primer pair (F-R1) resulted in multiple products from *ok1104* animals and a single band from wild-type animals (data not shown). A single RT-PCR product was detected in *ok1104* and wild-type animals with a



**Figure 2.** Effects of *mec-10* RNAi. **A**, RNAi against *mec-10* in *lin-35* ( $n=745$ ) has no effect on animals with wild-type *mec-10* or animals with the *ok1104* deletion allele and enhances the touch sensitivity of animals with missense mutations in *mec-10*. Animals were fed bacteria expressing dsRNA against either GFP (white bars) or *mec-10* (black bars) and assayed for touch response as described in Materials and Methods. Bars are mean  $\pm$  SEM for  $n = 41$ –81 animals. Significance in all panels from Student's *t* test: ns, not significant; \* $p < 0.05$ ; \*\* $p < 0.01$ ; \*\*\* $p < 0.0001$ . Numbers in parentheses represent the number of animals that were completely unresponsive. **B**, RNAi against *mec-10* results in a partial loss of touch sensitivity in a strain that is hypersensitive to RNAi [ $P_{unc-119}sid-1 P_{unc-119}gfp P_{mec-6}; lin-15b(n744)$ ], whereas RNAi against *mec-4* produces a more dramatic loss of touch sensitivity. Animals were fed bacteria expressing dsRNA against either GFP (control), *mec-10*, or *mec-4* as indicated and assayed for touch response as described in Materials and Methods (mean  $\pm$  SEM,  $n = 60$  for each). **C**, RNAi against *mec-10* in a hypersensitive RNAi background ( $P_{unc-119}sid-1 P_{unc-119}gfp P_{mec-6}$ ) reduces the touch sensitivity of animals with wild-type *mec-10* (control) and does not affect the touch response of animals with a deletion in *mec-10* (*ok1104* or *tm1552*). Animals were fed bacteria expressing dsRNA against either GFP (white bars) or *mec-10* (black bars) and assayed for touch response as described in Materials and Methods (mean  $\pm$  SEM,  $n = 90$ –100 for each).

second primer pair (F-R2) that spans a region including that covered by the first primer pair. We sequenced the RT-PCR product from *ok1104* animals from the F-R2 primer pair and two of the products from the F-R1 primer. Conceptual translation of these three gene products revealed the following (Fig. 1D): a transcript encoding an aberrant MEC-10 product with a deletion of 47 aa (L190 to G236) and two transcripts encoding premature stop codons. This analysis indicates that the *ok1104* deletion allele disrupts transcription of the *mec-10* gene but leaves open the possibility that *ok1104* animals might express a mutant MEC-10 protein.

We further tested the effects of reduced MEC-10 activity on touch sensitivity *in vivo* using RNAi. Initially, we used strains carrying *lin-35* ( $n=745$ ), which increases the efficiency of RNAi in the TRNs (Lehner et al., 2006). RNAi against *mec-10* in these animals had no effect on touch sensitivity (Fig. 2A), whereas RNAi against *mec-4* reduced touch sensitivity as found previously (Lehner et al., 2006).

If MEC-10 were required for touch sensitivity, we would expect animals treated with *mec-10* RNAi to have touch sensitivity similar to that of animals carrying the *ok1104* deletion allele (Fig. 1A). RNAi against *mec-10* in *lin-35* ( $n=745$ ) animals, however, had no detectable effect on the touch response. Because this discrepancy could be attributable to incomplete

knockdown of *mec-10*, we retested *mec-10* RNAi in animals whose neurons were made very sensitive to RNAi by neuronal expression of the gene *sid-1* (Calixto et al., 2010). RNAi against *mec-10* in these animals produced partially touch-insensitive animals (Fig. 2B). However, RNAi against *mec-4* produced an even more dramatic reduction in touch sensitivity in *sid-1* (+) transgenic animals. These results mirror the more severe touch-insensitive phenotype of *mec-4* null mutants compared with *mec-10* deletion animals. The phenotype of *ok1104* animals and the effects of knockdown of *mec-10* suggest that MEC-10 is not essential for touch sensation. This result could explain why no null alleles of *mec-10* were identified in previous screens for touch-insensitive animals.

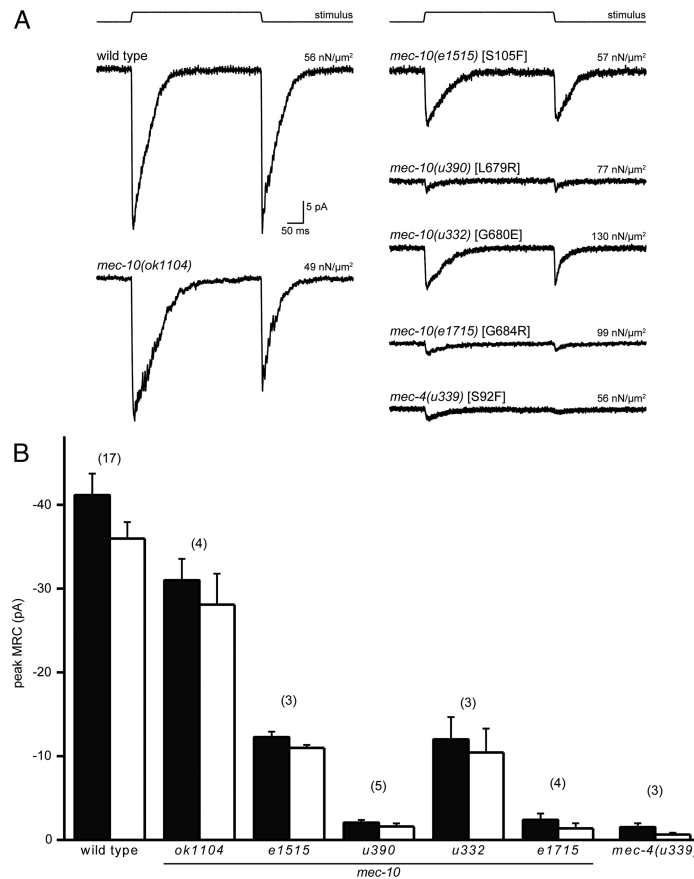
These RNAi results suggest that the *ok1104* deletion causes a loss of functional MEC-10 protein. If, however, *ok1104* resulted in a polypeptide that interfered with proper function of the channel complex, then knockdown of *mec-10* expression by RNAi in *ok1104* animals should rescue their touch response (the *ok1104* allele has >90% of the region targeted by *mec-10* RNAi). In contrast, we found that RNAi against *mec-10* had no effect on the touch response in *ok1104* mutants with either the *lin-35* mutation (Fig. 2A) or the *sid-1* (+) transgene (Fig. 2C). These results suggest that either a truncated protein is not made in *ok1104* animals, or if it is made, it does not interfere with the function of the touch receptor complex.

We also tested the behavioral response of trans-heterozygotes with one copy of *e1515*, *u20*, *u390*, *u332*, or *e1715* and one copy of *ok1104*. The touch responses of these animals were indistinguishable from homozygous *mec-10* mutant animals (supplemental Fig. 1A, B, available at [www.jneurosci.org](http://www.jneurosci.org) as supplemental material). This result also suggests that *ok1104* is a loss-of-function allele.

Chatzigeorgiou et al. (2010a,b) reported that *mec-10(tm1552)*, an allele with a deletion in the region of the gene that encodes the extracellular domain [as with *mec-10(ok1104)*], also produced partial touch insensitivity. Therefore, both *ok1104* and *tm1552* are probably similar loss-of-function alleles. Moreover, a similarly deleted region in *mec-4(u253)* results in a loss-of-function allele (Hong et al., 2000). We used *ok1104* in our experiments because RNAi against *mec-10* did not alter touch sensitivity. In contrast, RNAi for *mec-10* increased the touch sensitivity of *tm1552* animals (Fig. 2C).

Chatzigeorgiou et al. (2010a) also reported that the deletion in *mec-10(tm1552)* results in differential touch insensitivity along the length of the TRN processes. In contrast, we found that wild-type, *mec-10(ok1104)*, and *mec-10(tm1552)* animals all showed a reduced response to touch near the ALM cell body compared with touch near the second pharyngeal bulb (supplemental Fig. 1, available at [www.jneurosci.org](http://www.jneurosci.org) as supplemental material). No difference in response was detected from the two ends of the PLM neurons.

Chatzigeorgiou et al. (2010b) have proposed that MEC-10 is essential for harsh touch sensitivity. Neither animals homozygous for missense mutations in *mec-10* (Huang and Chalfie, 1994) nor animals with both a *mec-4* null mutation (*u253*) and a *mec-10* deletion (*tm1552*) were insensitive to harsh touch (this study). All wild-type animals responded to prodding by a platinum wire, whereas only  $15 \pm 8\%$  (mean  $\pm$  SEM,  $n = 20$  for all) of *mec-3(e1338)* animals, which are defective in sensing harsh touch (Way and Chalfie, 1989), responded. However,  $85 \pm 8\%$  of *mec-4(u253)* and  $80 \pm 9\%$  of *mec-10(ok1104)mec-4(u253)* double-mutant animals responded to harsh touch stimuli.



**Figure 3.** *mec-10* and *mec-4* mutants have MRCs with decreased amplitude. **A**, Examples of *in vivo* recordings of MRCs from PLM touch receptor neurons in wild-type, *mec-10*, and *mec-4* animals (at  $-74$  mV) in response to a saturating mechanical stimulus (top). Each trace is an average of 20 sweeps. Stimulus pressure is indicated above each trace. **B**, Maximum peak amplitude of MRC recorded from PLM touch receptor neurons (at  $-74$  mV), at the onset (black bars) and offset (white bars) of a response to a saturating mechanical stimulus (mean  $\pm$  SEM, numbers in parentheses indicate number of cells tested).

***mec-10* alleles that result in touch insensitivity contain gain-of-function mutations**

The results presented thus far suggest that loss of *mec-10* causes only mild touch insensitivity (Figs. 1A, 2B), whereas several mutant *mec-10* alleles result in greater loss of touch sensitivity (Fig. 1A). To test whether this more severe defect is caused by gain-of-function mutations in the *mec-10* alleles, we used RNAi to knock down expression of mutant *mec-10*. In contrast to the effects of RNAi against *mec-10* in animals carrying either wild-type *mec-10* or the *ok1104* allele, RNAi against *mec-10* reduced the penetrance and expressivity of touch insensitivity of *mec-10* mutant animals (Fig. 2A). Thus, decreasing expression of mutant MEC-10 proteins resulted in animals that responded more often to repeated stimuli and fewer animals completely failed to respond to touch (Fig. 2A). These results support the conclusion that the *mec-10* mutations are gain-of-function mutations.

**Transduction channel subunits are positioned normally in *mec-10* mutant animals**

The MEC-4/MEC-10 channel complex is localized in puncta along the process of the TRNs (Chelur et al., 2002; Zhang et al., 2004). The partial or complete loss of touch sensitivity in *mec-10* animals could be a result of inefficient or improper localization of transduction channel subunits in the TRNs. To test for defects in the localization of the receptor complex in *mec-10* deletion and mutant animals, we assayed the localization of two components of the channel complex, MEC-4 and MEC-2. Using MEC-4::YFP and an anti-MEC-2 antibody, we found that the transduction channel in *mec-10* mutant animals was localized in a punctate pattern similar to that seen in wild-type animals (supplemental Fig. 2, available at [www.jneurosci.org](http://www.jneurosci.org) as supplemental material). This result indicates that the touch insensitivity seen in *mec-10* animals is likely a result of interference with the function and not a gross mislocalization of the transduction channel.

**Loss of MEC-10 decreases MRC amplitude but not single-channel conductance or pressure sensitivity**

We recorded MRCs from PLM touch receptor neurons in live animals to determine how loss of MEC-10 affects channel function. Application and removal of a mechanical stimulus elicits large inward MRCs in both wild-type and *mec-10(ok1104)* deletion mutants (Fig. 3A). Loss of *mec-10* did not detectably affect the latency of MRC activation at either the onset or offset of a touch but slowed the rate of MRC activation and adaptation of the onset response (Table 1). Specifically, rates for activation ( $\tau_1$ ) and adaptation ( $\tau_2$ ) of “on” MRCs were  $\tau_1 = 2.6 \pm 0.2$  ms and  $\tau_2 = 51 \pm 3$  ms for wild-type animals but were  $\tau_1 = 4.2 \pm 0.3$  ms and  $\tau_2 = 67 \pm 3$  ms

in *mec-10(ok1104)* animals ( $p < 0.05$  by one-way ANOVA). Thus, MEC-10 is required for normal MRC kinetics *in vivo*. TRNs from animals with the *ok1104* mutation also had smaller peak MRC amplitudes, ~75% that of wild-type animals.

We tested whether the change in MRC size reflected a decrease in single-channel conductance. Using noise analysis to estimate the apparent single-channel conductance, we found that it was similar in wild-type and *ok1104* mutants:  $15.6 \pm 0.8$  pS for wild type ( $n = 25$ ) and  $15.0 \pm 1.8$  pS for *ok1104* ( $n = 9$ ). Thus, the effect of the *ok1104* deletion on MRC amplitude is not attributable to a decrease in single-channel conductance. This *in vivo* observation is consistent with previous work showing that coexpressing MEC-10 with MEC-4 in *Xenopus* oocytes has no effect on the single-channel conductance measured directly in outside-out membrane patches (Brown et al., 2008).

**Table 1. Kinetics of “on” and “off” MRCs**

Genotype	On			Off		
	Latency (ms)	$\tau_1$ (ms)	$\tau_2$ (ms)	Latency (ms)	$\tau_1$ (ms)	$\tau_2$ (ms)
Wild type	0.7 ± 0.1 (n = 23)	2.6 ± 0.2 (n = 12)	51 ± 3 (n = 12)	1.9 ± 0.1 (n = 23)	2.0 ± 0.2 (n = 12)	49 ± 6 (n = 12)
<i>ok1104</i>	0.7 ± 0.1 (n = 10)	4.2 ± 0.3* (n = 10)	67 ± 3* (n = 10)	1.8 ± 0.1 (n = 10)	1.6 ± 0.1 (n = 10)	41 ± 3 (n = 10)
<i>e1515</i>	1.0 ± 0.2 (n = 5)	2.7 ± 0.5 (n = 5)	48 ± 6 (n = 5)	3.0 ± 0.3* (n = 5)	2.3 ± 0.2 (n = 5)	47 ± 3 (n = 5)
<i>u332</i>	0.8 ± 0.1 (n = 8)	2.9 ± 0.2 (n = 7)	49 ± 4 (n = 7)	2.7 ± 0.2* (n = 8)	1.5 ± 0.1 (n = 7)	20 ± 2* (n = 7)

Average latency, activation ( $\tau_1$ ), and adaptation ( $\tau_2$ ) time constants were calculated from MRC responses to stimuli of at least 40 nN/ $\mu\text{m}^2$  [mean ± SEM, n is number of recordings; \* $p < 0.05$ , one-way ANOVA and subsequent pairwise comparisons (Tukey's test)].

Next, we investigated whether the decrease in MRC size in *mec-10(ok1104)* mutants was attributable to a loss of pressure sensitivity and found that normalized pressure–response curves were similar in wild-type and *mec-10(ok1104)* mutants (supplemental Fig. 3A, B, available at [www.jneurosci.org](http://www.jneurosci.org) as supplemental material). Collectively, these results indicate that MEC-10 is not essential for the formation of pressure-sensitive ion channels in the PLM neurons but fine tunes the time course of activation and adaptation. Additionally, the results suggest that the reduction in MRC size reflects a decrease in either the number of channels available to be opened by external force *in vivo*, a decrease in the peak open probability, or a combination of both factors.

#### Missense mutations in *mec-10* and *mec-4* decrease MRC amplitude

In contrast to TRNs in *mec-10(ok1104)* mutants, which have nearly wild-type MRCs, TRNs from animals carrying *mec-10* missense alleles exhibited a dramatic reduction in peak MRC size. For instance, *mec-10(e1515)* animals had MRCs with a maximum amplitude that was ~30% of that in wild-type animals. Because the *e1515* mutation replaces a conserved serine in the N terminus of MEC-10 with a phenylalanine (S105F), this result suggests that the N terminus is essential for normal DEG/ENaC function *in vivo*. To learn whether this effect was specific to MEC-10 or a more general feature of DEG/ENaC channels, we recorded from *mec-4(u339)* animals in which the homologous residue in MEC-4 is identically changed (S92F) (Fig. 1B). We found that MRCs in *mec-4(u339)* animals were reduced to 4% of their wild-type amplitude. MRC amplitude was also dramatically decreased by the *u332*, *u390*, and *e1715* alleles, which affect conserved residues in the second transmembrane domain (TM2) of MEC-10 (Fig. 3). The effect of *mec-10* mutations on MRC amplitude mirrored the severity of the behavioral defects such that mutations that give rise to mild defects in behavior such as *e1515* also retain larger-amplitude MRCs.

As in wild-type animals, MRC amplitude increased with applied pressure in *e1515* and *u332* mutants. Thus, mutant channel complexes retain their ability to detect external force. Consistent with this idea, neither *e1515* nor *u332* showed an increase in the stimulus pressure required to fully saturate MRC amplitude (supplemental Fig. 3C, D, available at [www.jneurosci.org](http://www.jneurosci.org) as supplemental material). (The MRCs in *u390* and *e1715* animals were too small to analyze.) The pressure–response curve for *e1515* was slightly shifted to the right (supplemental Fig. 3C, available at [www.jneurosci.org](http://www.jneurosci.org) as supplemental material):  $P_{50}$  values were  $15 \pm 4$  nN/ $\mu\text{m}^2$  ( $n = 3$ ) and  $8 \pm 1$  nN/ $\mu\text{m}^2$  ( $n = 17$ ) in *e1515* and wild-type animals, respectively. Thus, larger pressures were required for half-maximal amplitude MRC activation in *e1515* an-

imals, suggesting that the mutation in *e1515* in the N terminus of the protein influences channel gating. Pressure–response curves in *u332* animals, in contrast, were indistinguishable from wild type (supplemental Fig. 3, available at [www.jneurosci.org](http://www.jneurosci.org) as supplemental material).

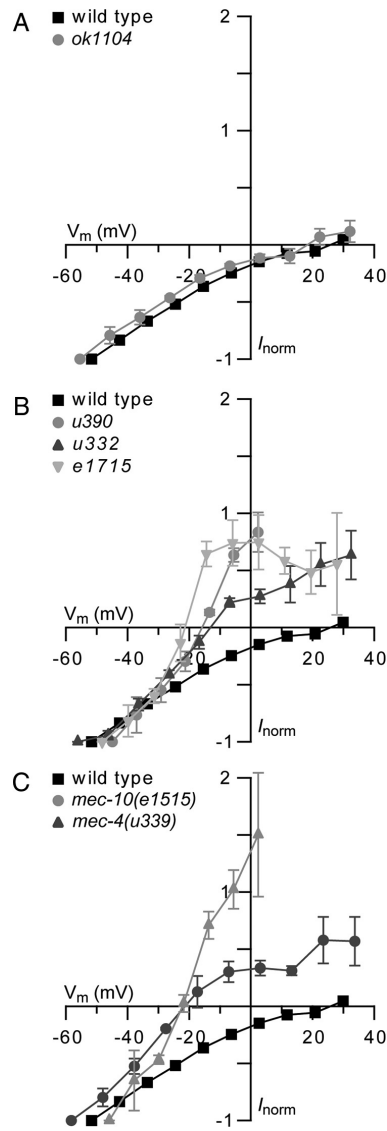
We also examined the latencies for MRC activation at the onset and the offset of the mechanical stimulus in *e1515* and *u332* mutant animals (Table 1; MRCs in *u390* and *e1715* were too small to analyze). The measured response latencies are <1 ms and represent an upper bound on the time elapsed between the delivery (or removal) of the mechanical stimulus and activation of channels *in vivo*. Latencies for channel activation in response to stimulus onset were similar to wild type in both *e1515* and *u332* mutants. In contrast, latencies for the “off” response were increased. As in wild-type animals, MRCs in *mec-10* missense mutants activated rapidly and adapted during continuous stimulation (Fig. 3A). The time course of MRCs in *e1515* mutants was similar to that recorded in wild-type PLM neurons (Table 1). MRCs in *u332*, however, showed a 2.5-fold increase in the adaptation rate ( $\tau_2$ ) of the off response. Previous work also showed an increased rate of adaptation and response latency in MRCs recorded from *mec-10(u20)* animals (O'Hagan et al., 2005).

To determine whether mutations in *mec-10* and *mec-4* specifically affect MRCs or they affect the general excitability of TRNs, we recorded the response of voltage-gated currents to a series of voltage steps. These currents are generated in response to voltage pulses and are independent of the mechanosensitive response. Peak and steady-state voltage-gated currents recorded from all mutant animals were qualitatively similar to those recorded from wild-type animals and from previous studies (O'Hagan et al., 2005) (supplemental Fig. 4, available at [www.jneurosci.org](http://www.jneurosci.org) as supplemental material). Hence, these mutations appear to affect mechanotransduction specifically.

#### Missense mutations in *mec-10*, but not loss of MEC-10, alter MRC ion selectivity

Recordings of MRCs in wild-type animals demonstrate that the MEC-4/MEC-10 transduction channel is Na<sup>+</sup> selective (O'Hagan et al., 2005). Such selectivity is preserved when MEC-4/MEC-10 channels are expressed in *Xenopus* oocytes and is insensitive to the presence or absence of MEC-10 (Goodman et al., 2002; Brown et al., 2007). Consistent with the properties of channels expressed in oocytes, MRCs reversed polarity near +20 mV in both wild-type and *ok1104* animals (Fig. 4A). Thus, loss of MEC-10 does not appear to affect ion selectivity *in vivo*. In contrast, mutations in MEC-10 shifted the reversal potential for MRCs by –40 mV or more (Fig. 4B, C). The negative reversal potential of the MRC in *mec-10* mutant animals suggests that mutant channels have increased permeability to K<sup>+</sup> ions. A similar effect was reported previously for MRCs recorded from *mec-10(u20)* and *mec-4(u2)* animals (O'Hagan et al., 2005). This result suggests that the shift in ion selectivity is caused by gain-of-function mutations in *mec-10* rather than a nonfunctional MEC-10.

To test this interpretation, we measured the MRC–voltage relationship in *mec-4(u339)* animals. If the gain-of-function mutation in *e1515* is responsible for the shift in ion selectivity, a mutation in the conserved S92 residue in *mec-4(u339)* should cause a similar shift in the reversal potential of the MRCs. We found that this was the case: MRCs recorded in both *mec-10(e1515)* and *mec-4(u339)* animals reversed polarity near –20 mV (Fig. 4C).



**Figure 4.** Point mutations in *mec-10* and *mec-4* alter the reversal potential of the MRC, whereas a deletion in *mec-10* does not affect the reversal potential. Current–voltage relations for MRCs recorded from PLM cells at the onset of a saturating mechanical stimulus in mutant (gray) and wild-type (black) animals (mean  $\pm$  SEM). MRCs were recorded at  $-114$  to  $+66$  mV in  $20$  mV increments. Current was normalized ( $I_{norm}$ ) to the current recorded at a holding potential of  $-114$  mV, and membrane potential ( $V_m$ ) was adjusted for voltage attenuation as described in Materials and Methods. **A**, *mec-10(ok1104)* ( $n = 4$ ) compared with wild-type ( $n = 7$ ). **B**, *mec-10(u390)* ( $n = 3$ ), *mec-10(u332)* ( $n = 4$ ), and *mec-10(e1715)* ( $n = 4$ ) compared with wild-type ( $n = 7$ ). **C**, *mec-10(e1515)* ( $n = 3$ ) and *mec-4(u339)* ( $n = 3$ ) compared with wild-type ( $n = 7$ ).

**Mutant MEC-10 requires MEC-2**

In addition to MEC-4 and MEC-10, several non-pore-forming accessory subunits form part of the mechanosensory channel complex. These accessory subunits include MEC-2, a PHB-

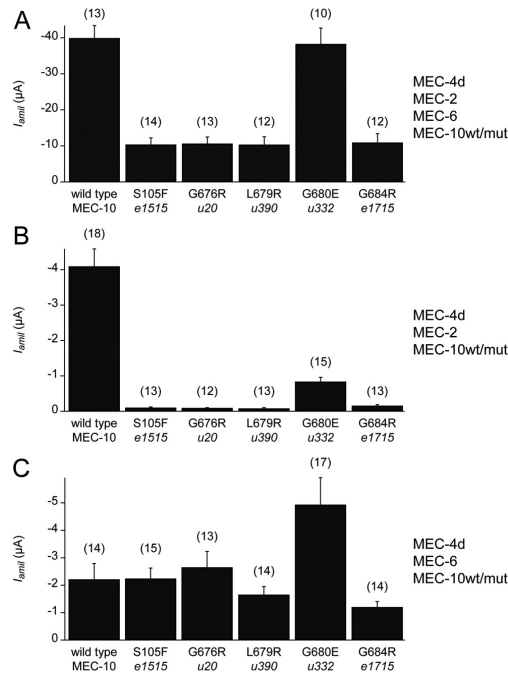
domain protein, and MEC-6, a paraoxonase-like protein. These proteins colocalize with the channel along the process of the TRN and interact with MEC-4 and MEC-10 (Chelur et al., 2002; Goodman et al., 2002; Zhang et al., 2004). Expression of MEC-2 and MEC-6 in *Xenopus* oocytes affects both the size and the properties of the MEC-4 current. To investigate how mutant MEC-10 proteins interact with other subunits of the channel complex, we expressed wild-type and mutant forms of MEC-10 along with MEC-4, MEC-2, and MEC-6 in *Xenopus* oocytes. As in previous studies, we used a constitutively active MEC-4 isoform [MEC-4d also known as MEC-4(A713T)] (Goodman et al., 2002).

Coexpression of MEC-10 with MEC-4d, MEC-2, and MEC-6 reduced the amiloride-sensitive current recorded from *Xenopus* oocytes compared with current recorded from oocytes expressing MEC-4d, MEC-2, and MEC-6 (our unpublished observation). We found that mutant MEC-10 proteins further reduced the current. Current recorded from oocytes expressing MEC-4d, MEC-2, MEC-6 and mutant MEC-10 was as low as 25% of the current recorded from oocytes expressing MEC-4d, MEC-2, MEC-6 and wild-type MEC-10 (Fig. 5A). Therefore, oocytes expressing MEC-4d/MEC-10/MEC-2/MEC-6 channel complexes recapitulate the gain-of-function effects of the *mec-10* mutations *in vivo*. The one exception was MEC-10(G680E), corresponding to the *u332* allele, which resulted in an amiloride-sensitive current with an amplitude comparable with that recorded from oocytes expressing channel complexes with wild-type MEC-10. The mutant phenotype produced by the *u332* allele may result from interactions with other proteins of the channel complex *in vivo*.

The reduction of the amiloride-sensitive current by mutant versions of MEC-10 did not require MEC-6. The current was decreased by  $>95\%$  relative to channel complexes with wild-type MEC-10 for all the MEC-10 mutant proteins coexpressed with MEC-4d and MEC-2 in the absence of MEC-6 except MEC-10(G680E), which decreased the current by 80% (Fig. 5B).

In contrast, the reduction of the amiloride-sensitive current by mutant MEC-10 proteins required MEC-2. Coexpression of MEC-10 mutant proteins with MEC-4d and MEC-6 produced currents that were similar to channel complexes with wild-type MEC-10 (Fig. 5C). The exception was MEC-10(G680E), which produced more than twofold larger current than wild-type MEC-10 when coexpressed with MEC-4d/MEC-6.

The effect of the mutation in the *u332* allele [MEC-10(G680E)] was anomalous to the other *mec-10* alleles in heterologously expressed channels. MEC-10(G680E) decreased the current recorded from the MEC-4d/MEC-2/MEC-10 channel complexes less, relative to wild-type MEC-10, than any of the other four MEC-10 mutant proteins. MEC-10(G680E) also increased the current from the MEC-4d/MEC-6/MEC-10 complex relative to wild type, whereas the other mutant proteins functioned similarly to wild-type MEC-10. The net effect of the MEC-10(G680E) mutation, however, was similar to the effect of wild-type MEC-10 in MEC-4d/MEC-2/MEC-6 channel complexes. However, both behavioral responses of *u332* animals and *in vivo* recordings from these animals were similar to the other *mec-10* mutant animals. Differences in heterologously expressed channels could be attributable to an interaction between the residue mutated in *u332* with the activating mutation in MEC-4d, which is in close proximity to the site of the *mec-10* mutations. Conversely, these differences could be caused by additional proteins that interact with the MEC-4/MEC-10 complex *in vivo* but are not present in the heterologous system.



**Figure 5.** MEC-10 mutant proteins inhibit the amiloride-sensitive current in *Xenopus* oocytes in a MEC-2-dependent manner. Amiloride-sensitive current ( $I_{ami}$ ) recorded at  $-85$  mV from the MEC-4d channel complex expressed with wild-type and mutant forms of MEC-10 as indicated beneath each bar (mean  $\pm$  SEM, numbers in parentheses represent number of cells tested). **A**, Oocytes expressing MEC-4d, MEC-2, MEC-6, and wild-type and mutant forms of MEC-10 as noted. Except for the G680E variant, currents recorded from channels with MEC-10 variants were significantly different from currents from channels with wild-type MEC-10 ( $p < 0.00001$ , Student's  $t$  test). **B**, Oocytes expressing MEC-4d, MEC-2, and wild-type and mutant forms of MEC-10 as noted. Currents recorded from channels with MEC-10 variant proteins were significantly different from those from channels with wild-type MEC-10 ( $p < 0.00001$ , Student's  $t$  test). **C**, Oocytes expressing MEC-4d, MEC-6, and wild-type and mutant forms of MEC-10 as noted. Currents recorded from channels with G680E were significantly larger than currents from channels with wild-type MEC-10 ( $p < 0.05$ , Student's  $t$  test). No significant difference in current between channels with any of the other MEC-10 variants and those with wild-type MEC-10 ( $p = 0.12$ – $0.97$ , Student's  $t$  test).

Next we tested whether the mutations in the *mec-10* alleles decrease the association between mutant MEC-10 proteins and MEC-4d in *Xenopus* oocytes. We found that all mutant forms of MEC-10 coimmunoprecipitated with MEC-4d when coexpressed with MEC-2 (supplemental Fig. 5A, available at [www.jneurosci.org](http://www.jneurosci.org) as supplemental material). We also tested whether coexpression of mutated MEC-10 proteins resulted in fewer MEC-4d channel complexes expressed at the surface of the cell. We found that MEC-4d is expressed at the surface of the oocyte when coexpressed with either wild-type or mutant forms of MEC-10 and MEC-2 (supplemental Fig. 5B, available at [www.jneurosci.org](http://www.jneurosci.org) as supplemental material). Together, these results indicate that the effects of the MEC-10 mutations on the current recorded from heterologously expressed MEC-4d channels are likely attributable to an effect on the function of the channel complex and not interactions between the channel subunits or trafficking to the surface of the oocyte. These findings are in agreement with *in vivo* recordings of MRCs.

## Discussion

### Functional diversity of DEG/ENaC channel subunits

Although the amino acid sequences of MEC-4 and MEC-10 are 54% identical, these pore-forming channel subunits are not interchangeable. *mec-4* null animals, which retain the wild-type *mec-10* gene, lack MRCs (O'Hagan et al., 2005), and overexpression of one gene cannot rescue the touch insensitivity caused by mutation of the other gene (Huang and Chalfie, 1994). Because *mec-10(ok1104)* animals have substantial MRCs, MEC-10 is not essential to form channels in the PLM neurons. MEC-10 is needed, however, for optimal ion channel activity *in vivo*. MRCs generated in response to saturating mechanical stimuli in *mec-10* deletion mutants are smaller than in wild-type PLM neurons, and these animals show reduced touch sensitivity in behavioral assays. Previous observations had also suggested a minor role for MEC-10 based on the differential sensitivity of the TRNs to activating *d* mutations in *mec-4* and *mec-10* (Huang and Chalfie, 1994). Thus, as with  $\beta$  or  $\gamma$ ENaC (Canessa et al., 1993, 1994; Lingueglia et al., 1993) and ASIC2b (Lingueglia et al., 1997; Hesselager et al., 2004), MEC-10 cannot form functional channels on its own and plays a regulatory role in MEC-4 mechanotransduction complexes.

The *mec-10* gene is expressed in the gentle touch-sensitive TRNs and the harsh touch-sensitive PVD and FLP neurons (Huang and Chalfie, 1994). However, only the TRNs that sense gentle touch coexpress *mec-4*. In PLM, loss of MEC-10 decreases, but does not eliminate, the maximal MRC evoked by low-intensity or "gentle" stimuli. Recently, Chatzigeorgiou et al. (2010b) reported that the response to harsh touch in the PVD neurons and in the TRNs absolutely requires MEC-10 and another DEG/ENaC protein, DEGT-1. [Harsh touch sensitivity in FLP requires MEC-10 but not DEGT-1 (Chatzigeorgiou and Schafer, 2011).] Our experiments lead us to question the role of MEC-10 in the PVD neurons. First, using the same deletion (*tm1552*) used by Chatzigeorgiou et al. (2010b), we could not detect a significant loss of harsh touch sensitivity in animals lacking *mec-4*. Second, if *mec-10* were essential for the harsh touch channel of the PVD neurons and acted similarly to its role in the MEC-4 channel complex, one might expect that animals with the recessive gain-of-function mutations in *mec-10* would also be harsh touch insensitive, but they are not (Huang and Chalfie, 1994). We propose that *mec-10* is not likely to be essential in either the TRNs or the PVD neurons.

### Interactions between subunits in the mechanoreceptor channel complex

MEC-2 and MEC-6 synergistically increase the current from the MEC-4d/MEC-10 channel complex *in vitro* by increasing the number of channels in an active state (Chelur et al., 2002; Brown et al., 2008). We show that heterologously expressed mutant MEC-10 proteins decrease currents from the MEC-4d/MEC-10 channel, analogous to the *in vivo* effects of mutations in *mec-10*. This effect is dependent on the presence of MEC-2 but not MEC-6. Previous work showed that MEC-2 decreases the amiloride sensitivity of the channel and increases single-channel conductance, suggesting that MEC-4 and MEC-10 together form an amiloride-binding site that can be modified by MEC-2 (Chelur et al., 2002; Brown et al., 2008). The MEC-2 dependence of the gain-of-function effects of the MEC-10 missense mutations may indicate that the interaction between MEC-2 and MEC-4 causes a conformational change. This conformational change could render the channel complex susceptible to interference by the

MEC-10 mutations. Alternatively, or additionally, MEC-2 could directly affect MEC-10 conformation.

#### Structural basis of ion selectivity in DEG/ENaC channels

Five *mec-10* alleles (*u20*, *u390*, *u332*, *e1715*, and *e1515*) and two *mec-4* alleles (*u2*, *u339*) encode point mutations that alter the reversal potential of MRCs *in vivo* (this study and O'Hagan et al., 2005). Whereas wild-type MRCs reverse polarity near the equilibrium potential for Na<sup>+</sup> ions, mutant MRCs reverse polarity 40 mV negative to this value, on average (Fig. 4) (O'Hagan et al., 2005, their Fig. 6C). The simplest explanation for this change in reversal potential is that point mutations encoded by *mec-10* and *mec-4* missense alleles increase K<sup>+</sup> permeability. Such an increase in permeability could arise from an increase in the diameter of the mutant pore, because the selectivity sequence of wild-type DEG/ENaC channels mirrors ionic size (Kellenberger and Schild, 2002).

Five of the seven missense *mec-10* and *mec-4* alleles analyzed *in vivo* result in amino acid substitutions of conserved residues in TM2 of MEC-10 and MEC-4 (Fig. 1B). A high-resolution crystal structure of a related DEG/ENaC channel, chicken ASIC1a, reveals that TM2 forms a long  $\alpha$  helix, tilted at 50° with respect to the plane of the membrane (Gonzales et al., 2009). All of the affected TM2 residues are predicted to lie on the same side of the TM2 helix and localize to the cytoplasmic side of the putative gate. Four of five mutations affect conserved glycines (the fifth is a lysine residue that is conserved in many but not all family members). Our experimental data support the idea that main-chain carbonyl oxygen atoms at such glycine residues coordinate permeant ions in the open-channel conformation (Gonzales et al., 2009). Indeed, two of the glycine residues proposed to coordinate ions in the open-channel state by Gonzales et al. (2009) correspond to the residues affected in *u332* and *e1715*. Mutations at the position equivalent to the site mutated in *e1715* affect ion selectivity in vertebrate ENaC channels (for review, see Kellenberger and Schild, 2002). A third glycine, which is mutated in both *mec-10(u20)* and *mec-4(u2)* and conserved across phyla, was proposed to form a desensitization gate in cASIC1a (Gonzales et al., 2009). Our current and previous results (O'Hagan et al., 2005) demonstrate that this glycine has an additional role in regulating ion selectivity and may also coordinate permeant ions in the open channel.

Loss of MEC-10 has little or no effect on MRC reversal potential (Fig. 4A), implying that homomeric MEC-4 channels (formed in *mec-10* deletion mutants) and heteromeric MEC-4/MEC-10 channels have identical ion selectivity profiles. Similar results were seen when these channel proteins were expressed in *Xenopus* oocytes (Goodman et al., 2002; Brown et al., 2007) and underscores the importance of the glycine surface in TM2, which is identical in MEC-4 and MEC-10, for regulating pore size and coordinating permeant ions.

The *mec-10* gain-of-function alleles affect more than a common surface on TM2; the *e1515* and *u339* mutations affect a conserved serine residue in the N terminus of MEC-10 and MEC-4, respectively (Fig. 1B). These mutations reduce the peak amplitude of the MRCs and change the ion selectivity of the transduction channel. Thus, the N terminus of MEC-4 and MEC-10 is involved in ion selectivity *in vivo*. The contribution of the N terminus to selectivity is shared by vertebrate DEG/ENaC proteins because mutating the homologous position in ASIC2 and ASIC3 also increases K<sup>+</sup> permeability (Coscoy et al., 1999).

In principle, such a selectivity change could offset the effect of degeneration-inducing mutations in MEC-4 by limiting the de-

polarization induced by constitutive channel activation in the mutants. Consistent with this idea, transgenic expression of a *u339* [MEC-4(S92F)] mutant isoform suppresses degeneration induced by the toxic MEC-4(A713V) protein *in vivo* (Hong et al., 2000). The structural basis for the effect of the N terminus on selectivity is unknown but could involve direct interactions with the pore-lining TM2 in the open-channel state.

In this study and that of O'Hagan et al. (2005), we identified five residues (in TM2 and the cytoplasmic N terminus) that can mutate to alter selectivity. These data imply that the structural basis of ion selectivity in DEG/ENaC is distinct from the well-characterized selectivity filter of K<sup>+</sup>-selective ion channels (Armstrong, 2003). In particular, K<sup>+</sup>-selective channels rely on a highly conserved 3 aa sequence oriented such that backbone carbonyls form closely spaced binding sites for K<sup>+</sup> ions in the pore. The Na<sup>+</sup> selectivity of DEG/ENaC channels, in contrast, appears to rely on residues distributed across at least three helical turns in TM2 and extending into the N terminus. Thus, the body plan of the selectivity filter of DEG/ENaC channels is distinct from that of ion channels that contain a pore-loop motif similar to that found in bacterial and eukaryotic K<sup>+</sup> and Na<sup>+</sup> channels. Because DEG/ENaC channels are conserved in animals and absent from both plant and bacterial genomes (Goodman and Schwarz, 2003; Hunter et al., 2009), this type of ion selectivity filter may represent an animal-specific motif in ion channels.

#### References

- Armstrong CM (2003) Voltage-gated K channels. *Sci STKE* 2003:re10.
- Brenner S (1974) The genetics of *Caenorhabditis elegans*. *Genetics* 77:71–94.
- Brown AL, Fernandez-Illasas SM, Liao Z, Goodman MB (2007) Gain-of-function mutations in the MEC-4/ENaC sensory mechanotransduction channel alter gating and drug blockade. *J Gen Physiol* 129:161–173.
- Brown AL, Liao Z, Goodman MB (2008) MEC-2 and MEC-6 in the *Caenorhabditis elegans* sensory mechanotransduction complex: auxiliary subunits that enable channel activity. *J Gen Physiol* 131:605–616.
- Calixto A, Chelur D, Topalidou I, Chen X, Chalfie M (2010) Enhanced neuronal RNAi in *C. elegans* using SID-1. *Nat Methods* 7:554–559.
- Canessa CM, Horisberger JD, Rossier BC (1993) Epithelial sodium channel related to proteins involved in neurodegeneration. *Nature* 361:467–470.
- Canessa CM, Schild L, Buell G, Thorens B, Gautschi I, Horisberger JD, Rossier BC (1994) Amiloride-sensitive epithelial Na<sup>+</sup> channel is made of three homologous subunits. *Nature* 367:463–467.
- Chalfie M, Au M (1989) Genetic control of differentiation of the *Caenorhabditis elegans* touch receptor neurons. *Science* 243:1027–1033.
- Chalfie M, Sulston J (1981) Developmental genetics of the mechanosensory neurons of *Caenorhabditis elegans*. *Dev Biol* 82:358–370.
- Chalfie M, Wolinsky E (1990) The identification and suppression of inherited neurodegeneration in *Caenorhabditis elegans*. *Nature* 345:410–416.
- Chatzigeorgiou M, Schafer WR (2011) Lateral facilitation between primary mechanosensory neurons controls nose touch perception in *C. elegans*. *Neuron* 70:299–309.
- Chatzigeorgiou M, Grundy L, Kindt KS, Lee WH, Driscoll M, Schafer WR (2010a) Spatial asymmetry in the mechanosensory phenotypes of the *C. elegans* DEG/ENaC gene *mec-10*. *J Neurophysiol* 104:3334–3344.
- Chatzigeorgiou M, Yoo S, Watson JD, Lee WH, Spencer WC, Kindt KS, Hwang SW, Miller DM 3rd, Treinin M, Driscoll M, Schafer WR (2010b) Specific roles for DEG/ENaC and TRP channels in touch and thermosensation in *C. elegans* nociceptors. *Nat Neurosci* 13:861–868.
- Chelur DS, Ernstrom GG, Goodman MB, Yao CA, Chen L, O'Hagan R, Chalfie M (2002) The mechanosensory protein MEC-6 is a subunit of the *C. elegans* touch-cell degenerin channel. *Nature* 420:669–673.
- Coscoy S, de Weille JR, Lingueglia E, Lazdunski M (1999) The pretransmembrane 1 domain of acid-sensing ion channels participates in the ion pore. *J Biol Chem* 274:10129–10132.
- Driscoll M, Chalfie M (1991) The *mec-4* gene is a member of a family of *Caenorhabditis elegans* genes that can mutate to induce neuronal degeneration. *Nature* 349:588–593.
- Fraser AG, Kamath RS, Zipperlen P, Martinez-Campos M, Sohrmann M,



- Ahringer J (2000) Functional genomic analysis of *C. elegans* chromosome I by systematic RNA interference. *Nature* 408:325–330.
- Gonzales EB, Kawate T, Gouaux E (2009) Pore architecture and ion sites in acid-sensing ion channels and P2X receptors. *Nature* 460:599–604.
- Goodman MB, Schwarz EM (2003) Transducing touch in *Caenorhabditis elegans*. *Annu Rev Physiol* 65:429–452.
- Goodman MB, Ernstrom GG, Chelur DS, O'Hagan R, Yao CA, Chalfie M (2002) MEC-2 regulates *C. elegans* DEG/ENaC channels needed for mechanosensation. *Nature* 415:1039–1042.
- Heinemann SH, Conti F (1992) Nonstationary noise analysis and application to patch clamp recordings. *Methods Enzymol* 207:131–148.
- Hesselager M, Timmermann DB, Ahring PK (2004) pH dependency and desensitization kinetics of heterologously expressed combinations of acid-sensing ion channel subunits. *J Biol Chem* 279:11006–11015.
- Hobert O, Moerman DG, Clark KA, Beckerle MC, Ruvkun G (1999) A conserved LIM protein that affects muscular adherens junction integrity and mechanosensory function in *Caenorhabditis elegans*. *J Cell Biol* 144:45–57.
- Hong K, Mano I, Driscoll M (2000) *In vivo* structure–function analyses of *Caenorhabditis elegans* MEC-4, a candidate mechanosensory ion channel subunit. *J Neurosci* 20:2575–2588.
- Huang M, Chalfie M (1994) Gene interactions affecting mechanosensory transduction in *Caenorhabditis elegans*. *Nature* 367:467–470.
- Huang M, Gu G, Ferguson EL, Chalfie M (1995) A stomatin-like protein necessary for mechanosensation in *C. elegans*. *Nature* 378:292–295.
- Hunter S, Apweiler R, Attwood TK, Bairoch A, Bateman A, Binns D, Bork P, Das U, Daugherty L, Duquenne L, Finn RD, Gough J, Haft D, Hulo N, Kahn D, Kelly E, Laugraud A, Letunic I, Lonsdale D, Lopez R, et al. (2009) InterPro: the integrative protein signature database. *Nucleic Acids Res* 37:D211–D215.
- Kamath RS, Ahringer J (2003) Genome-wide RNAi screening in *Caenorhabditis elegans*. *Methods* 30:313–321.
- Kellenberger S, Schild L (2002) Epithelial sodium channel/degenerin family of ion channels: a variety of functions for a shared structure. *Physiol Rev* 82:735–767.
- Lehner B, Calixto A, Crombie C, Tischler J, Fortunato A, Chalfie M, Fraser AG (2006) Loss of LIN-35, the *Caenorhabditis elegans* ortholog of the tumor suppressor p105Rb, results in enhanced RNA interference. *Genome Biol* 7:R4.
- Lingueglia E, Voilley N, Waldmann R, Lazdunski M, Barbry P (1993) Expression cloning of an epithelial amiloride-sensitive Na<sup>+</sup> channel. A new channel type with homologies to *Caenorhabditis elegans* degenerins. *FEBS Lett* 318:95–99.
- Lingueglia E, de Weille JR, Bassilana F, Heurteaux C, Sakai H, Waldmann R, Lazdunski M (1997) A modulatory subunit of acid sensing ion channels in brain and dorsal root ganglion cells. *J Biol Chem* 272:29778–29783.
- Lu X, Horvitz HR (1998) *lin-35* and *lin-53*, two genes that antagonize a *C. elegans* Ras pathway, encode proteins similar to Rb and its binding protein RbAp48. *Cell* 95:981–991.
- Mello C, Fire A (1995) DNA transformation. *Methods Cell Biol* 48:451–482.
- Miller DM, Shakes DC (1995) Immunofluorescence microscopy. *Methods Cell Biol* 48:365–394.
- O'Hagan R, Chalfie M, Goodman MB (2005) The MEC-4 DEG/ENaC channel of *Caenorhabditis elegans* touch receptor neurons transduces mechanical signals. *Nat Neurosci* 8:43–50.
- Papadopoulos JS, Agarwala R (2007) COBALT: constraint-based alignment tool for multiple protein sequences. *Bioinformatics* 23:1073–1079.
- Way JC, Chalfie M (1989) The *mec-3* gene of *Caenorhabditis elegans* requires its own product for maintained expression and is expressed in three neuronal cell types. *Genes Dev* 3:1823–1833.
- Zhang S, Árnadóttir J, Keller C, Caldwell GA, Yao CA, Chalfie M (2004) MEC-2 is recruited to the putative mechanosensory complex in *C. elegans* touch receptor neurons through its stomatin-like domain. *Curr Biol* 14:1888–1896.

Appendix II. Characterization of other POML proteins

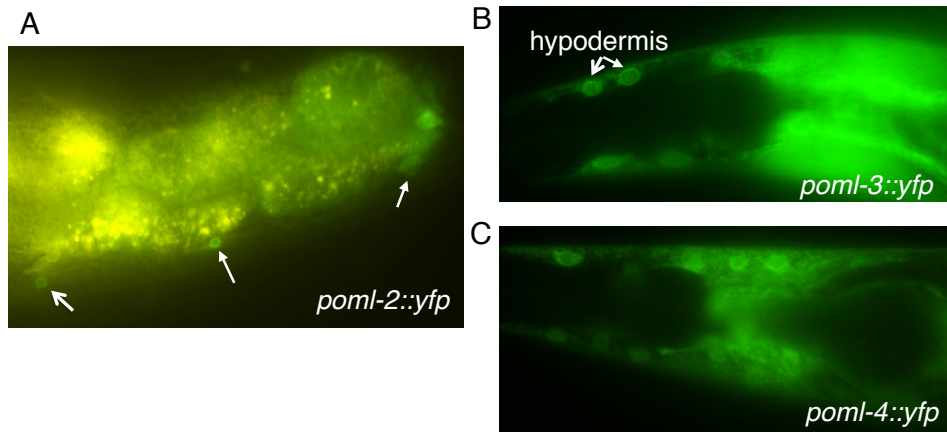


Figure V. Expression pattern of POML-2, POML-3, and POML-4.

Table V. Summary of *C. elegans* PONs

PONs	Gene expression	Loss-of-function phenotype	RNAi
MEC-6	Many neurons (TRNs, HSN, PVD, IL1, male tail sensory rays, and etc), muscles (body wall, vulval, intestinal, anal depressor and sphincter muscles), and excretory canal (from Chelur et al., 2002)	Mec	RNAi in <i>poml-4(ok1834)</i> resulted in 20% Dpy animals.
POML-1	TRNs, IL1, AIM, ALN, BDU	Mec in the sensitized background	ND
POML-2	DA neuron, intestinal-rectalvalve, rectal glands	Small brood size	ND
POML-3	hyp6, hyp-7, and intestine	none	RNAi in <i>poml-4(ok1834)</i> resulted in 30% Dpy animals.
POML-4	hyp6, hyp-7, and intestine	none	ND